Supporting information

Minimising conformational bias in fluoroprolines through vicinal difluorination†

Gert-Jan Hofman,[a,b] Emile Ottoy,[b] Mark Light,[a] Bruno Kieffer,[c] Ilya Kuprov,[a] Jose C. Martins,[b,*] Davy Sinnaeve,[b,*] and Bruno Linclau[a,*]

Table of Contents

1 Synthesis

1.1 Synthesis of 3,4-difluoroproline 7

1.1.1 (2S)-N-t-Butyloxycarbonyl-3,4-dehydroproline benzyl ester **9**.

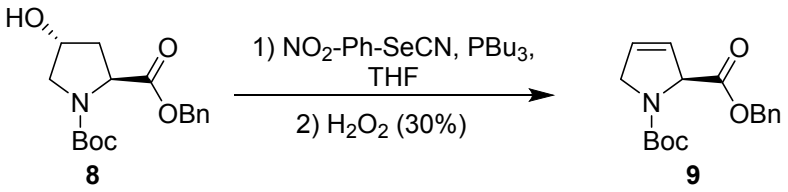

8 **9**

63% over 2 steps

At 0 °C, tributylphosphine (1.2 mL, 4.951 mmol) and 2-nitrophenyl selenocyanate (913.5 mg, 4.023 mmol) were added to a solution of **8** (994.5 mg, 3.095 mmol) in THF (15.0 mL). After stirring at rt for 7 h, a saturated aqueous solution of $NaHCO_3$ (5.0 mL) and H_2O_2 (30% w/w, 10.0 mL) were added, and the mixture was stirred at rt. After 12 h, the mixture was cooled on ice and slowly quenched with a saturated aqueous solution of $Na_2S_2O_3$ (20 mL). The aqueous phase was extracted with DCM (3 x 30 mL). The organic phases were washed with brine (30 mL), dried over $MgSO_4$ and the solvent was evaporated *in vacuo*. Purification by flash chromatography (hexane/EtOAc 90:10 to 75:25) yielded alkene **9** (591.2 mg, 63 %) as a slightly yellow oil. **$[\alpha]_D$** -130 (c 1.2, $CHCl_3$, 22 °C); **Rf** 0.35 (hexane/acetone 90:10); **^{1}H NMR** (400 MHz, $CDCl_3$): (63:37 rotamer ratio) δ 7.41–7.29 (m, $5H_{(M)}$+$5H_{(m)}$, Ph), 6.04–5.91 (m, 2H, $C_\gamma H_{(M+m)}$), 5.80–5.70 (m, 2H, $C_\beta H_{(M+m)}$), 5.32–4.98 (m, 4H, $CH_2Ph_{(M+m)}$ + 2H, $C_\alpha H_{(M+m)}$), 4.35–4.14 (m, 4H, $C_\delta H_{2(M+m)}$), 1.49 (s, 9H, $CO_2C(C\underline{H}_3)_{3\surd}$), 1.36 (s, 9H, $CO_2C(C\underline{H}_3)_{3(M)}$) ppm; **^{13}C NMR** (100 MHz, $CDCl_3$): δ 170.4 ($\underline{C}O_{2(M)}$), 170.1 ($\underline{C}O_{2(m)}$), 153.8 ($\underline{C}O_2C(CH_3)_{3(m)}$), 153.4 ($\underline{C}O_2C(CH_3)_{3(M)}$), 135.7 ($\underline{C}_{Ph(m)}$), 135.5 ($\underline{C}_{Ph(M)}$), 129.5 ($C_{\gamma(M)}$), 129.4 ($C_{\gamma(m)}$), 128.6–128.0 ($\underline{C}H_{Ph(M+m)}$), 124.7 ($C_{\beta(m)}$), 124.6 ($C_{\beta(M)}$), 80.2 ($CO_2\underline{C}(CH_3)_{3(M)}$), 80.1 ($CO_2\underline{C}(CH_3)_{3(m)}$), 66.8–66.4 ($\underline{C}H_2Ph_{(M+m)}$ + $C_{\alpha(M+m)}$), 53.5 ($C_{\delta(m)}$), 53.3 ($C_{\delta(M)}$), 28.4 ($CO_2C(\underline{C}H_3)_{3(m)}$), 28.2 ($CO_2C(\underline{C}H_3)_{3(M)}$) ppm; **MS** (ESI)(*m/z*): 326.4 $(M+Na)^+$; **HRMS** (ESI) for $C_{17}H_{21}NNaO_4$ $[M+Na]^+$ Calcd. 326.1360; Found 326.1364; **IR** 2976 (m), 1753 (s), 1703 (s) cm^{-1}.

This compound is reported in the patent literature without characterisation data.[1, 2]

1.1.2 Determination of the regioselectivity of the Grieco elimination reaction

Comparison of the NMR spectrum of the 3,4-alkene, the 4,5-alkene, and the crude reaction mixture:

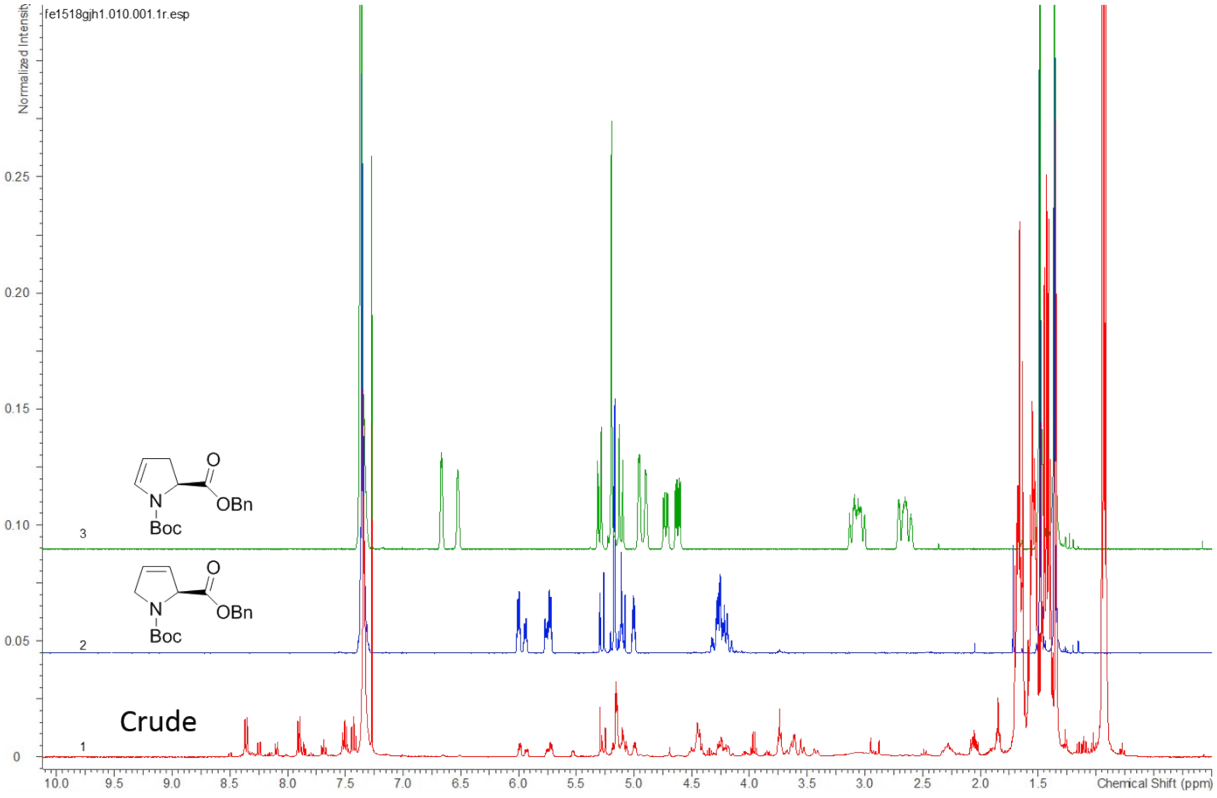

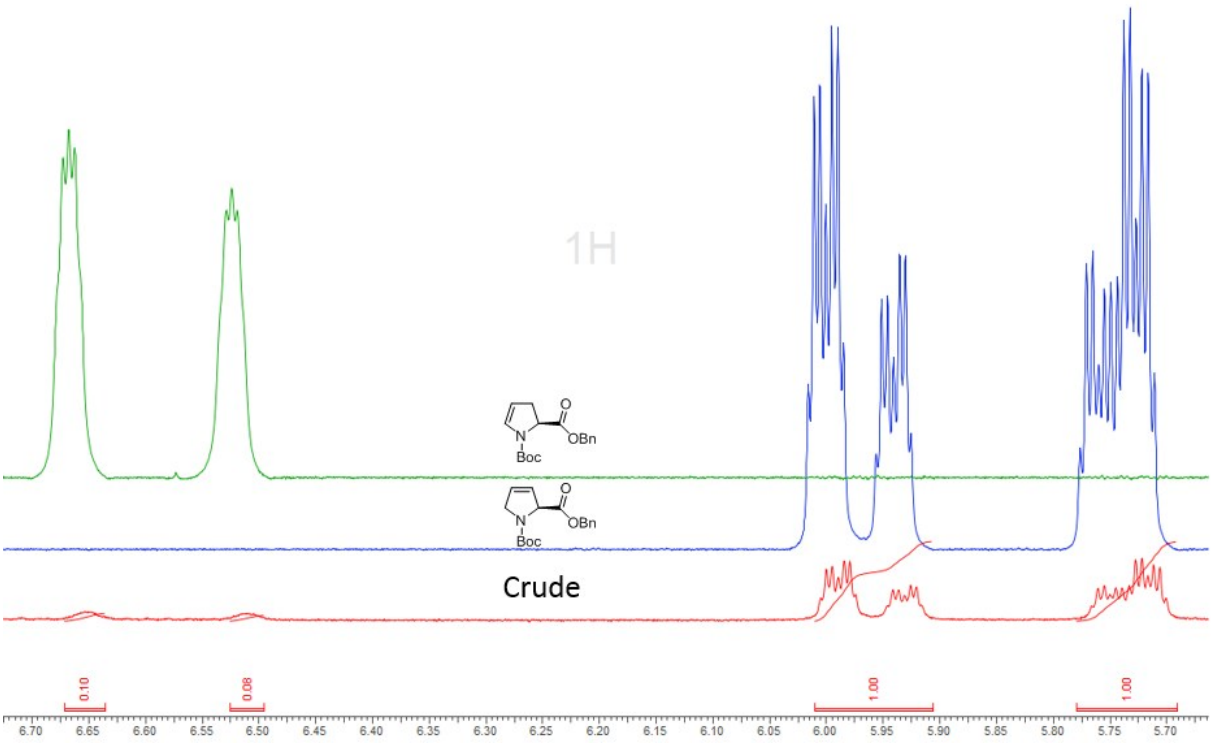

1.1.3 Verification of the 3,4-dehydroproline enantiopurity

Enantiopure N-Boc-(4*R*)-hydroxyproline is used as a starting material so the absolute configuration is known. In the course of the elimination reaction, there si the potential tfor epimerisation of the 3,4-dehydroproline product. For example, this is the case when 3,4-dehydroproline was synthesised via a mesylate elimination using DBU as base. In our hands, a 25% loss of enantiopurity was observed in this case, as determined chiral HPLC. In contrast, the Grieco elimination procedure proceeds without loss of enantiopurity, as shown below.

Chiral HPLC analyses were performed on an Agilent 1120 Compact LC, equipped with an autosampler, a VMD UV detector and a porous silica guard column. A Chiralcel OD-H column, coated with Cellulose tris (3,5-dimethylphenylcarbamate) on 5 µm silica-gel (4.6 x 250 mm internal diameter) was used for chiral analysis. The samples were run isocratically with 2.5% isopropanol in hexane with an elution volume of 0.5 mL/min. Detection was done at 250nm.

Mesylate elimination

Area % Report

Data File: C:\EZChrom Elite\Enterprise\Projects\Default\Data\GJH\240318\GJH-7985-46 (2)_2.dat
Method: C:\EZChrom Elite\Enterprise\Projects\Default\Method\untitled.met
Acquired: 24/03/2018 14:32:08
Printed: 24/03/2018 16:10:21

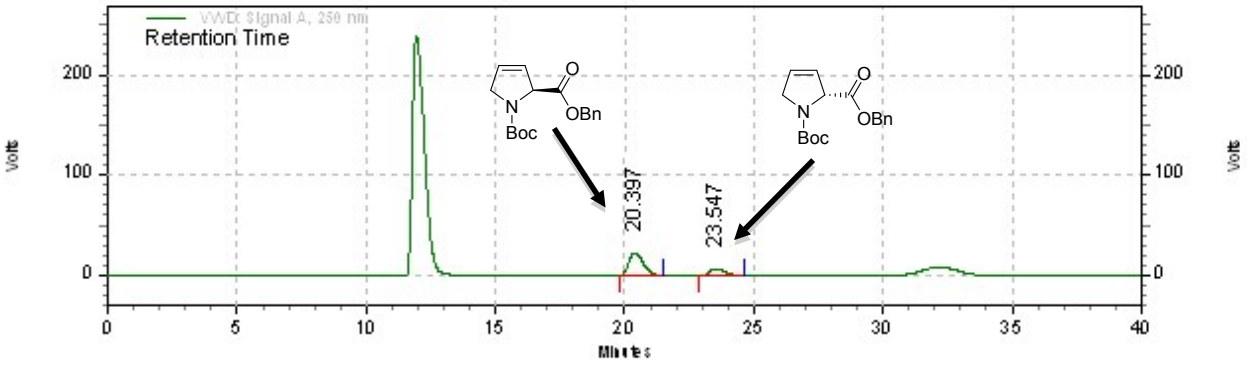

VWD: Signal A, 250 nm Results

Retention Time	Area	Area %	Height	Height %
20.397	14662521	75.20	372192	75.85
23.547	4834695	24.80	118518	24.15
Totals	19497216	100.00	490710	100.00

Grieco elimination

Page 1 of 1

Area % Report

Data File: C:\EZChrom Elite\Enterprise\Projects\Default\Data\GJH\240318\GJH-8254-64_1.dat
Method: C:\EZChrom Elite\Enterprise\Projects\Default\Method\GJH\ODH-0.5ML-2.5IPA_250NM.met
Acquired: 24/03/2018 15:14:18
Printed: 24/03/2018 16:04:50

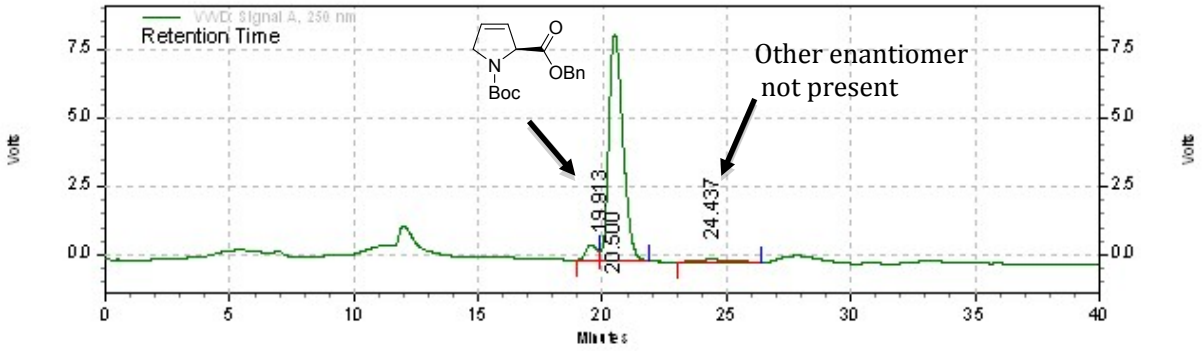

VWD: Signal A, 250 nm Results

Retention Time	Area	Area %	Height	Height %
19.913	306156	5.10	5135	3.53
20.500	5471260	91.21	138554	95.15
24.437	221062	3.69	1929	1.32
Totals	5998478	100.00	145618	100.00

1.1.4 (2S,3R,4S)-N-t-Butyloxycarbonyl-3,4-dihydroxyproline benzyl ester **10**.

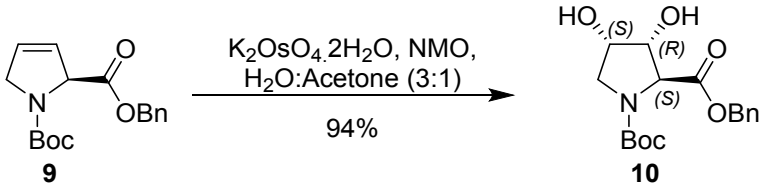

9 **10**

To a solution of **9** (5.95 g, 19.6 mmol) in acetone (45.0 mL) and water (15.0 mL), NMO (5.75 g, 49.1 mmol) and $K_2OsO_4.2H_2O$ (50.0 mg, 0.136 mmol) were added. After 2.5 d at rt, the mixture was quenched with a saturated aqueous solution of $Na_2S_2O_3$ (20 mL) and stirred for 1 h. The aqueous layer was extracted with EtOAc (4×50 mL). The organic phases were washed with brine (50 mL), dried over $MgSO_4$ and evaporated *in vacuo*. Purification by flash chromatography (hexane/acetone 70:30) yielded diol **10** as a clear oil (6.21 g, 94%). **$[\alpha]_D$** -12 (c 1.4, $CHCl_3$, 22 °C); **Rf** 0.25 (hexane/acetone 70:30); **^{1}H NMR** (400 MHz, $CDCl_3$): (63:37 rotamer ratio) δ 7.41–7.29 (m, $5H_{(M)}$+$5H_{(m)}$, Ph), 5.27 (d, *J*=12.4 Hz, 1H, CHH'-$Ph_{(m)}$), 5.20 (d, *J*=12.5 Hz, 1H, CHH'-$Ph_{(M)}$), 5.16 (d, *J*=12.5 Hz, 1H,

major CHH'-Ph), 5.11 (d, *J*=12.5 Hz, 1H, CHH'-$Ph_{(m)}$), 4.44–4.12 (m, 2H, $C_\alpha H_{(M+m)}$ + 2H, $C_\beta H_{(M+m)}$ + 2H, $C_\gamma H_{(M+m)}$), 3.72–3.13 (m, 4H, $C_\delta H_{2(M+m)}$ + 2H, $C_\beta OH_{(M+m)}$ + 2H, $C_\gamma OH_{(M+m)}$), 1.44 (s, 9H, $CO_2C(CH_3)_{3(m)}$), 1.31 (s, 9H, $CO_2C(CH_3)_{3(M)}$) ppm (no assignment possible of C_γ, C_β and C_α); **^{13}C NMR** (100 MHz, $CDCl_3$): δ 171.4 ($CO_{2(M)}$), 171.1 ($CO_{2(m)}$), 154.5 ($CO_2C(CH_3)_{3(m)}$), 154.0 (major $CO_2C(CH_3)_3$), 135.4 ($C_{Ph(m)}$), 135.2 ($C_{Ph(M)}$), 128.6–128.1 ($CH_{Ph(M+m)}$), 80.8 (major $CO_2C(CH_3)_3$), 80.7 ($CO_2C(CH_3)_{3(m)}$), 75.7 (M), 74.6 (m), 70.5 (m), 69.8 (M), 67.2 ($CH_2Ph_{(m)}$), 67.1 ($CH_2Ph_{(M)}$), 64.8 (major), 64.7 (m), 50.9 ($C_{\delta(m)}$), 50.6 (major C_δ), 28.3 ($CO_2C(CH_3)_{3(m)}$), 28.1 (major $CO_2C(CH_3)_3$) ppm; **IR** 3412 (br. m), 1745 (s), 1677 (s), 1411 (s), 1172 (s) cm^{-1}; **MS** (ESI)(*m/z*): 338.4 $(M+H)^+$, 360.4 $(M+Na)^+$; **HRMS** (ESI) for $C_{17}H_{23}NNaO_6$ $[M+Na]^+$ Calcd. 360.1418; Found 360.1423.

This compound is reported in the patent literature without characterisation data.[1]

Note: While this manuscript was in preparation, Geyer et al also described the diastereoselective dihydroxylation with potassium osmate.[3]

1.1.5 (2*R*,3*S*,4*R*)-*N*-*t*-Butyloxycarbonyl-3,4-difluoroproline benzyl ester **11**.

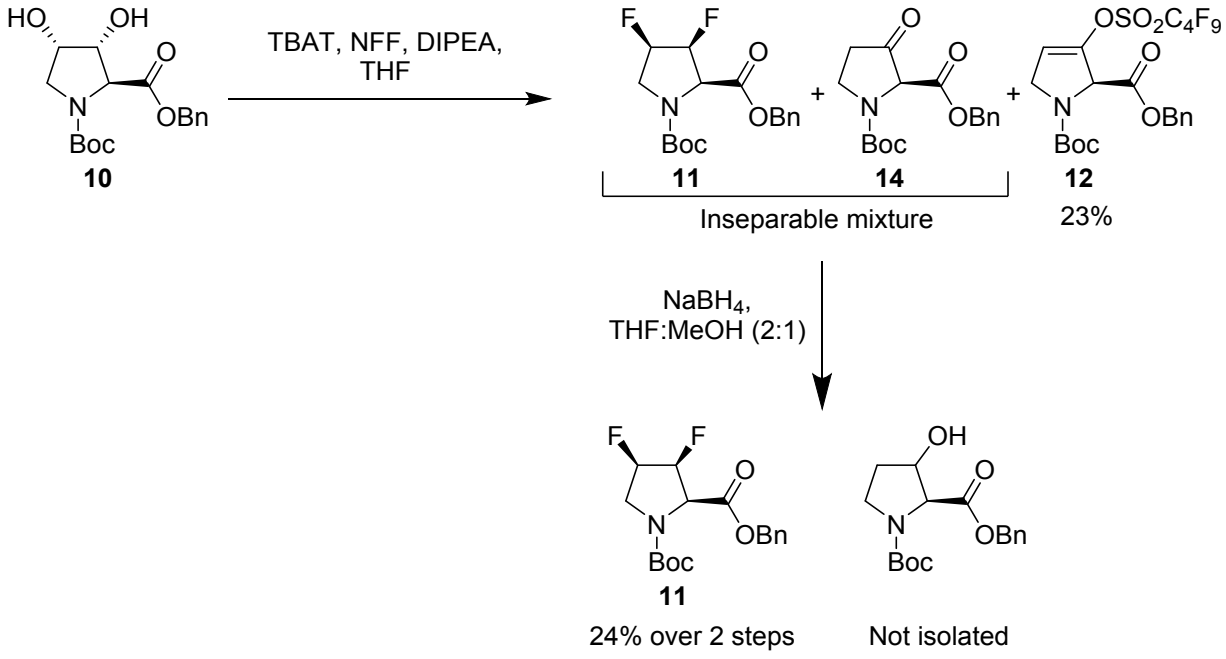

To a solution of **10** (4.30 g, 12.8 mmol) in THF (50.0 mL); tetrabutylammonium difluorotriphenylsilicate (6.88 g, 12.8 mmol), DIPEA (6.66 mL, 38.25 mmol) and nonafluorobutanesulfonyl fluoride (6.87 mL, 38.25 mmol) were added. After 22 h, the solvent was removed *in vacuo* and the mixture was purified by flash chromatography (hexane/acetone 80:20) to yield enol sulfonate **12** (1.77 g, 23%) as a clear oil and an inseparable mixture of difluoroproline **11** and ketone **14**. While separation was possible by HPLC, it was considerably facilitated by reducing the ketone impurity to the corresponding

alcohol. Therefore, the mixture was dissolved in methanol (7.0 mL) and THF (14.0 mL) and cooled to 0 °C. $NaBH_4$ (38.6 mg, 1.020 mmol) was added in one portion and stirring at 0 °C was continued for 10 minutes. Next, the mixture was poured in water (20 mL) and extracted with EtOAc (3 × 20 mL). The combined organic phases were dried over $MgSO_4$ and evaporated *in vacuo*. Purification by flash chromatography (hexane/EtOAc 80:20) yielded difluoroproline **11** (1.022 g, 24%) as a clear oil. **$[\alpha]_D$** -31 (c 1.1, $CHCl_3$, 22 °C); **Rf** 0.54 (hexane/acetone 70:30); **^{1}H NMR** (400 MHz, $CDCl_3$): (60:40 rotamer ratio) δ 7.42–7.29 (m, $5H_{(M)}$+$5H_{(m)}$, Ph), 5.37–4.92 (m, 4H $CH_2Ph_{(M+m)}$ + 2H $C_\gamma H_{(M+m)}$ + 2H $C_\beta H_{(M+m)}$), 4.67 (dd, *J*=18.1, 6.0 Hz, 1H, $C_\alpha H_{(m)}$), 4.57 (dd, *J*=16.9, 6.2 Hz, 1H, $C_\alpha H_{(M)}$), 3.98-3.68 (m, 4H $C_\delta H_{2(M+m)}$), 1.47 (s, 9H, $CO_2C(C\underline{H}_3)_{3(m)}$), 1.33 (s, 9H, $CO_2C(C\underline{H}_3)_{3(M)}$) ppm; **^{13}C NMR** (100 MHz, $CDCl_3$): δ 166.7 (d, *J*=5.1 Hz, $\underline{C}O_{2(M)}$), 166.3 (d, *J*=6.6 Hz, $\underline{C}O_{2(m)}$), 153.7 ($\underline{C}O_2C(CH_3)_{3(m)}$), 153.1 ($\underline{C}O_2C(CH_3)_{3(M)}$), 135.3 ($\underline{C}_{Ph(m)}$), 135.2 ($\underline{C}_{Ph(M)}$), 128.6–128.2 ($\underline{C}H_{Ph(M+m)}$), 89.0 (dd, *J*=209.1, 14.7 Hz, $C_{\beta(M)}$), 88.4 (dd, *J*=197.3, 15.4 Hz, $C_{\beta(m)}$), 87.5 (dd, *J*=195.9, 16.1 Hz, $C_{\gamma(m)}$), 87.1 (dd, *J*=207.6, 15.4 Hz, $C_{\gamma(M)}$), 81.3 ($CO_2\underline{C}(CH_3)_{(M+m)}$), 67.4 ($\underline{C}H_2Ph_{(M+m)}$), 60.5 (d, *J*=21.3 Hz, $C_{\alpha(M)}$), 60.1 (d, *J*=22.0 Hz, $C_{\alpha(m)}$), 47.8 (br dd, *J*=25.7, 1.7 Hz, $C_{\delta(m)}$), 47.4 (br dd, *J*=25.7, 1.5 Hz, $C_{\delta(M)}$), 28.2 ($CO_2C(\underline{C}H_3)_{3(m)}$), 28.0 ($CO_2C(\underline{C}H_3)_{3(M)}$) ppm; **^{19}F NMR** (376 MHz, $CDCl_3$): (60:40 rotamer ratio) δ -204.9– -205.4 (m, $2F_{(M+m)}$), -208.1 (br dt, *J*=51.6, 15.0 Hz, $F'_{(M)}$), -208.6 (dtd, *J*=52.0, 15.0, 3.5 Hz, $F'_{(m)}$) ppm; **^{19}F {^{1}H} NMR** (376 MHz, $CDCl_3$): (60:40 rotamer ratio) δ -205.1 (d, *J*=5.2 Hz, $F_{(M)}$), -205.2 (d, *J*=5.2 Hz, $F_{(m)}$), -208.1 (d, *J*=5.2 Hz, $F'_{(M)}$), -208.6 (d, *J*=5.2 Hz, $F'_{(m)}$) ppm; **IR** 2978 (w), 1759 (m), 1702 (s) cm^{-1}; **MS** (ESI)(*m/z*): 364.2 $(M+Na)^+$; **HRMS** (ESI) for $C_{17}H_{21}F_2NNaO_4$ $[M+Na]^+$ Calcd. 364.1331; Found 364.1338.

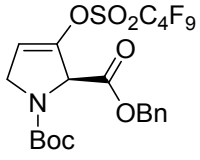

12

Data for enol sulfonate **12**: **$[\alpha]_D$** -42 (c 0.85, $CHCl_3$, 22 °C); **Rf** 0.29 (hexane/acetone 90:10); **^{1}H NMR** (500 MHz, $CDCl_3$): (65:35 rotamer ratio) δ 7.40–7.30 (m, $5H_{(M)}$+$5H_{(m)}$, Ph), 5.95 (app q, *J*=2.1 Hz, 1H, $C_\gamma H_{(M)}$), 5.89 (app q, *J*=2.0 Hz, 1H, $C_\gamma H_{(m)}$), 5.30 (d, *J*=12.4 Hz, 1H, $C\underline{H}H'$-$Ph_{(m)}$), 5.24 (d, *J*=12.1 Hz, 1H, $C\underline{H}H'$-$Ph_{(M)}$), 5.19 (d, *J*=12.1 Hz, 1H, $CH\underline{H}'$-$Ph_{(M)}$), 5.18 (d, *J*=12.4 Hz, 1H, $CH\underline{H}'$-$Ph_{(m)}$), 5.09 (ddd, *J*=6.4, 2.5, 1.8 Hz, 1H, $C_\alpha H_{(m)}$), 5.00 (ddd, *J*=6.4, 2.6, 1.8 Hz, 1H, $C_\alpha H_{(M)}$), 4.37-4.20 (m, 4H $C_\delta H_{2(M+m)}$), 1.48 (s, 9H, $CO_2C(C\underline{H}_3)_{3(m)}$), 1.34 (s, 9H, $CO_2C(C\underline{H}_3)_{3(M)}$) ppm; **^{13}C NMR** (100 MHz, $CDCl_3$): δ 167.6 ($\underline{C}O_{2(M)}$), 167.4 ($\underline{C}O_{2(m)}$), 153.0 ($\underline{C}O_2C(CH_3)_{3(m)}$), 152.6 ($\underline{C}O_2C(CH_3)_{3(M)}$), 141.0 ($C_{\beta(m)}$), 140.6 ($C_{\beta(M)}$), 135.0 ($\underline{C}_{Ph(m)}$), 134.8 ($\underline{C}_{Ph(M)}$), 128.7–128.2 ($\underline{C}H_{Ph(M+m)}$), 115.8 ($C_{\gamma(M)}$),

115.6 ($C_{\gamma(m)}$), 81.4 ($CO_2\underline{C}(CH_3)_{(M)}$), 81.3 ($CO_2\underline{C}(CH_3)_{(m)}$), 67.89 ($\underline{C}H_2Ph_{(M)}$), 67.85 ($\underline{C}H_2Ph_{(m)}$), 63.7 ($C_{\alpha(M)}$), 63.4 ($C_{\alpha(m)}$), 50.1 ($C_{\delta(m)}$), 49.7 ($C_{\delta(M)}$), 28.2 ($CO_2C(\underline{C}H_3)_{3(m)}$), 28.0 ($CO_2C(\underline{C}H_3)_{3(M)}$) ppm; **^{19}F NMR** (376 MHz, $CDCl_3$): δ -80.9 (m, 3F), -109.0 (br s, 2F), -121.2 (br s, 2F), -126.1 (br s, 2F) ppm; **^{19}F {^{1}H} NMR** (376 MHz, $CDCl_3$): δ -80.9 (m, 3F), -109.0 (br s, 2F), -121.2 (br s, 2F), -126.1 (br s, 2F) ppm; **IR** 2978 (w), 1757 (m), 1712 (s), 1395 (s), 1237 (s), 1200 (s), 1144 (s), 1114 (s) cm^{-1}; **MS** (ESI)(*m/z*): 602.1 $(M+H)^+$; 624.3 $(M+Na)^+$; **HRMS** (ESI) for $C_{21}H_{20}F_9NNaO_7S$ $[M+Na]^+$ Calcd. 624.0709; Found 624.0702.

1.1.6 (2*R*,3*S*,4*R*)-N-t-Butyloxycarbonyl-3,4-difluoroproline **13**.

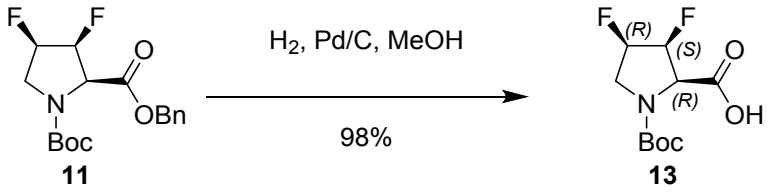

To a solution of **11** (180.9 mg, 0.530 mmol) in methanol (4.0 mL), 10 % Pd/C (25.6 mg) was added. The mixture was purged with one balloon volume of hydrogen gas. Subsequently, the mixture was kept under hydrogen atmosphere and stirred at room temperature. After 22 h, the mixture was filtered over a plug of celite and the solvent evaporated. **13** (130.4 mg, 98%) was obtained as an off-white solid and used as such in the next reaction.

1.1.7 *Rac*-(2*R*,3*S*,4*R*)-N-Acetyl-3,4-difluoroproline methyl ester **7.**

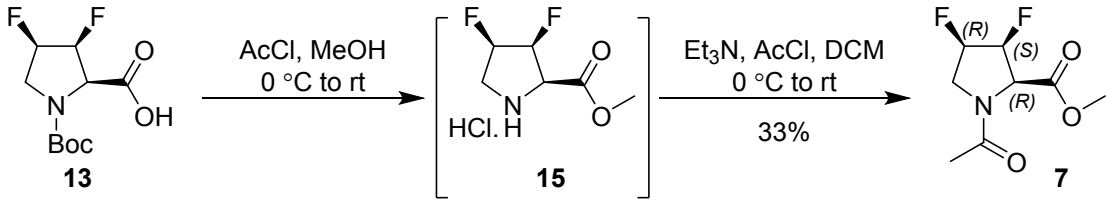

Racemic carboxylic acid **13** (112.9 mg, 0.449 mmol) was dissolved in methanol (2.0 mL) and cooled to 0 °C. Acetyl chloride (0.160 mL, 2.247 mmol) was added dropwise and stirring at 0 °C was continued. After 40 minutes, the mixture was allowed to warm to room temperature. After another 22 h, the mixture was concentrated by rotary evaporation to yield **15**. This product was then redissolved in DCM (2.0 mL) and cooled to 0 °C. Subsequently, triethylamine (0.150 mL, 1.078 mmol) was added and the solution was stirred for 30 minutes. Next, acetyl chloride (0.096 mL, 1.347 mmol) was added dropwise and the solution was allowed to warm to rt. After stirring for 21 hours, the mixture was poured into water (10 mL) and the aqueous layer was extracted with DCM (3 x 15 mL). The combined organic layers were dried over $MgSO_4$ and evaporated *in vacuo*. The crude product was purified by HPLC (hexane/acetone 50:50) to yield **7** (30.6 mg, 33%) as a

clear oil. **Rf** 0.56 (hexane/acetone 50:50); **^{1}H NMR** (400 MHz, $CDCl_3$): (78:22 rotamer ratio) δ 5.37–5.17 (m, 2H $C_{\beta}H_{(M+m)}$), 5.17–4.99 (m, 2H $C_{\gamma}H_{(M+m)}$), 4.73 (dd, *J*=20.3, 5.8 Hz, 1H, $C_{\alpha}H_{(M)}$), 4.57 (dd, *J*=11.0, 7.1 Hz, 1H, $C_{\alpha}H_{(m)}$), 4.08–3.75 (m, 4H $C_{\delta}H_{2(M+m)}$), 3.84 (s, 3H, $CO_2C\underline{H}_{3(m)}$), 3.79 (s, 3H, $CO_2C\underline{H}_{3(M)}$), 2.12 (s, 3H, $NCOC\underline{H}_{3(M)}$), 1.95 (s, 3H, $NCOC\underline{H}_{3(m)}$) ppm; **^{13}C NMR** (100 MHz, $CDCl_3$): δ 170.0 ($N\underline{C}OCH_{3(m)}$), 169.6 ($N\underline{C}OCH_{3(M)}$), 167.2(d, *J*=3.7 Hz, $\underline{C}O_2CH_{3\ (m)}$), 166.1 (d, *J*=6.6 Hz, $\underline{C}O_2CH_{3\ (M)}$), 89.1 (dd, *J*=204.7, 14.7 Hz, $C_{\beta(m)}$), 87.9 (dd, *J*=197.3, 14.7 Hz, $C_{\beta(M)}$), 87.3 (dd, *J*=198.8, 16.9 Hz, $C_{\gamma(M)}$), 86.8 (dd, *J*=192.2, 16.1 Hz, $C_{\gamma(m)}$), 60.5 (br d, *J*=22.0 Hz, $C_{\alpha(m)}$), 59.9 (dd, *J*=22.6, 1.5 Hz, $C_{\alpha(M)}$), 53.1 (s, $CO_2\underline{C}H_{3\ (m)}$), 52.7 (s, $CO_2\underline{C}H_{3\ (M)}$), 48.6 (br dd, *J*=26.4, 2.2 Hz, $C_{\delta(M)}$), 47.9 (br dd, *J*=24.6, 1.8 Hz, $C_{\delta(m)}$), 21.8 ($NCO\underline{C}H_{3\ (M)}$), 21.6 ($NCO\underline{C}H_{3\ (m)}$) ppm; **^{19}F NMR** (376 MHz, $CDCl_3$): (80:20 rotamer ratio) δ -202.5– -202.9 (m, $F_{(m)}$), -205.7– -206.0 (m, $F'_{(M)}$), -207.2– -207.5 (m, $F'_{(m)}$), -208.9– -209.2 (m, $F_{(M)}$), ppm; **^{19}F {^{1}H} NMR** (376 MHz, $CDCl_3$): (79:21 rotamer ratio) δ -202.6 (d, *J*=5.2 Hz, $F_{(m)}$), -205.7 (d, *J*=3.5 Hz, $F'_{(M)}$), -207.2 (d, *J*=5.2 Hz, $F'_{(m)}$), -208.9 (d, *J*=5.2 Hz, $F_{(M)}$) ppm; **IR** 1753 (s), 1653 (s), 1416 (s), 1202 (s) cm^{-1}; **MS** (ESI)(*m/z*): 208.3 $(M+H)^+$, 230.2 $(M+Na)^+$; **HRMS** (ESI) for $C_8H_{11}F_2NNaO_3$ $[M+Na]^+$ Calcd. 230.0599; Found 230.0594.

2 NMR experimental

2.1 general

For the conformational an kinetic analysis, all NMR measurements were performed on a Bruker Avance II spectrometer operating at a ^{1}H frequency of 500.13 MHz and equipped with a ^{1}H-^{13}C-^{19}F TXO probe with z-gradients. Quantitative 1D ^{1}H and 1D ^{19}F spectra with ^{1}H decoupling were measured with respectively an interscan delay of 21.6 s and 17.3 s, 65536 and 65536 time domain points and 10 ppm and 30 ppm spectral widths. To assign the rotamers of **7**, a ^{1}H-^{1}H NOESY spectrum with spectral width of 10 ppm, 2048 total time domain points in the direct dimension and 512 total time domain points in the indirect dimension was obtained. For compound **3**, 2D ^{19}F-^{19}F EXSY spectra were acquired with ^{1}H decoupling in both F_1 and F_2, with an interscan delay of 15.4 s, a spectral width of 5 ppm, 2048 total time domain points in the direct dimension and 256 total time domain points in the indirect dimension. For compounds **5** and **7**, 2D ^{1}H-^{1}H EXSY spectra were acquired with an interscan delay of 15.2 s, a spectral width of 10 ppm in F_2 and 1 ppm in F_1, 2048 total time domain points in the direct dimension and 256 total time domain points in the indirect dimension. All EXSY spectra were obtained at 35°C. For all EXSY spectra, time-domain weighting using a squared cosine bell function was applied, followed by zero-filling so that a 2048×2048 real data matrix was obtained.

To extract kinetic rate constants from an EXSY spectrum, diagonal peaks were integrated of the ^{19}F signal (compound **3**) or the acetyl CH_3 group (for **5** and **7**) of both rotamers, as well the cross-peaks between these signals. The $k_{cis\text{-}trans}$ and $k_{trans\text{-}cis}$ values were calculated using the same procedure as Renner *et al.*:[4]

$$k_{cis-trans} = \frac{\left(\frac{I_{ct}}{I_{cc}} + \frac{I_{tc}}{I_{tt}} K_{trans-cis}\right)}{2\tau_m}$$

$$k_{trans-cis} = \frac{\left(\frac{I_{ct}}{I_{cc} K_{trans-cis}} + \frac{I_{tc}}{I_{tt}}\right)}{2\tau_m}$$

With I_{tt} and I_{cc} denoting the diagonal peaks of the *trans* and *cis* forms respectively, I_{tc} the cross-peak at the F_1 frequency of the *trans* form and F_2 frequency of the *cis* form, I_{ct} the cross-peak at the F_1 frequency of the *cis* form and F_2 frequency of the *trans* form, $K_{trans\text{-}cis}$ the *trans*-to-*cis* ratio obtained at 35°C, and τ_m the mixing time. Three mixing times were measured for each compound: 0.5 s, 0.75 s and 1.0 s. The average of the obtained $k_{cis\text{-}trans}$ and $k_{trans\text{-}cis}$ values was taken, and the 95% error bars were calculated as the standard deviation multiplied by 1.96.

2.2 Spectra of the Ac-F-Pro-OMe model compounds

2.2.1 1D ^{1}H spectrum of Ac-Pro-OMe in D_2O, 298 K, 500 MHz.

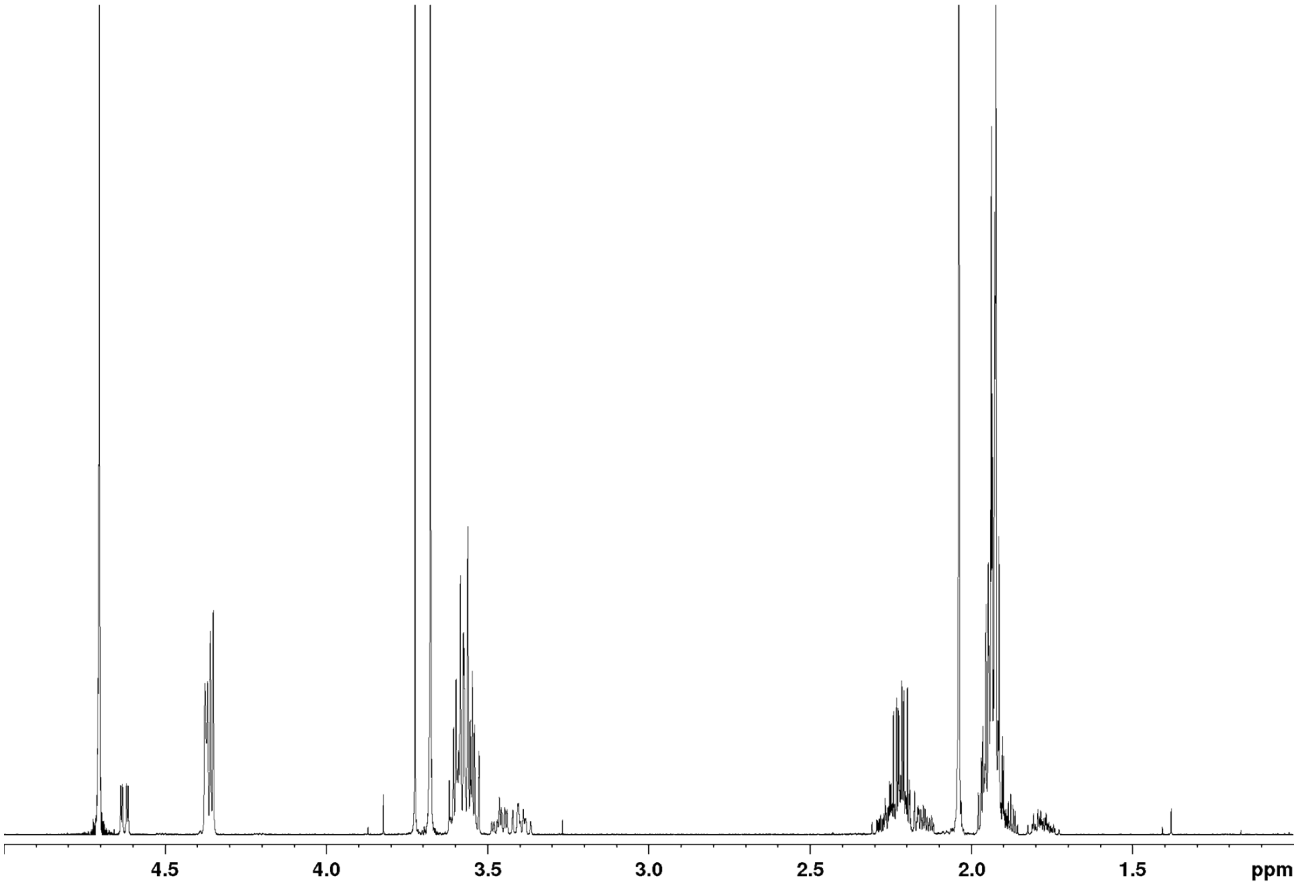

2.2.2 1D ^{1}H spectrum Ac-Pro-OMe in $CDCl_3$, 298 K, 500 MHz.

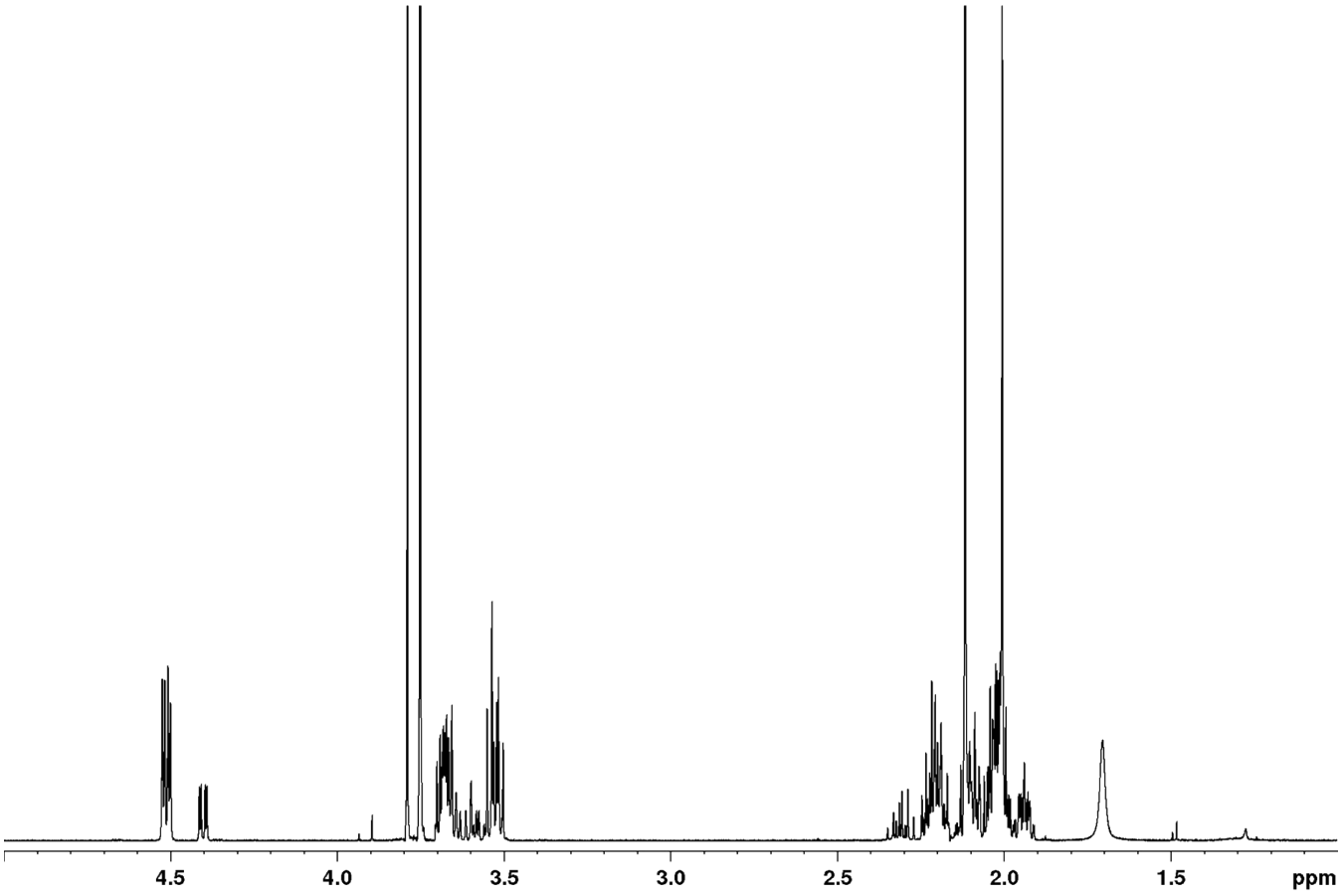

2.2.3 1D ^{1}H spectrum of Ac-(4R)-FPro-OMe **1** in D_2O, 298 K, 500 MHz.

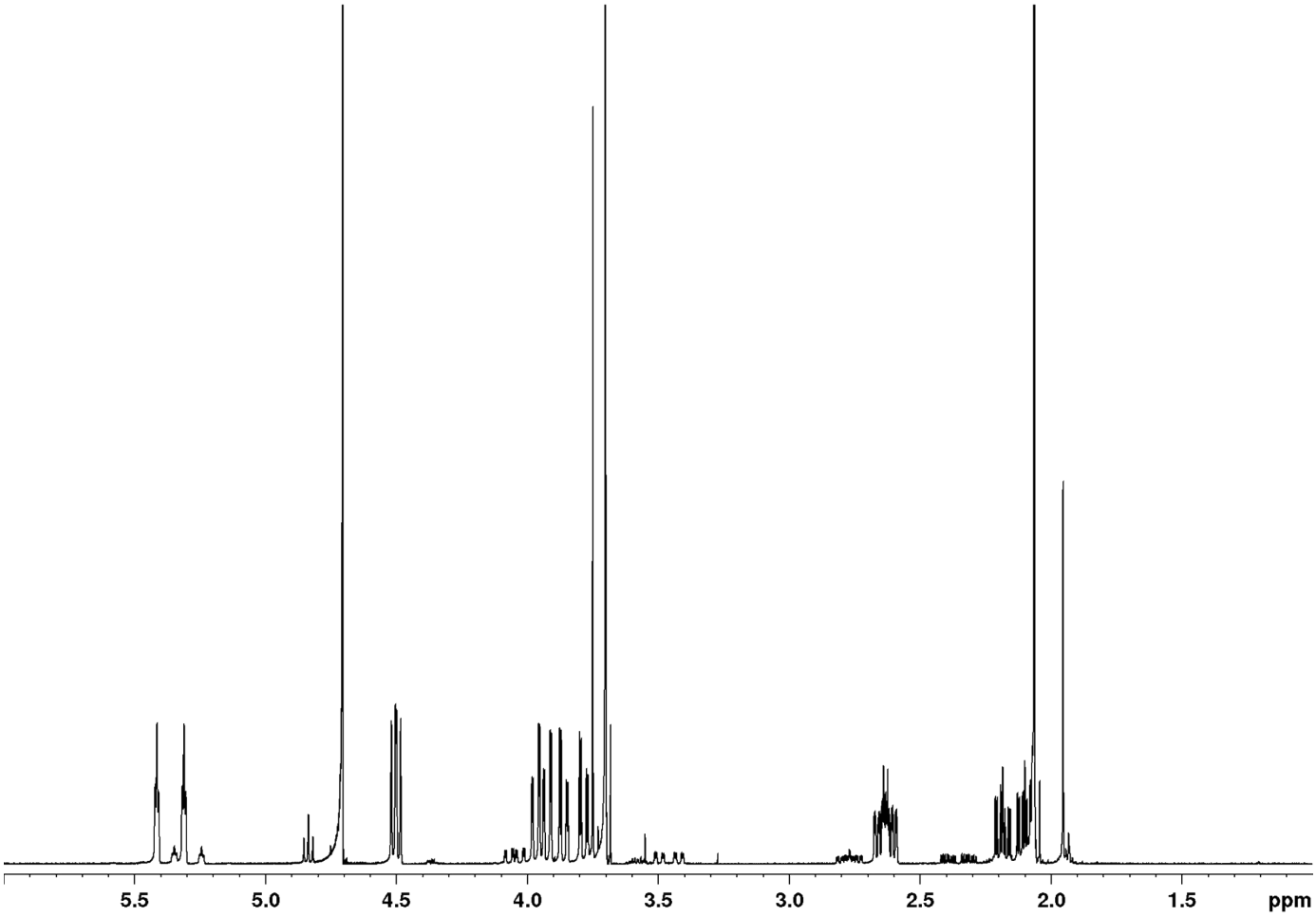

2.2.4 1D ^{1}H decoupled ^{19}F spectrum of Ac-(4R)-FPro-OMe **1** in D_2O, 298 K, 500 MHz.

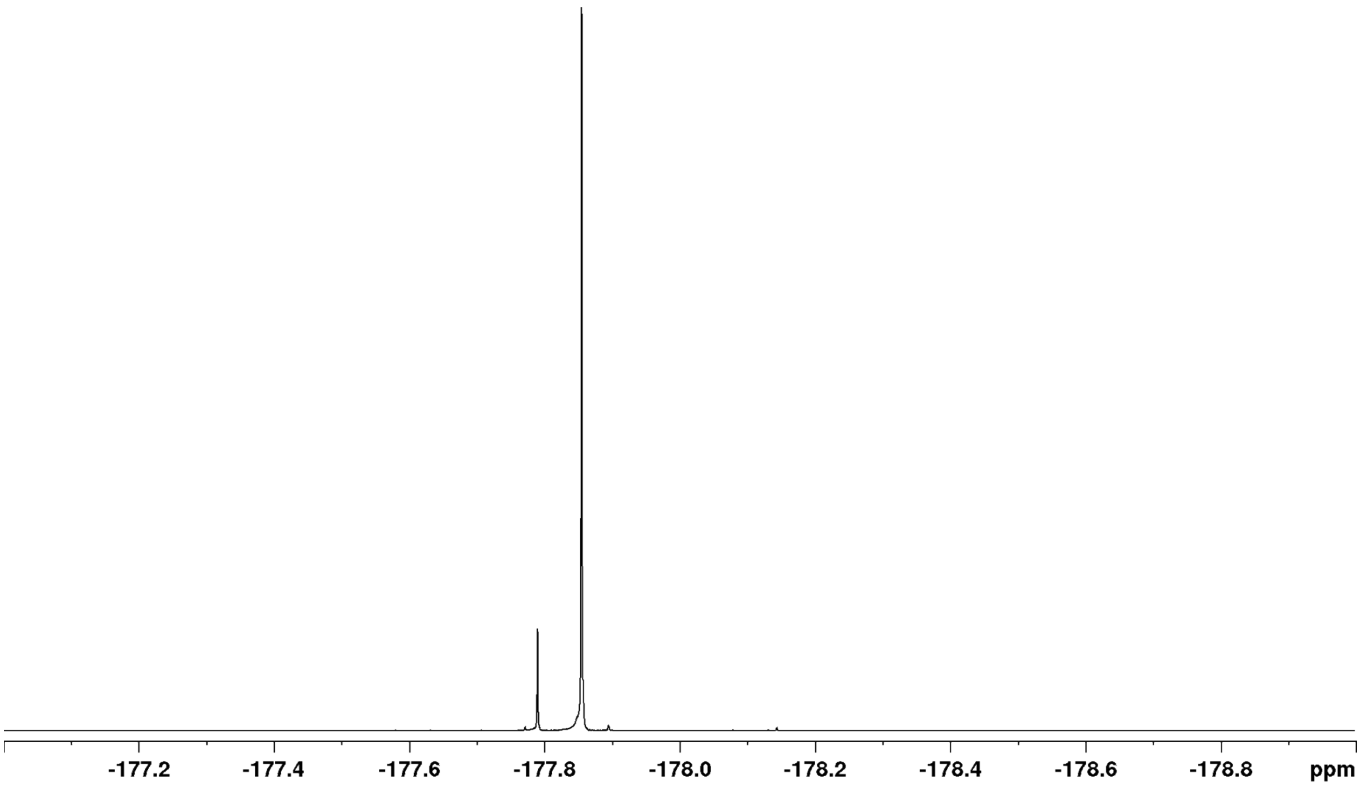

2.2.5 1D ^{1}H spectrum of Ac-(4R)-FPro-OMe **1** in $CDCl_3$, 298 K, 500 MHz

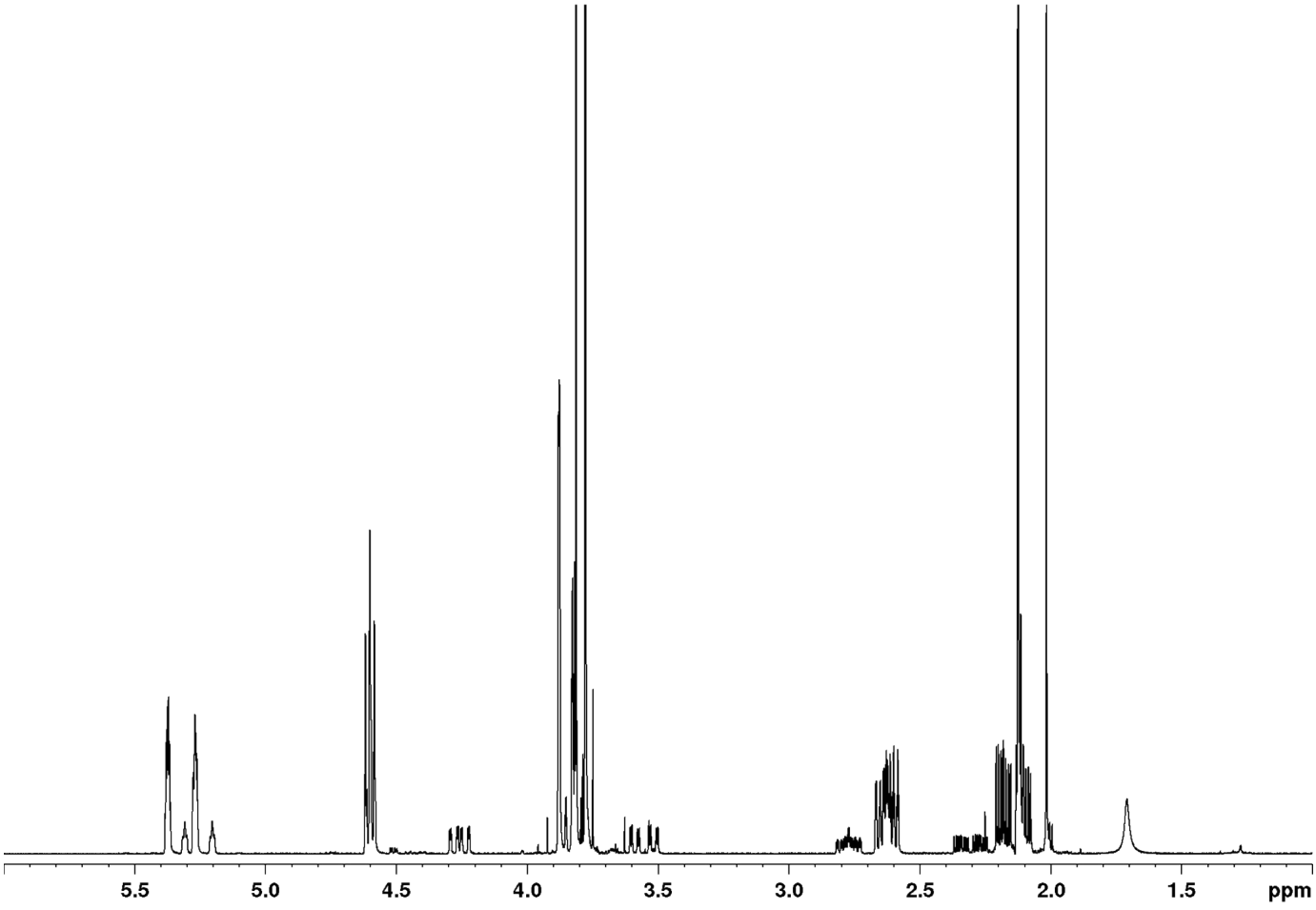

2.2.6 ^{1}H decoupled ^{19}F spectrum of Ac-(4R)-FPro-OMe **1** in $CDCl_3$, 298 K, 500 MHz

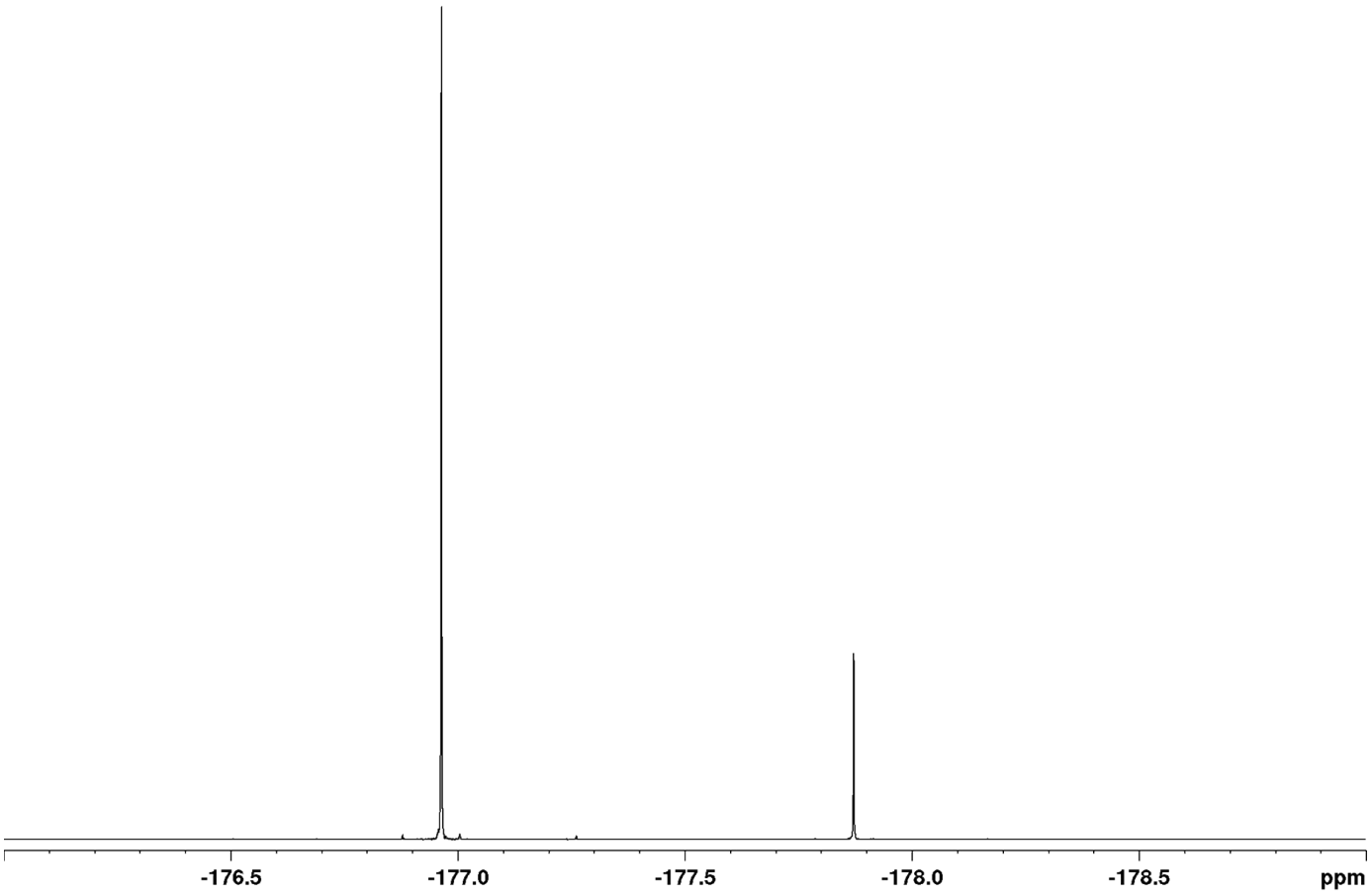

2.2.7 ^{1}H spectrum of Ac-(4S)-FPro-OMe **2** in D_2O, 298 K, 500 MHz

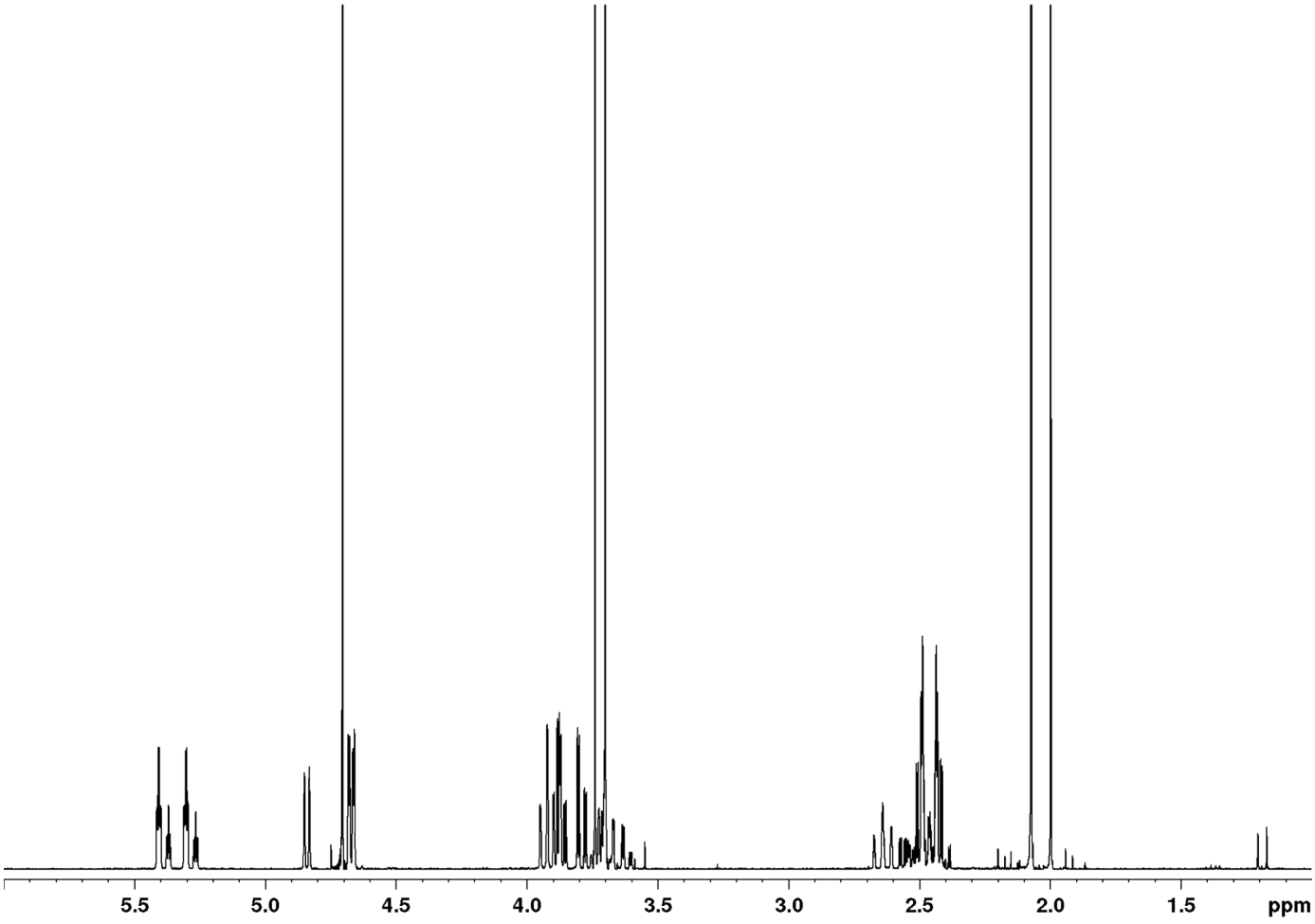

2.2.8 1D ^{1}H decoupled ^{19}F spectrum of Ac-(4S)-FPro-OMe **2** in D_2O, 298 K, 500 MHz

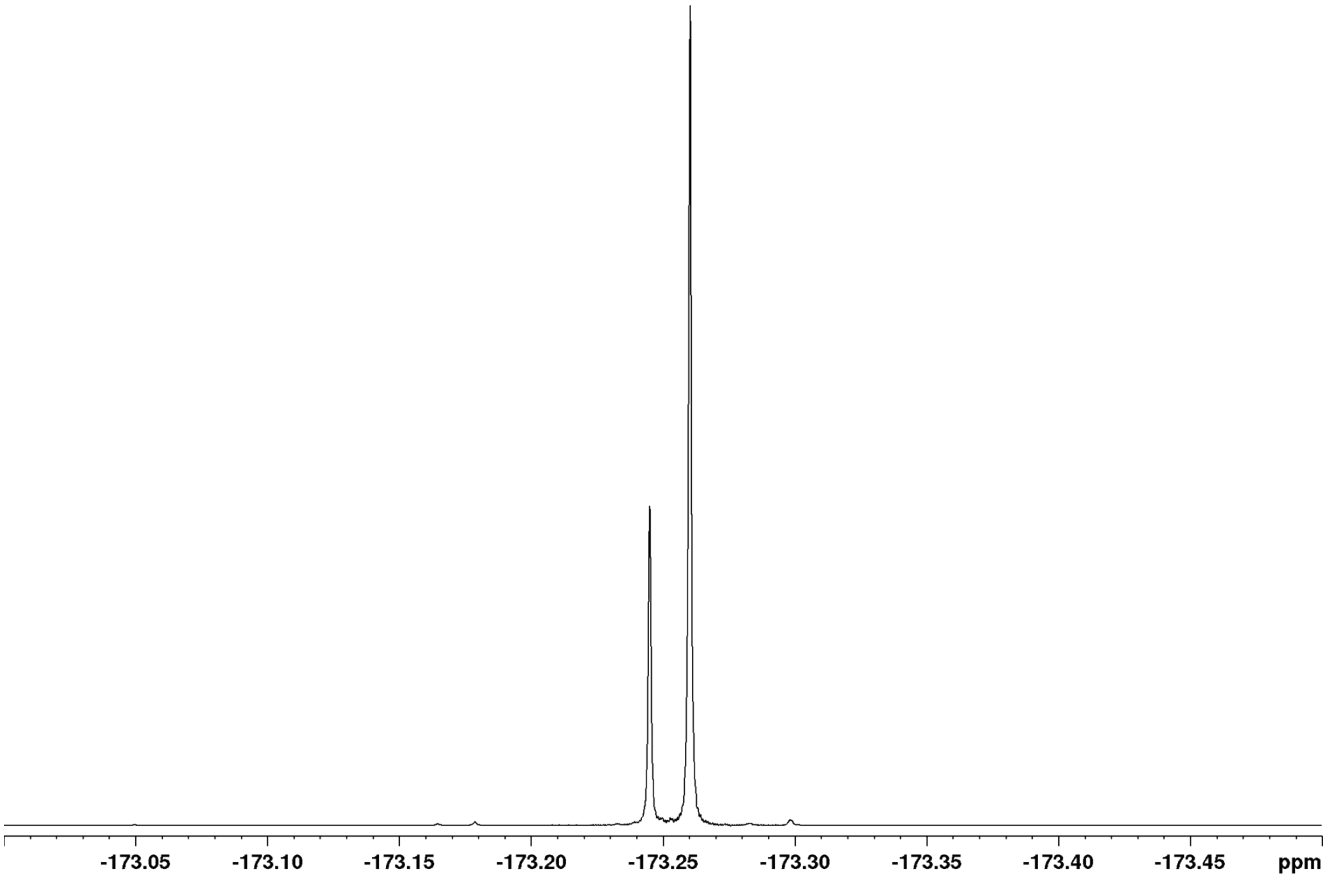

2.2.9 ^{1}H spectrum of Ac-(4S)-FPro-OMe **2** in $CDCl_3$, 298 K, 500 MHz.

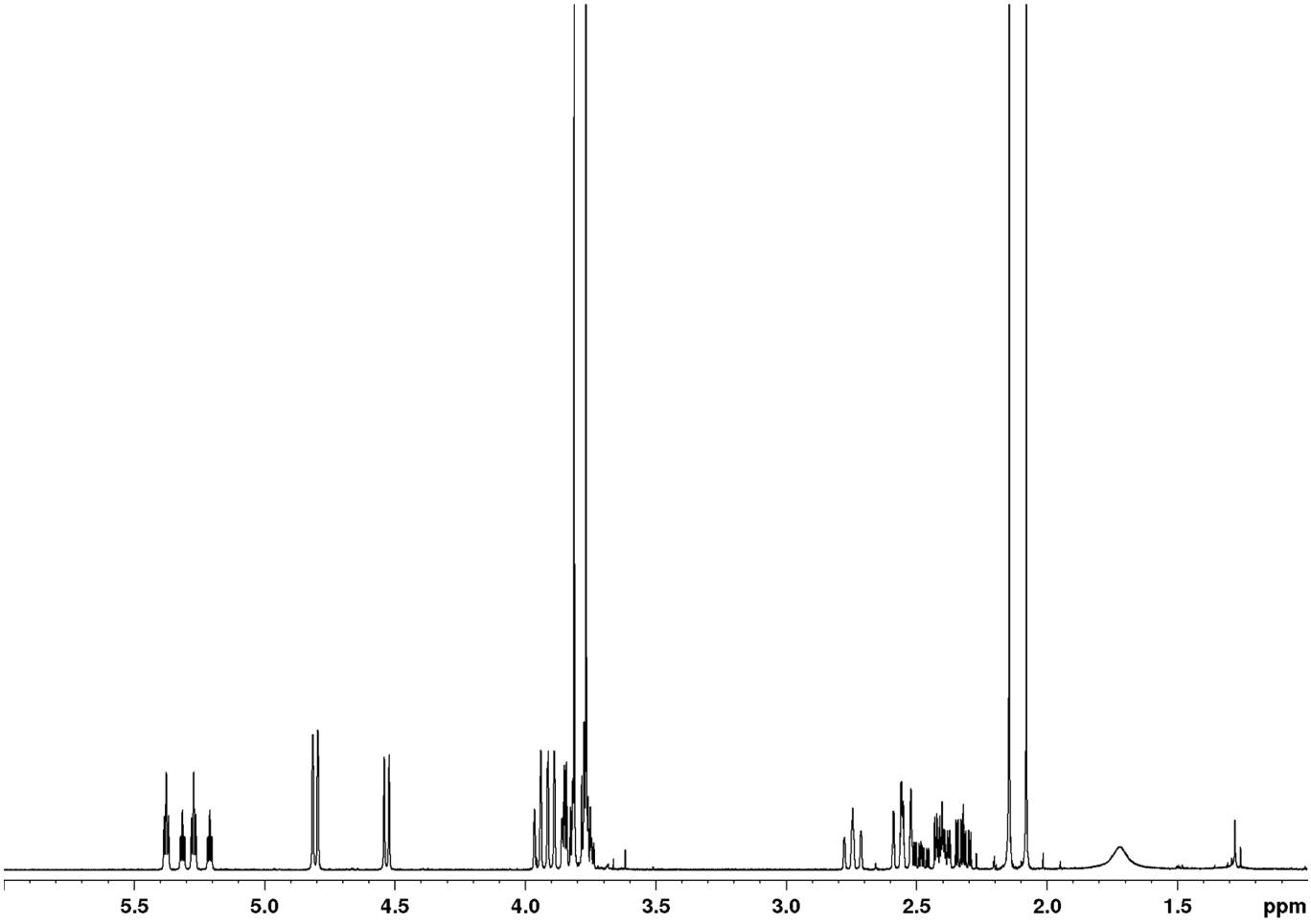

2.2.10 ^{1}H decoupled ^{19}F spectrum of Ac-(4S)-FPro-OMe **2** in $CDCl_3$, 298 K, 500 MHz

2.2.11 1D ^{1}H spectrum of Ac-(3R)-FPro-OMe **3** in D_2O, 298 K, 500 MHz.

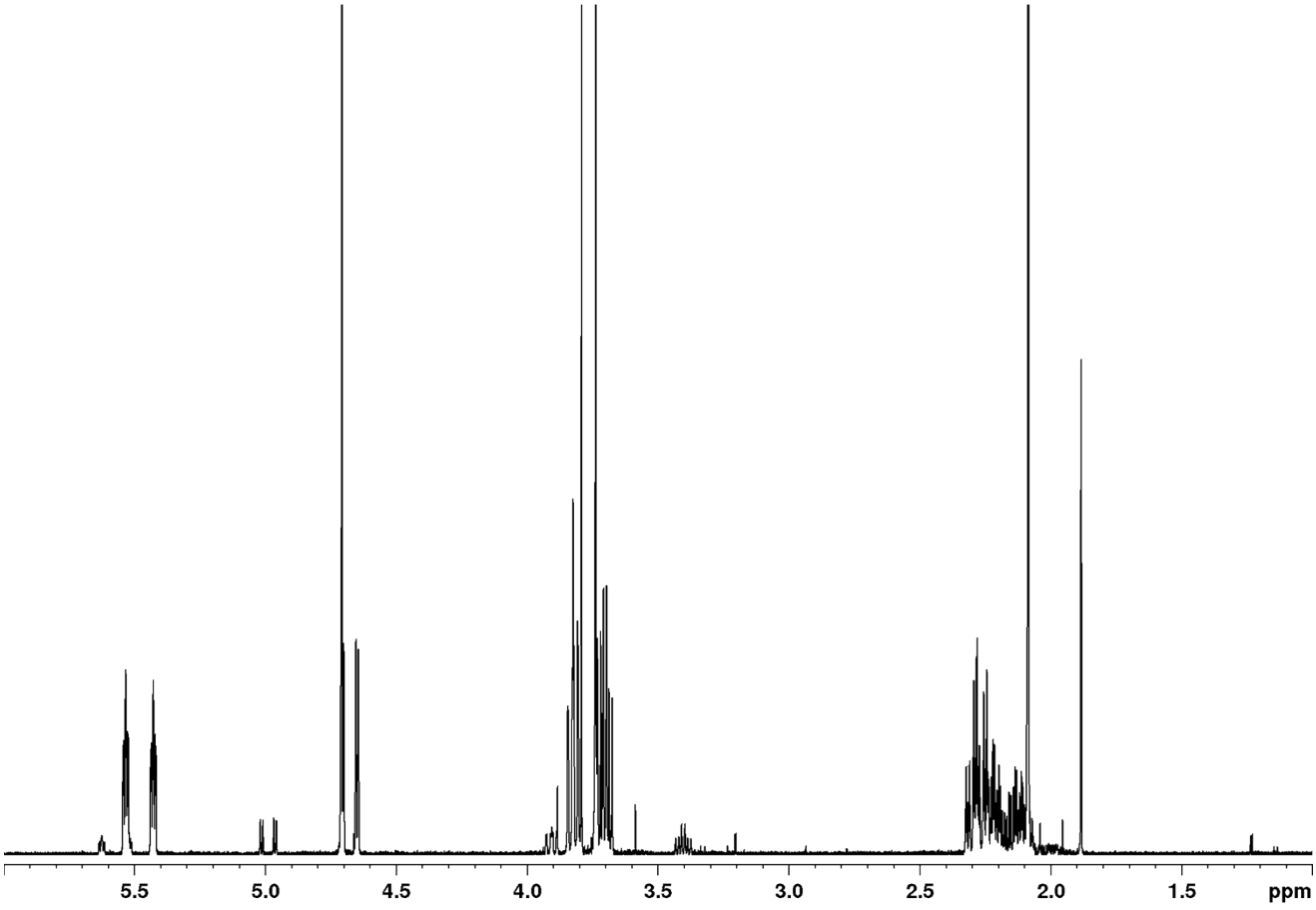

2.2.12 ^{1}H decoupled ^{19}F spectrum of Ac-(3R)-FPro-OMe **3** in D_2O, 298 K, 500 MHz.

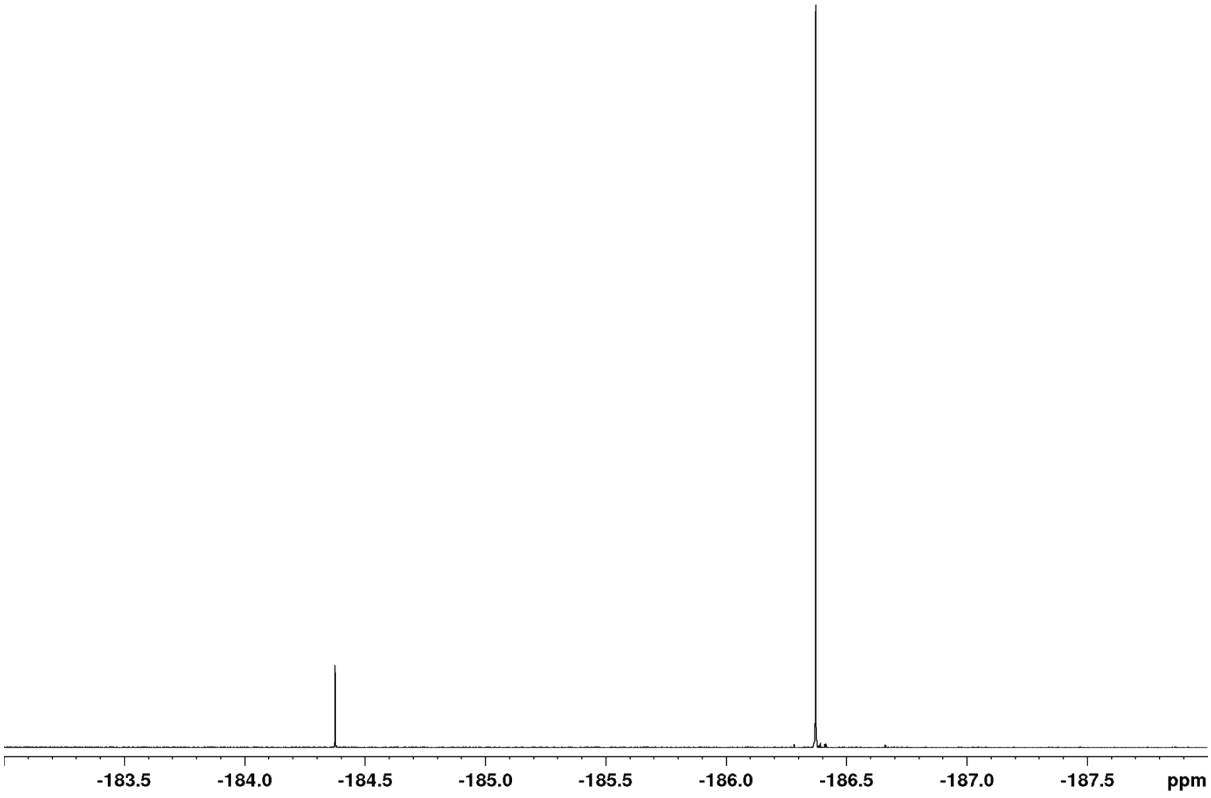

2.2.13 ^{1}H spectrum of Ac-(3R)-FPro-OMe **3** in $CDCl_3$, 298 K, 500 MHz.

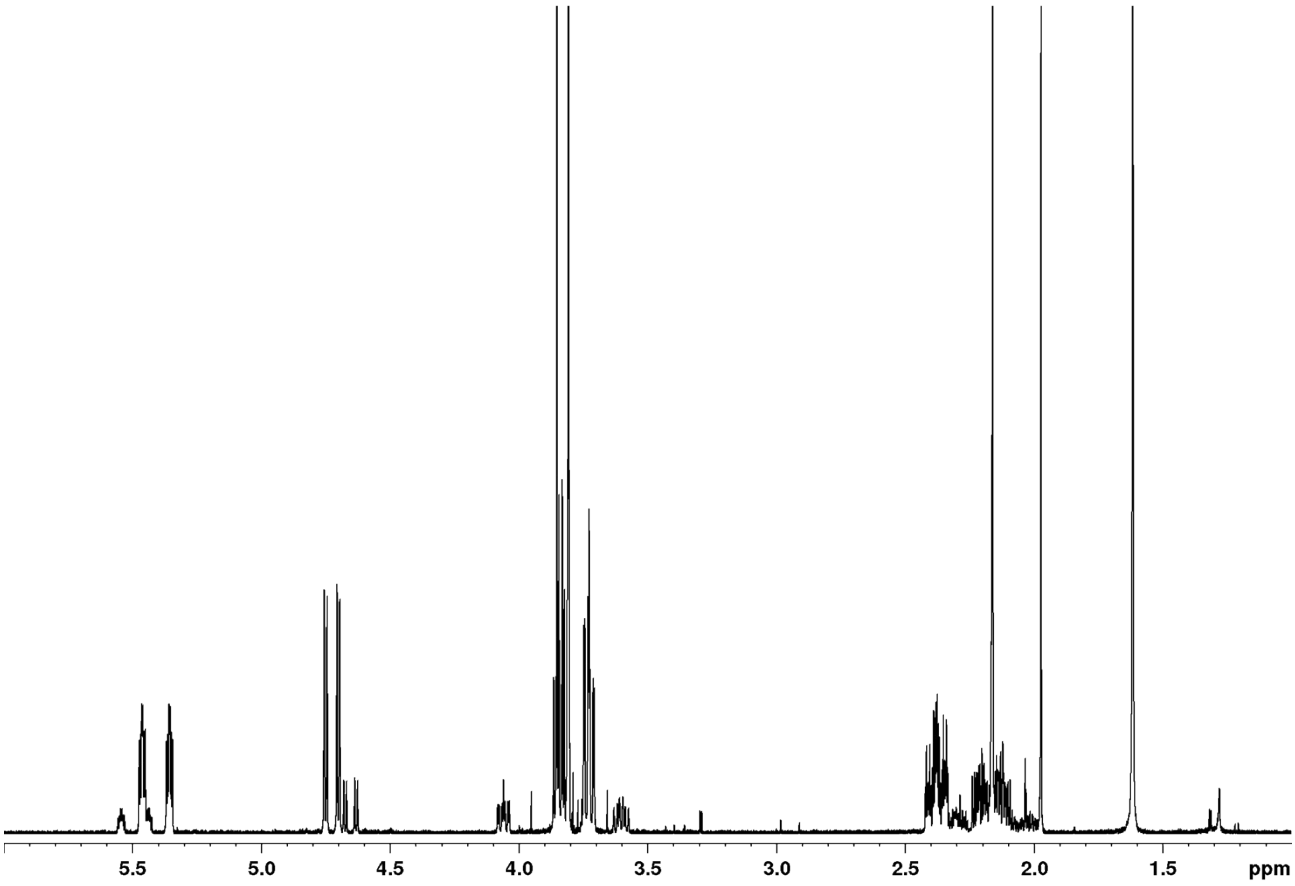

2.2.14 ^{1}H decoupled ^{19}F spectrum of Ac-(3R)-FPro-OMe **3** in $CDCl_3$, 298 K, 500 MHz.

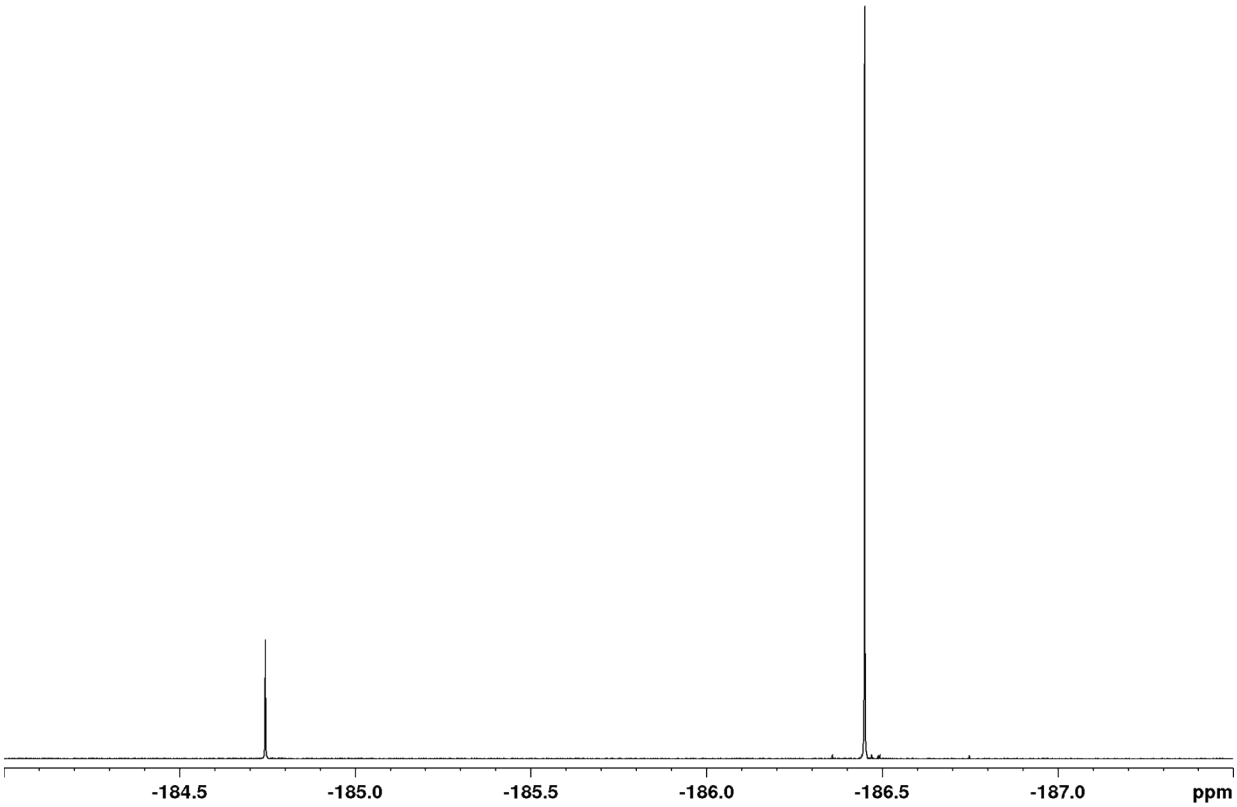

2.2.15 ^{1}H spectrum of Ac-4,4-F_2Pro-OMe **5** in D_2O, 298 K, 500 MHz

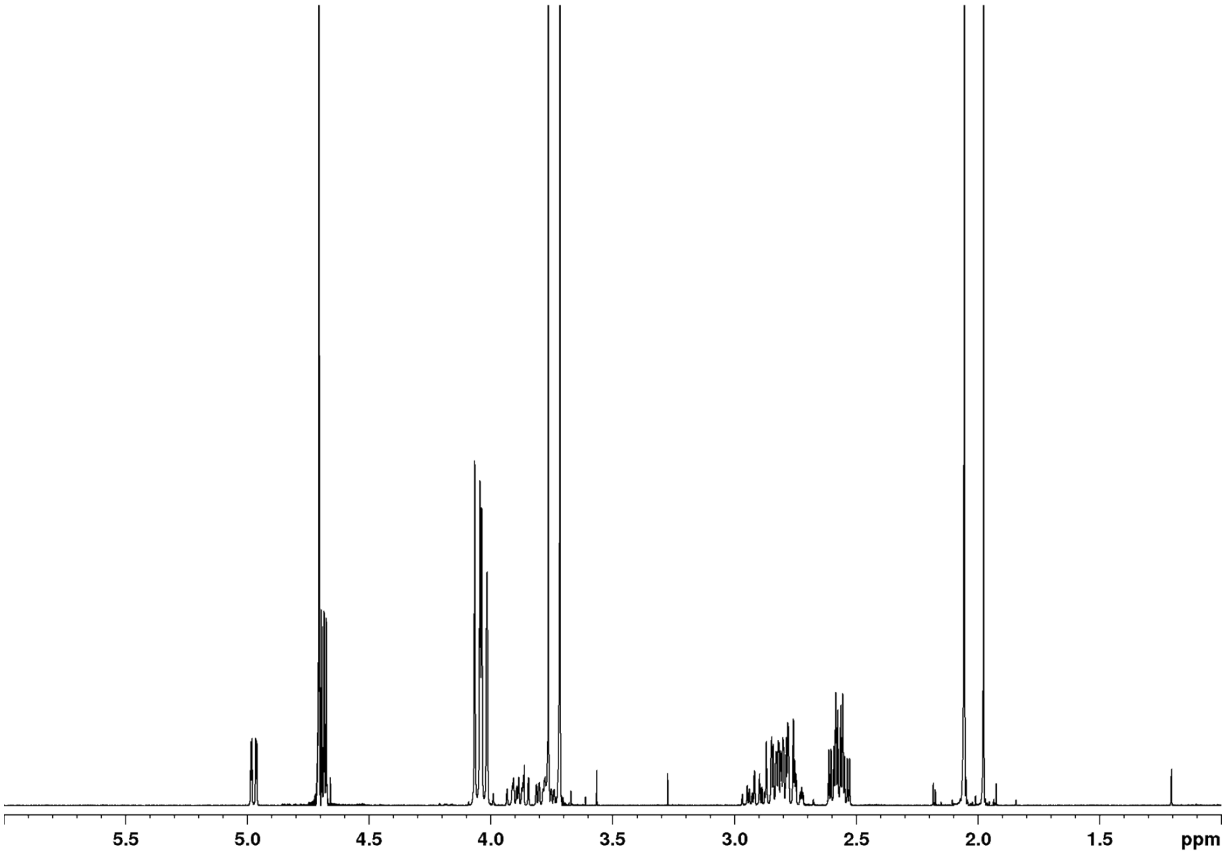

2.2.16 1D ^{1}H decoupled ^{19}F spectrum of Ac-4,4-F_2Pro-OMe **5** in D_2O, 298 K, 500 MHz.

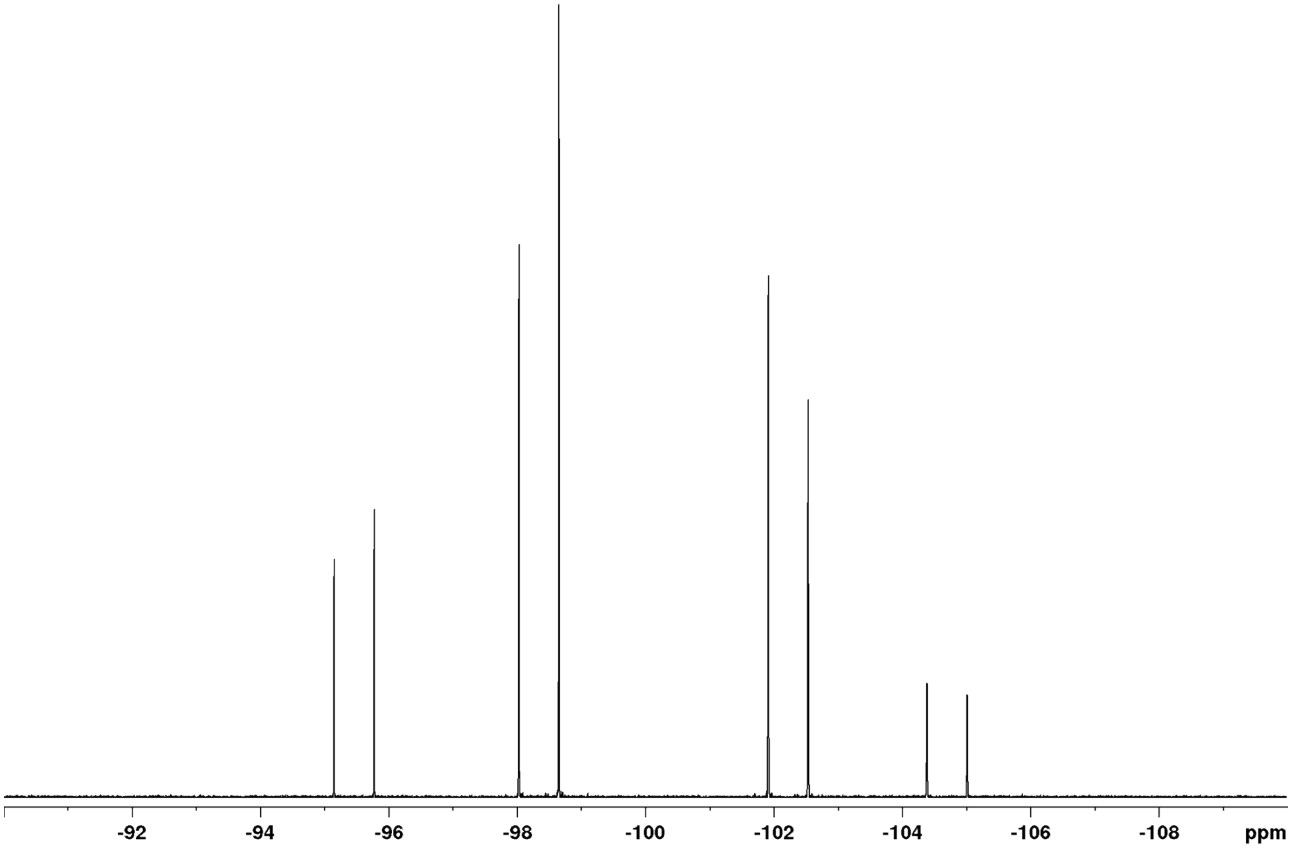

2.2.17 1D ^{1}H spectrum of Ac-4,4-F_2Pro-OMe **5** in $CDCl_3$, 298 K, 500 MHz.

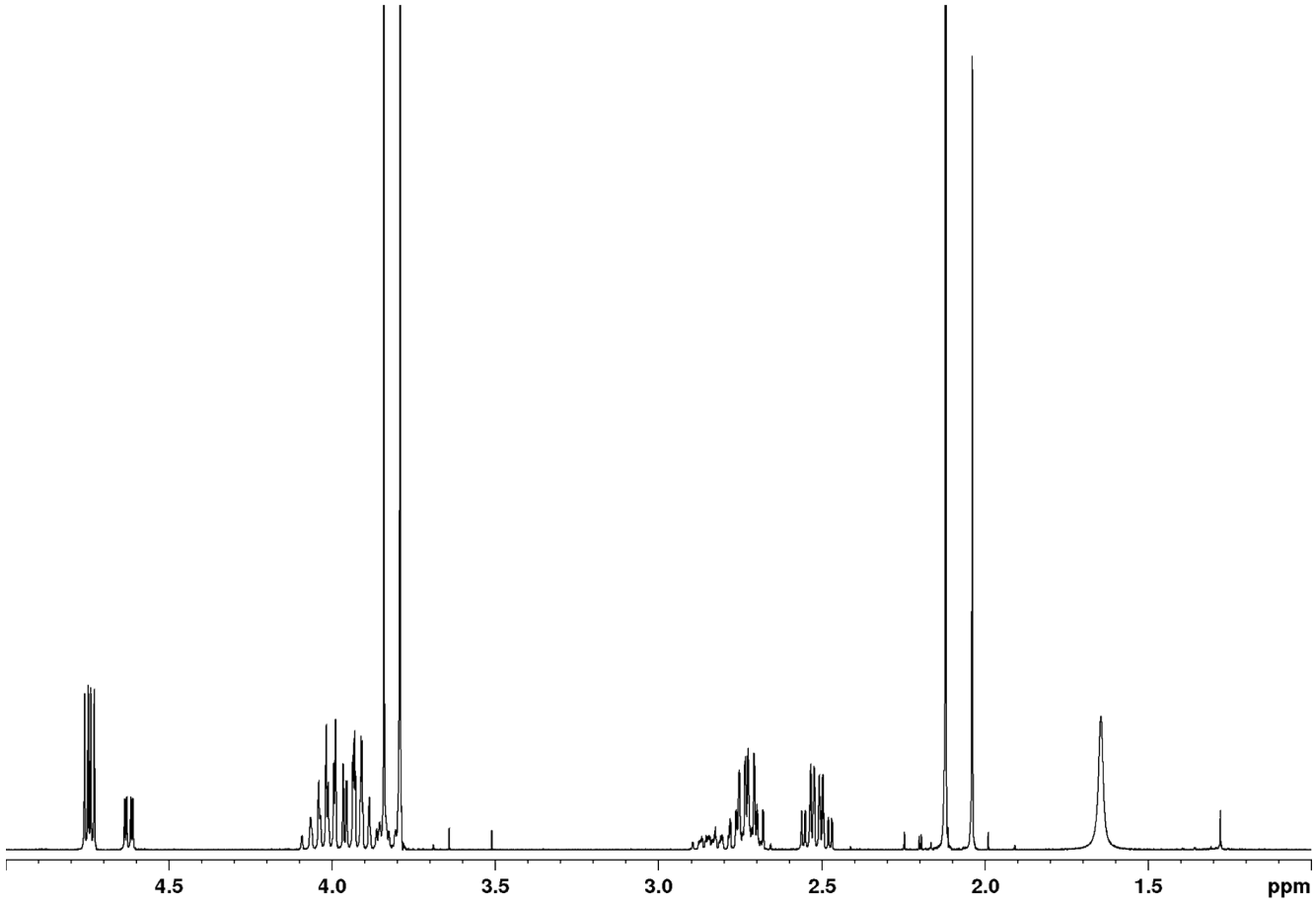
4.5
4.0
3.5
3.0
2.5
2.0
1.5
ppm

2.2.18 1D ^{1}H decoupled ^{19}F spectrum of Ac-4,4-F_2Pro-OMe **5** in $CDCl_3$, 298 K, 500 MHz

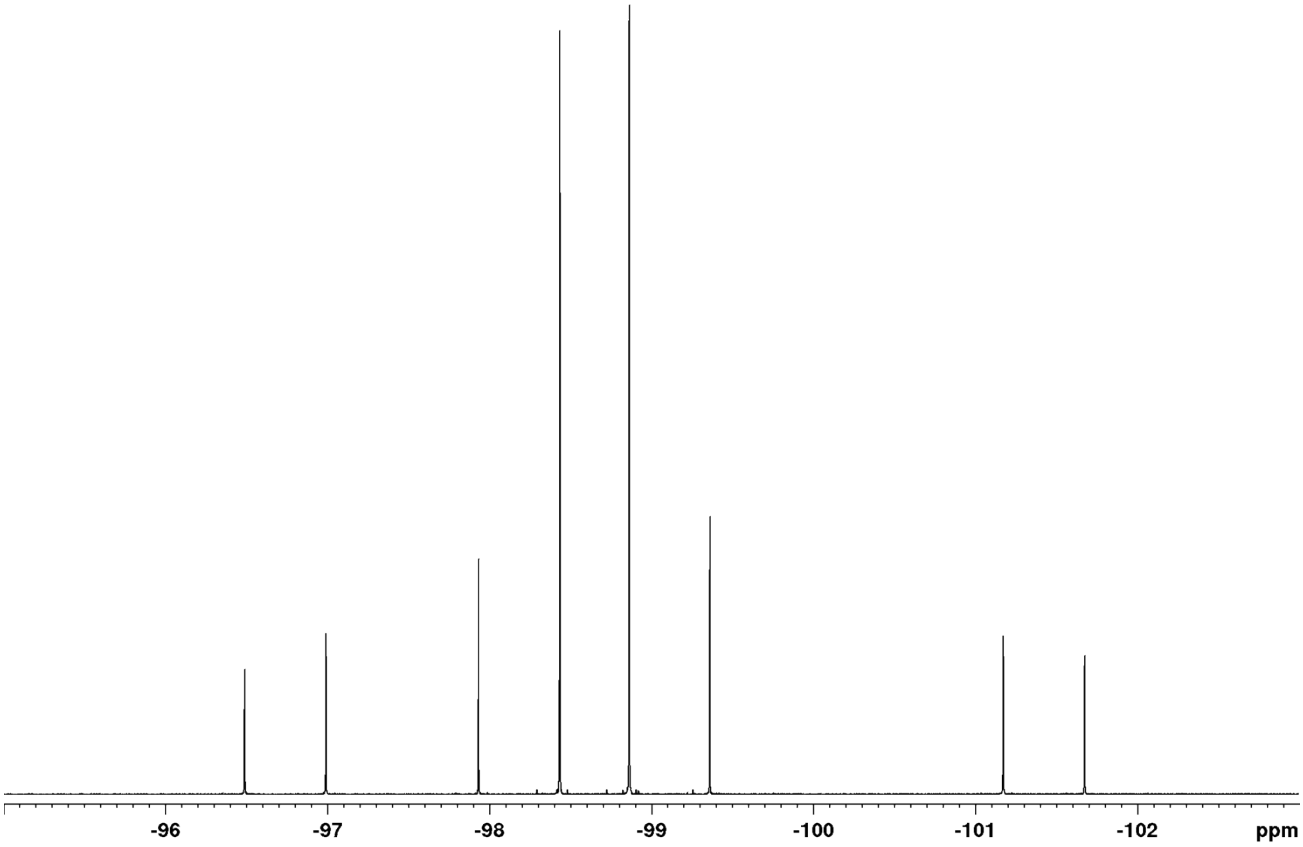

2.2.19 1D ^{1}H spectrum of Ac-(3S,4R)-F_2Pro-OMe **7** in D_2O, 298 K, 500 MHz.

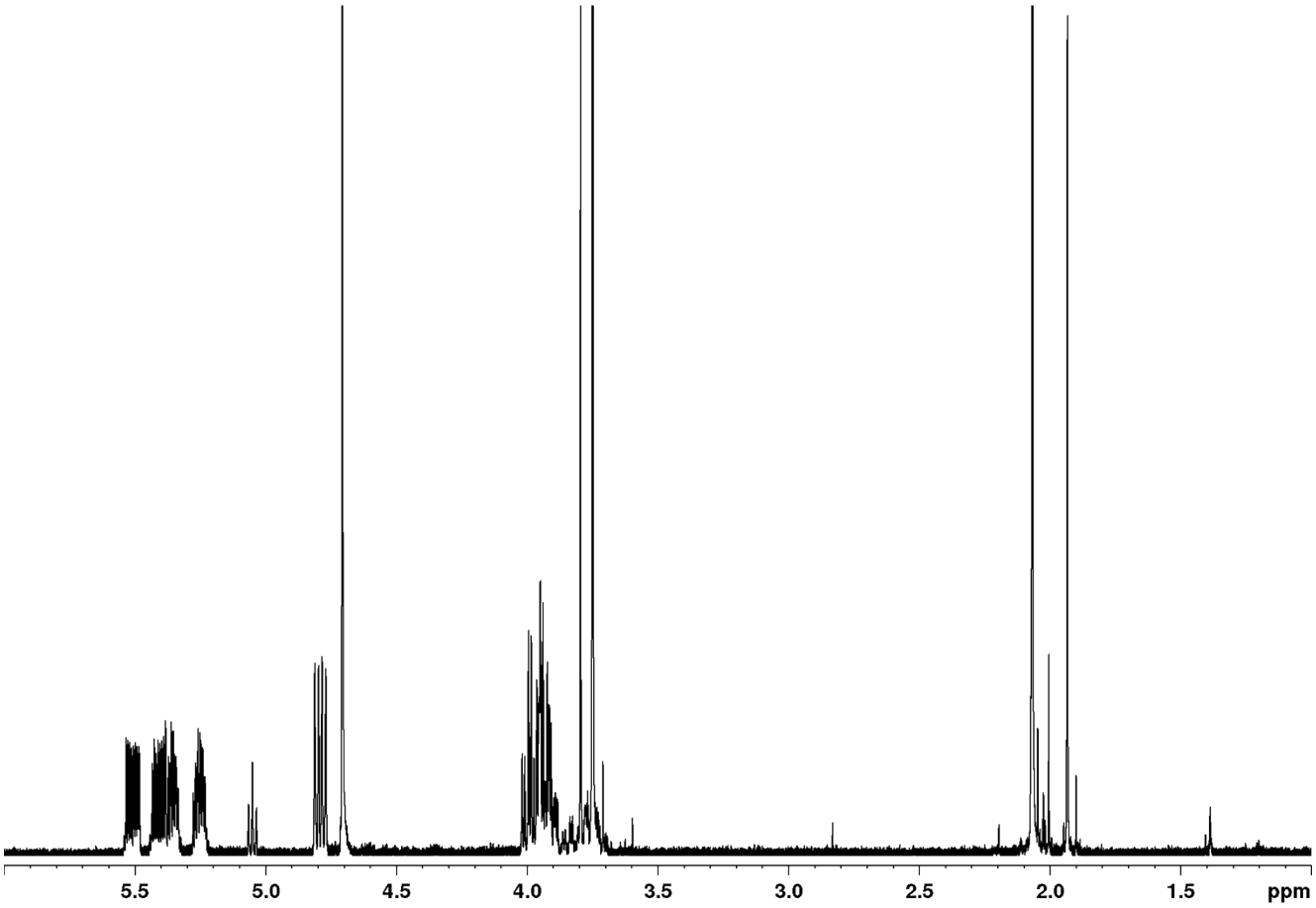

2.2.20 1D ^{1}H decoupled ^{19}F spectrum of Ac-(3S,4R)-F_2Pro-OMe **7** in D_2O, 298 K, 500 MHz.

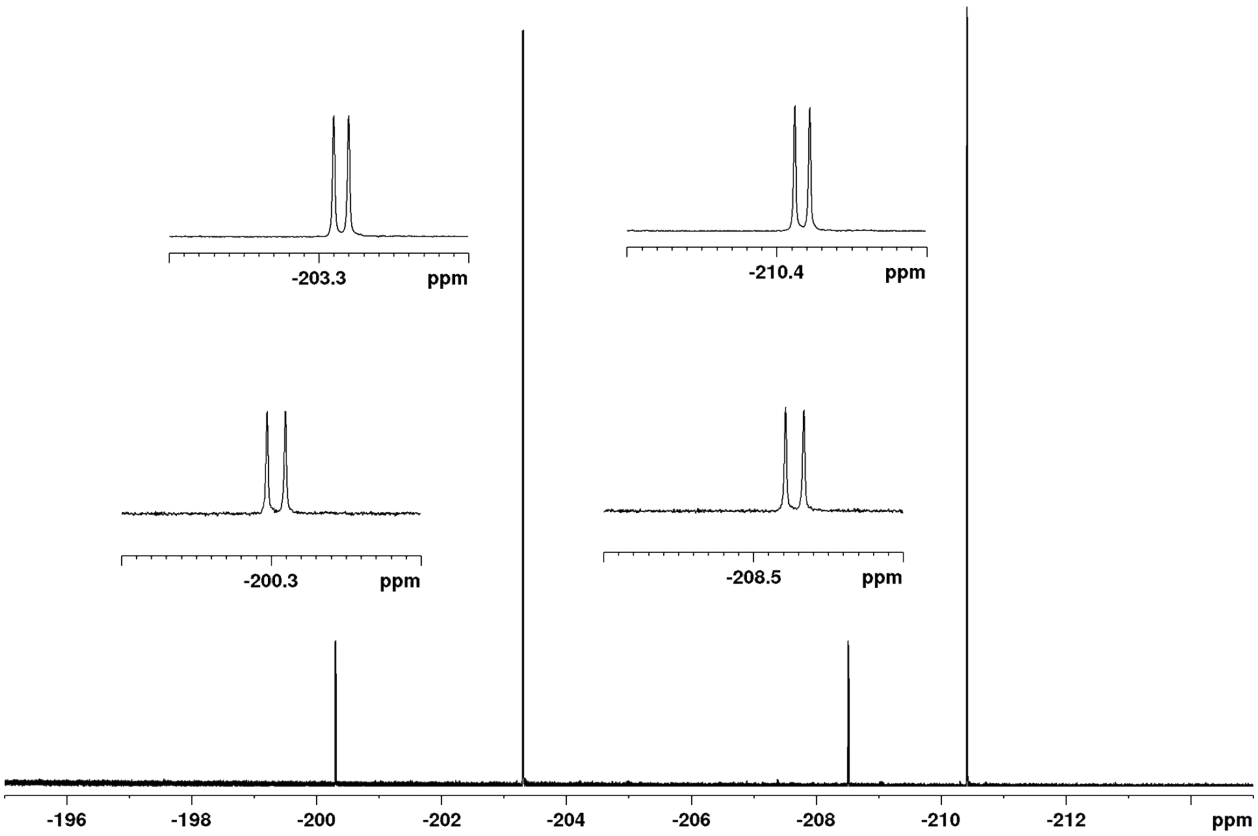

2.2.21 1D ^{1}H spectrum of Ac-(3S,4R)-F_2Pro-OMe **7** in $CDCl_3$, 298 K, 500 MHz.

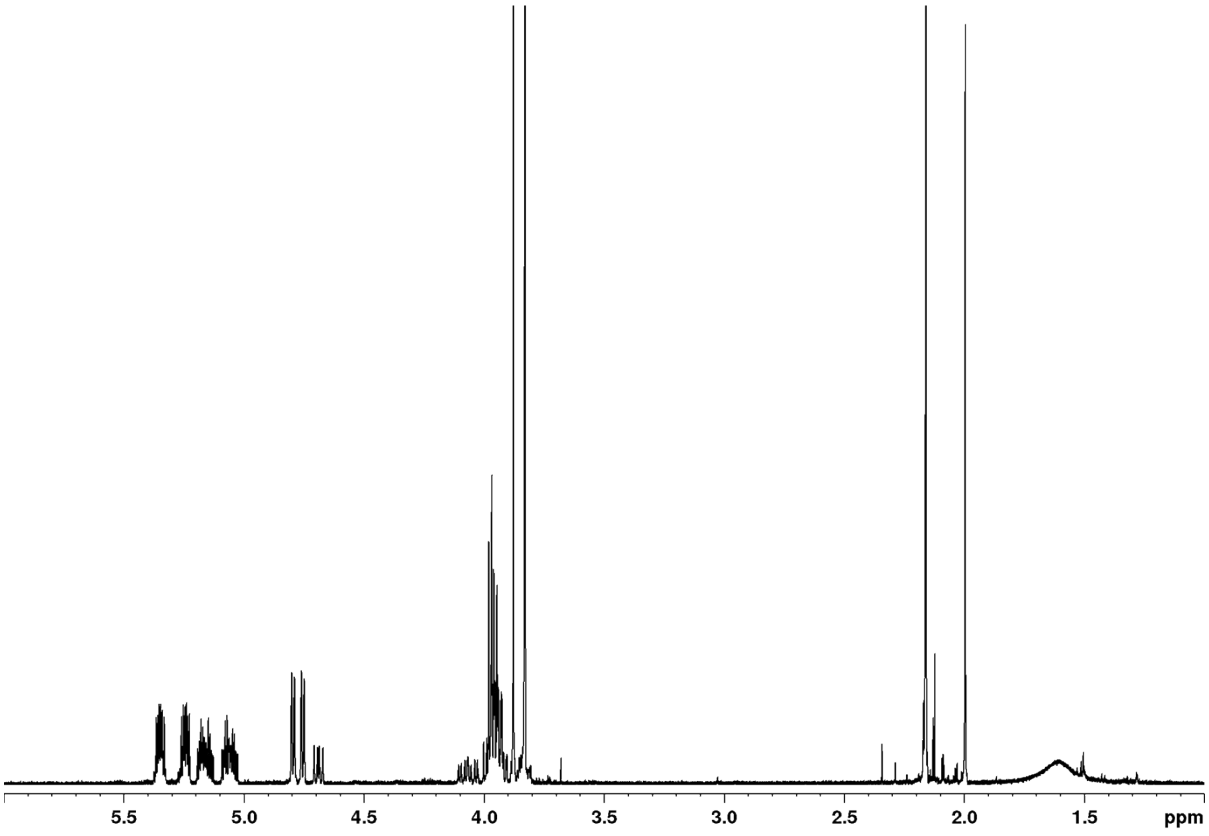

2.2.22 1D ^{1}H decoupled ^{19}F spectrum of Ac-(3S,4R)-F_2Pro-OMe **7** in $CDCl_3$, 298 K, 500 MHz.

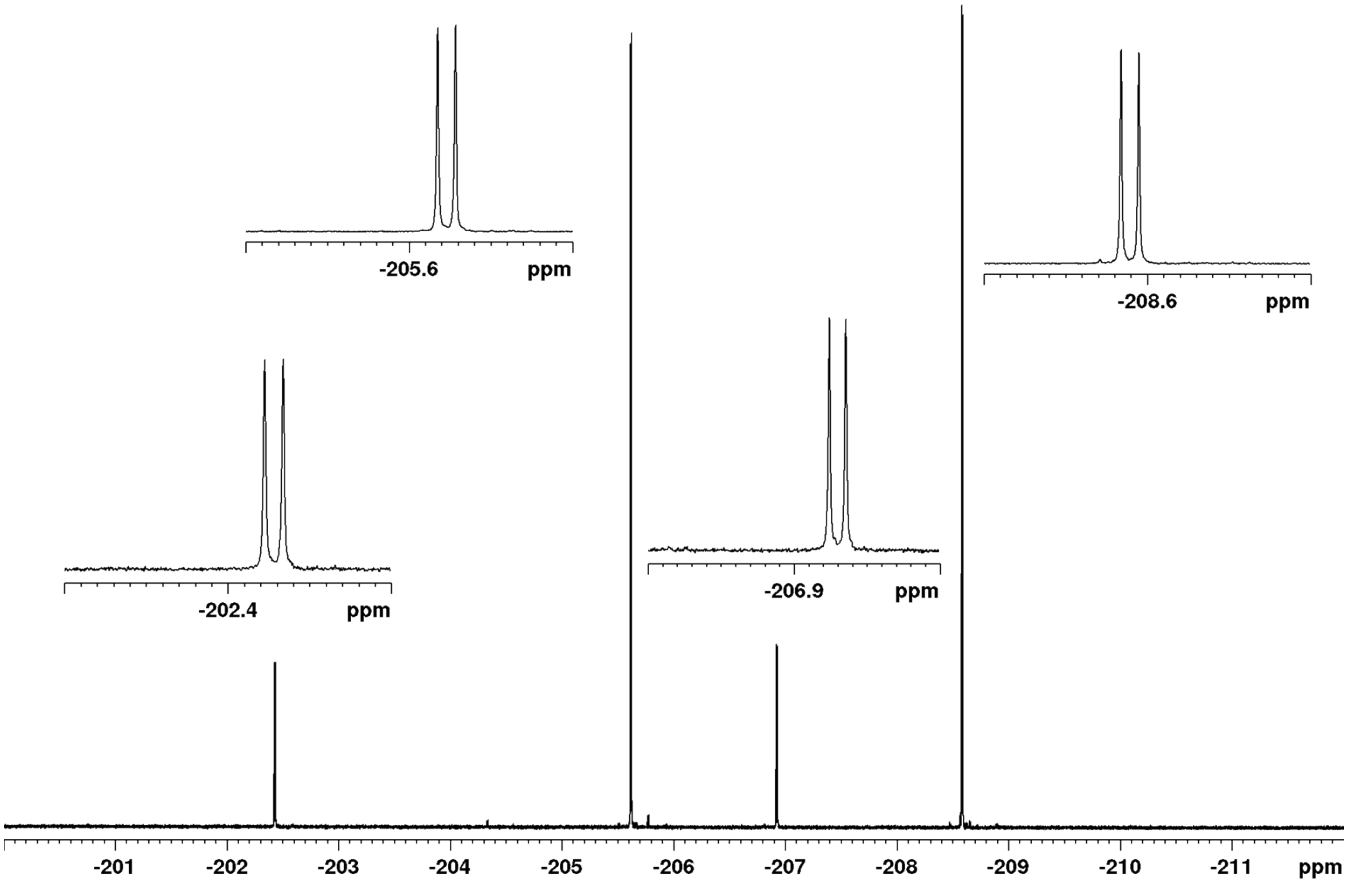

2.3 Experimental determination of cis/trans ratio's

2.3.1 1D ^{19}F spectrum with ^{1}H decoupling of compound **1** (D_2O)

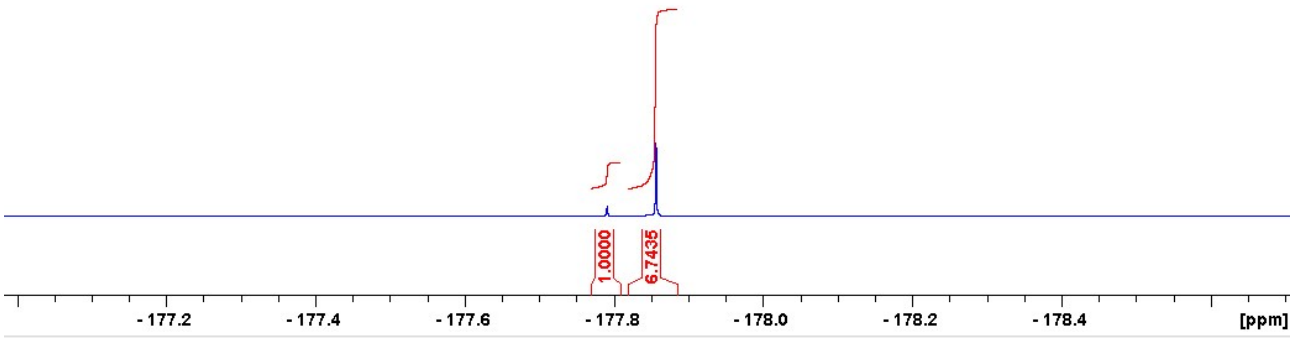

2.3.2 1D ^{19}F spectrum with ^{1}H decoupling of compound **1** ($CDCl_3$)

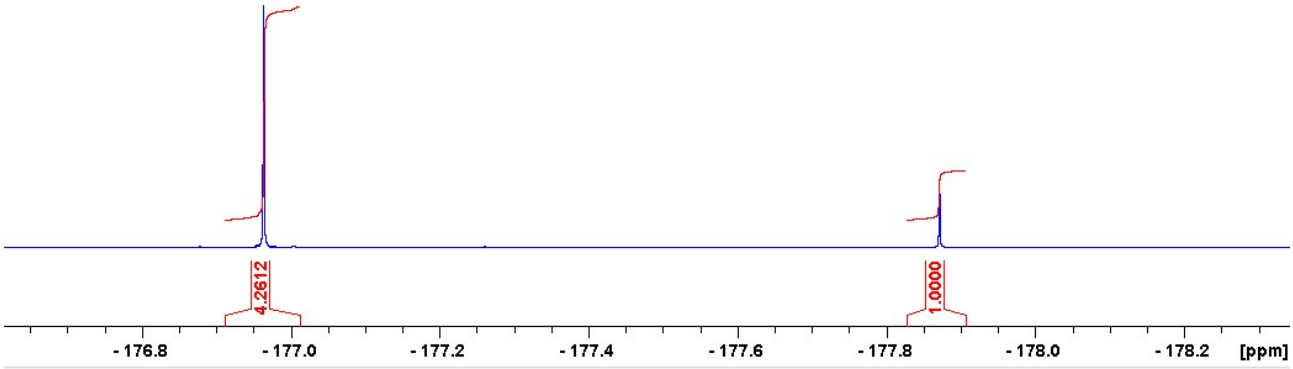

2.3.3 1D ^{19}F spectrum with ^{1}H decoupling of compound **2** (D_2O)

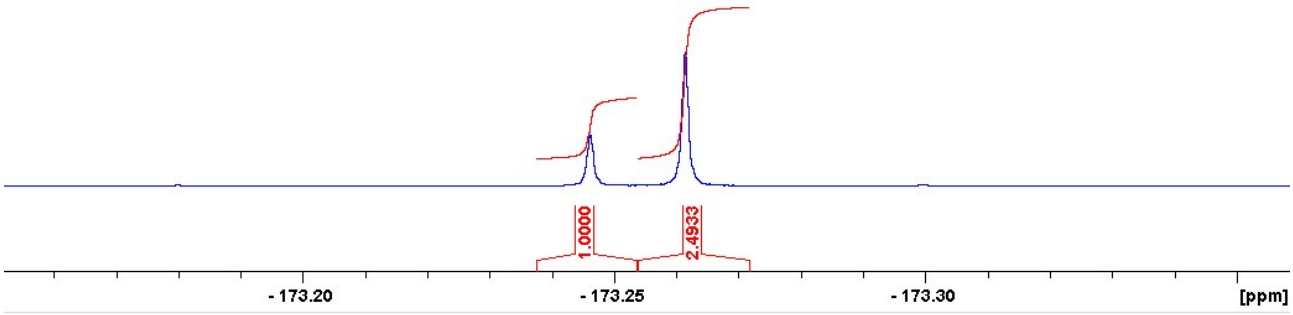

2.3.4 1D ^{19}F spectrum with ^{1}H decoupling of compound **2** ($CDCl_3$)

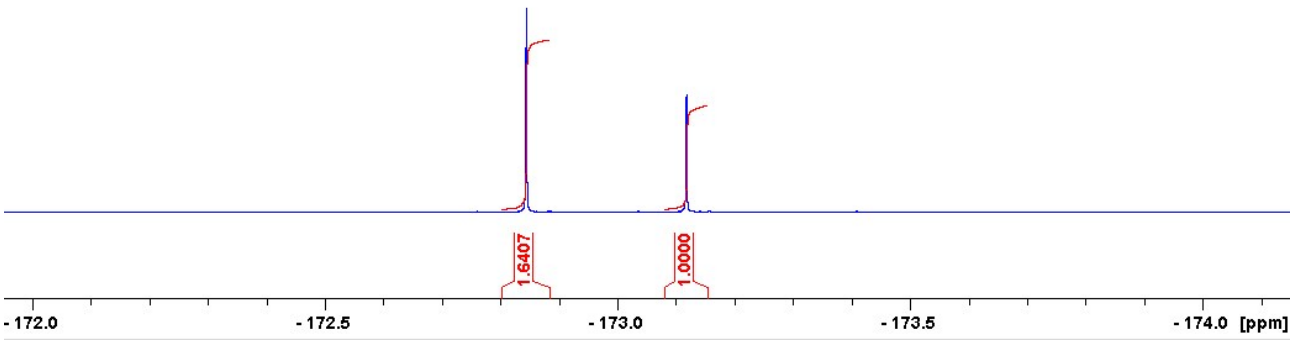

2.3.5 1D ^{19}F spectrum with ^{1}H decoupling of compound **3** (D_2O)

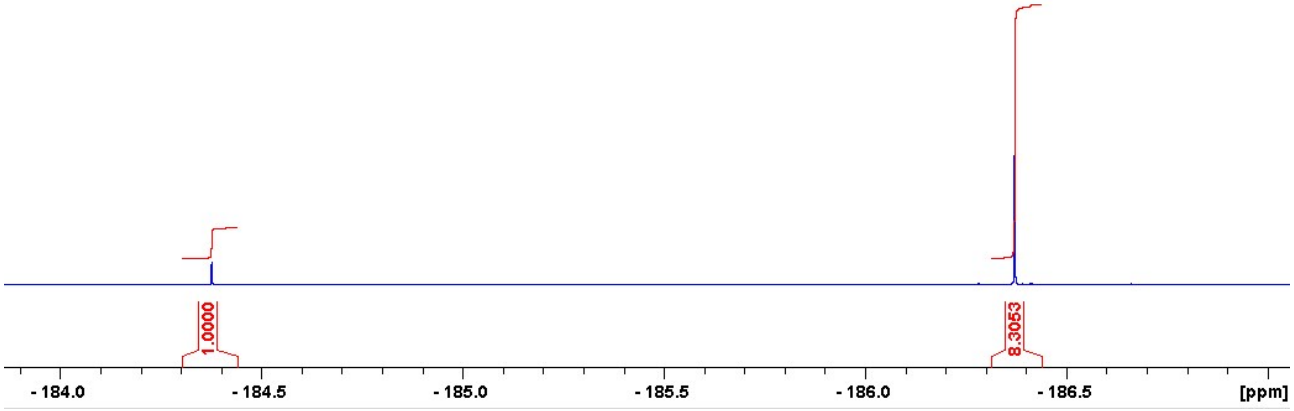

2.3.6 1D ^{19}F spectrum with ^{1}H decoupling of compound **3** ($CDCl_3$)

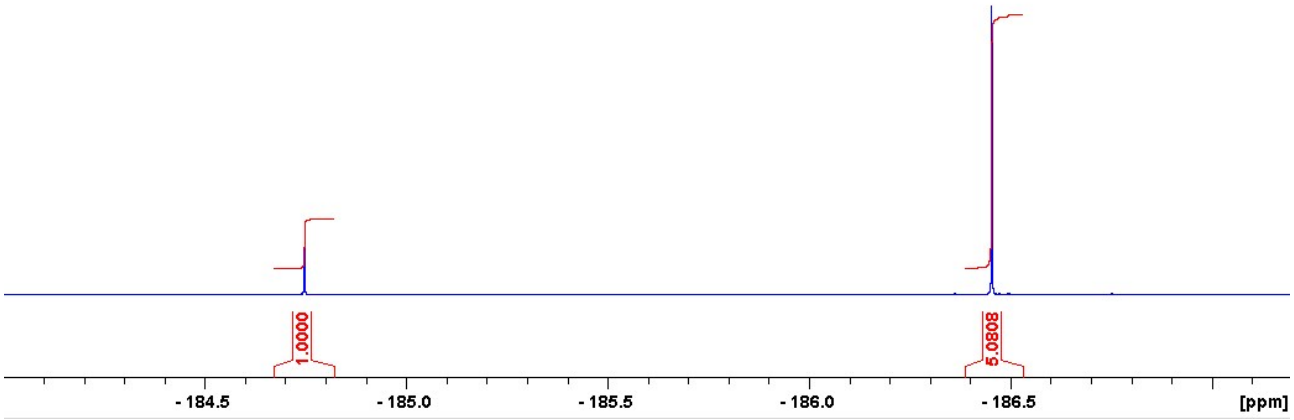

2.3.7 1D ^{1}H spectrum of compound **5** (D_2O)

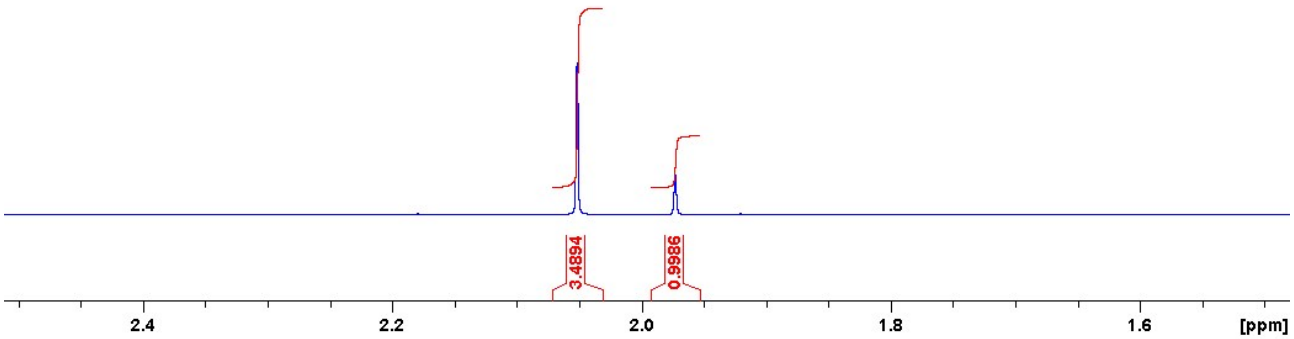

2.3.8 1D ^{1}H spectrum of compound **5** ($CDCl_3$)

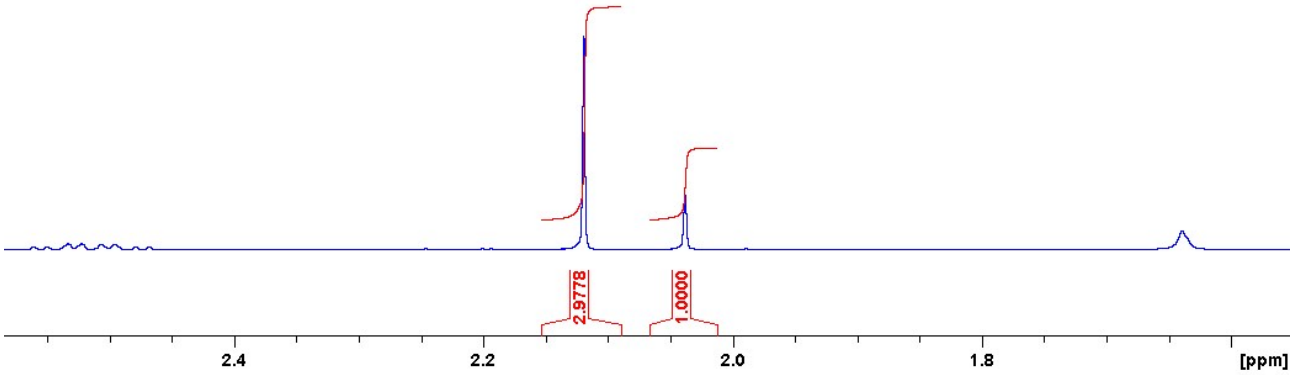

2.3.9 Compound **7** (H_2O)

2.3.9.1 Assignment of the rotamers

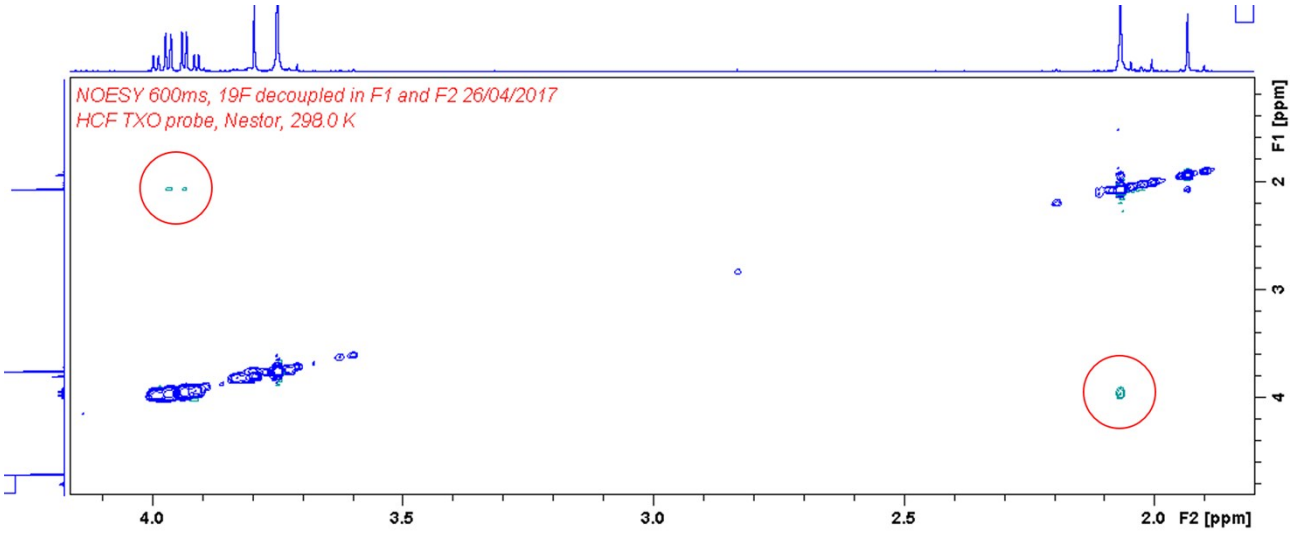

For the major form, a cross-peak can be seen between the acetyl methyl (2.07 ppm) signal and the δ protons (3.92 and 3.98 ppm), confirming the assignment as the *trans* rotamer. Such a cross-peak cannot be seen for the minor form, in agreement with the *cis* rotamer assignment.

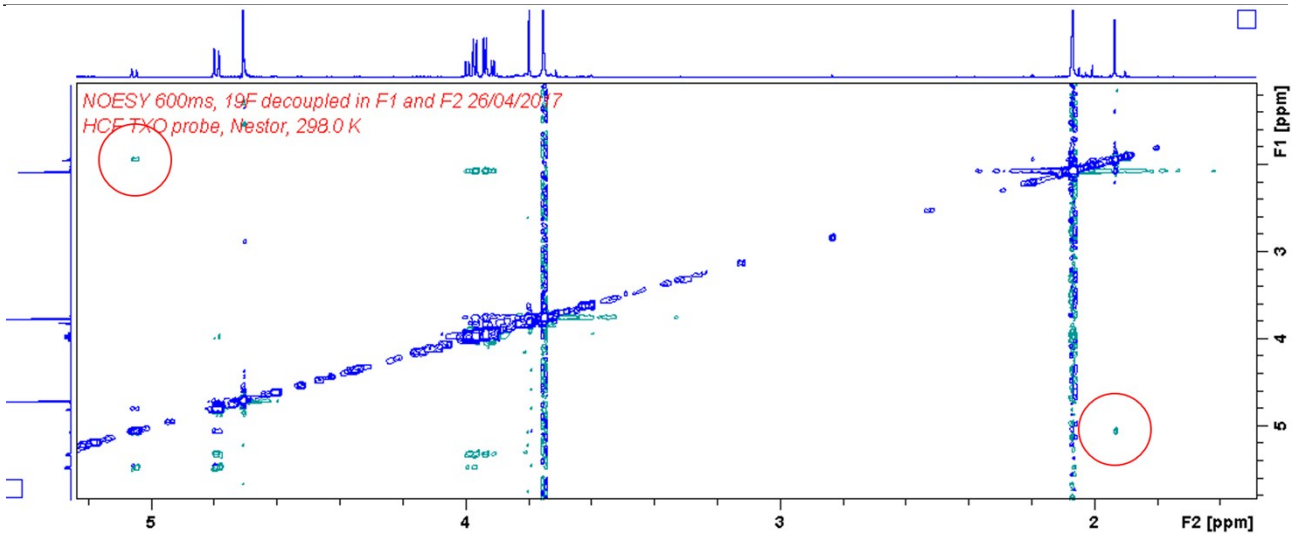

For the minor form, a cross peak between the acetyl methyl (2.07 ppm) signal and the alpha proton (5.05 ppm) can be seen which is an extra indication that this is the *cis* form.

2.3.9.2 1D ^{19}F spectrum with ^{1}H decoupling for ratio determination

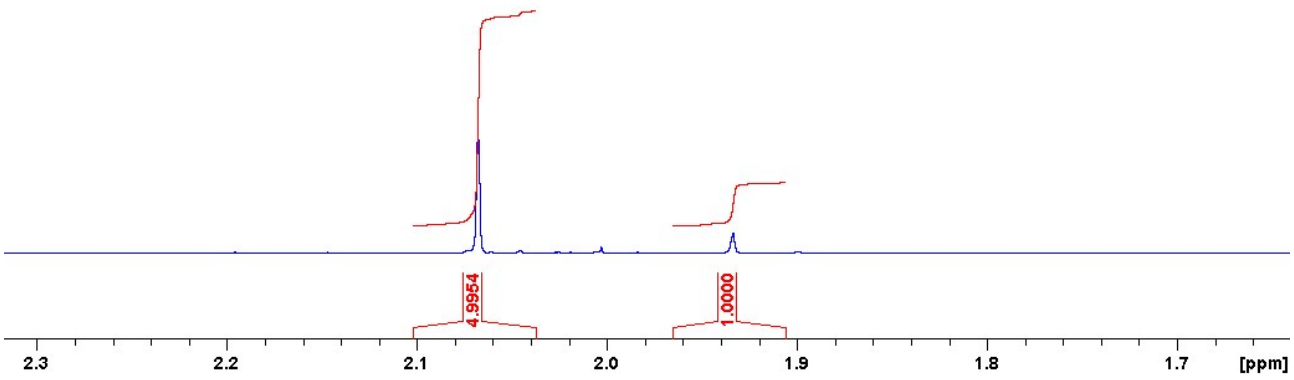

2.3.10 Compound **7** ($CDCl_3$)

2.3.10.1 Assignment of the rotamers of **7**

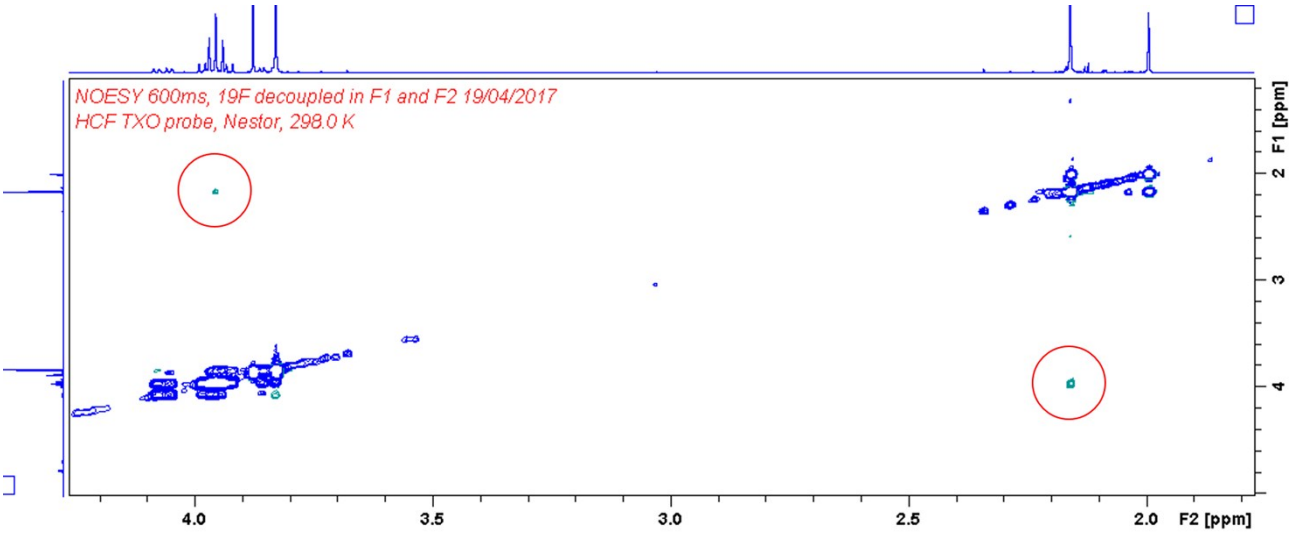

For the major form, a cross-peak can be seen between the acetyl methyl (2.16 ppm) signal and the δ protons (3.94 and 3.97 ppm), confirming the assignment as the *trans* rotamer. Such a cross-peak cannot be seen for the minor form, in agreement with the *cis* rotamer assignment.

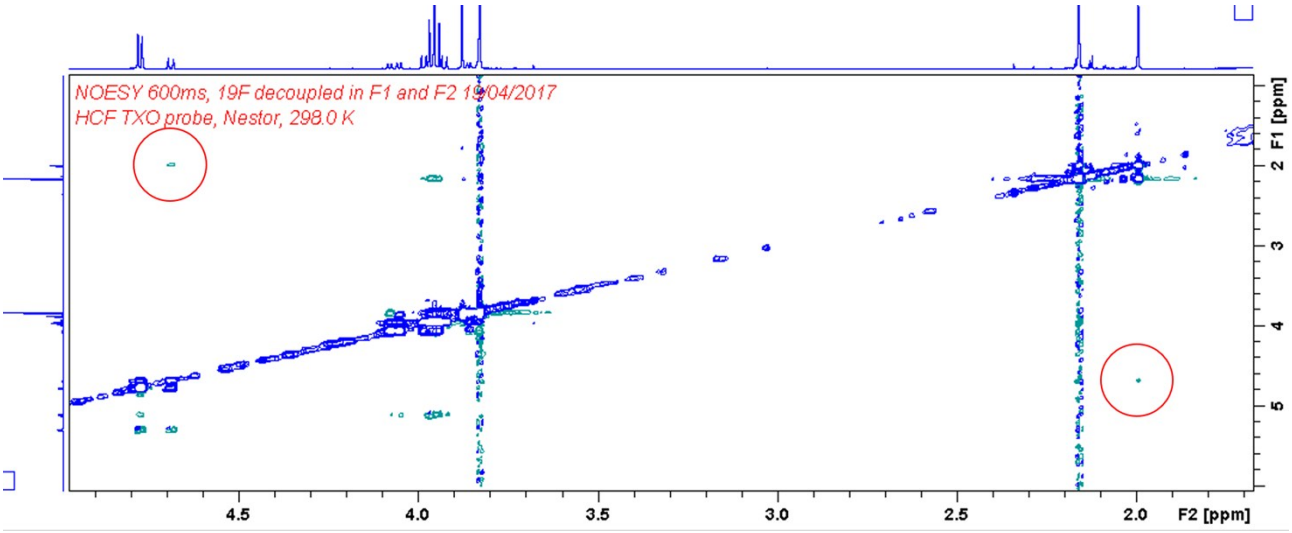

For the minor form, a cross peak between the acetyl methyl (2.16 ppm) signal and the alpha proton (4.69 ppm) can be seen which is an extra indication that this is the *cis* form.

2.3.10.2 Ratio determination of **7**, 1D ^{1}H spectrum

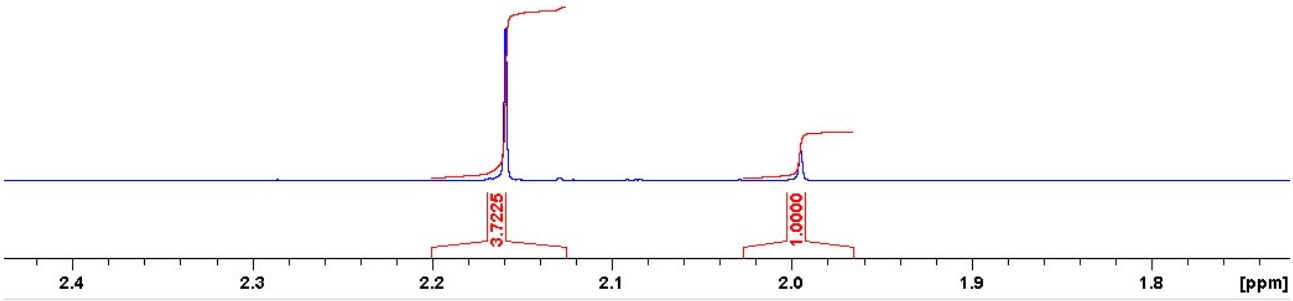

3 Computation

3.1 Computational assessment of the *endo/exo* and *cis/trans* fractions

For every molecule, four forms were considered in the calculations: *trans endo*, *trans exo*, *cis endo*, and *cis exo*. All calculations were performed with the Gaussian16 package,[5] using the same level of theory: M06[6]/cc-pVDZ. Geometries were optimized and the sum the electronic and thermal free energies at 298.15 K (G_{298}) were calculated. Solvent effects were taken into account using the SMD model.[7]

The G_{298} values were subsequently used to calculate the Boltzmann populations (p_i) using the following formula.

$$p_i = \frac{\exp\left(-\frac{G_i}{k_B T}\right)}{\sum_i \exp\left(-\frac{G_i}{k_B T}\right)}$$

In which *i* stands for one of the four forms, k_B is the Boltzmann constant and *T* the temperature (298.15 K).

Table 1 Gibbs free energies (in kJ/mol) of every form relative to the minimal energy form of every molecule. Calculated at the M06/cc-pVDZ level of theory for the geometry optimized molecules (same level of theory). Solvent is H_2O.

	trans endo	*cis endo*	*trans exo*	*cis exo*
Ac-Pro-OMe	0	1.701	1.636	5.558
Ac-4,4-F_2Pro-OMe	0	0.407	2.941	5.569
Ac-(3*S*,4*R*)-F_2Pro-OMe	0	1.223	0.585	6.622
Ac-(4*R*)-FPro-OMe	6.409	8.388	0	4.497
Ac-(4*S*)-FPro-OMe	0	0.895	11.21	14.47
Ac-(3*R*)-FPro-OMe	4.303	4.739	0	4.177

Table 2 Gibbs free energies (in kJ/mol) of every form relative to the minimal energy form of every molecule. Calculated at the M06/cc-pVDZ level of theory for the geometry optimized molecules (same level of theory). Solvent is $CHCl_3$.

	trans endo	*cis endo*	*trans exo*	*cis exo*
Ac-Pro-OMe	0	2.282	3.579	7.695
Ac-4,4-F_2Pro-OMe	0	1.113	1.441	7.533
Ac-(3*S*,4*R*)-F_2Pro-OMe	0.869	1.268	0	4.327
Ac-(4*R*)-FPro-OMe	5.091	7.270	0	4.981
Ac-(4*S*)-FPro-OMe	0	1.058	8.961	13.06
Ac-(3*R*)-FPro-OMe	2.854	6.320	0	2.226

3.2 Table Comparison between experimental and computed cis/trans ratio's

	$CDCl_3$		D_2O	
	NMR	M06	NMR	M06
1 (4*R*)	81:19	86:14	87:13	84:16
2 (4*S*)	63:37	61:39	72:28	59:41
3 (3*R*)	84:16	73:27	90:10	78:22
5 (4,4)	75:25	69:31	78:22	58:42
7 (3*S*,4*R*)	79:21	69:31	84:16	72:28
Ac-Pro-OMe	80:20	73:27	81:19	71:29

4 Crystallographic data for 11

Submitted by: **Gert-Jan Hofman**

Supervisor: **Bruno Linclau**

Solved by: **Mark Edward Light**

Sample ID: **GJH-7985-56**

Crystal Data and Experimental

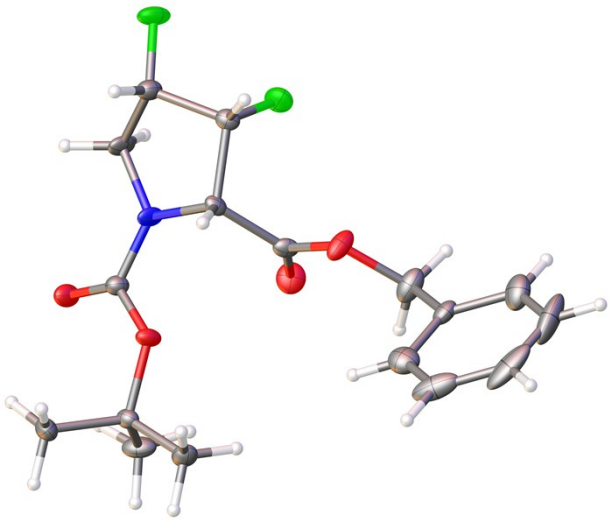

Figure 1: Thermal ellipsoids drawn at the 50% probability level. Second molecule omitted for clarity.

Experimental. Single clear colourless rod-shaped crystals of (**2017sot0006_K1_100K**) were recrystallised from --- by slow evaporation. A suitable crystal (0.25×0.04×0.03) mm^3 was selected and mounted on a MITIGEN holder silicon oil on a Rigaku AFC12 FRE-HF diffractometer. The crystal was kept at T = 100(2) K during data collection. Using **Olex2** (Dolomanov et al., 2009), the structure was solved with the **ShelXT** (Sheldrick, 2015) structure solution program, using the Intrinsic Phasing solution method. The model was refined with version 2016/6 of **ShelXL** (Sheldrick, 2015) using Least Squares minimisation.

Crystal Data. $C_{17}H_{21}F_2NO_4$, M_r = 341.35, orthorhombic, $Pna2_1$ (No. 33), a = 9.3962(3) Å, b = 10.8390(3) Å, c = 33.4374(9) Å, $\alpha = \beta = \gamma = 90^{\circ}$, V = 3405.45(17) $Å^3$, T = 100(2) K, Z = 8, Z' = 2, $\mu(MoK_\alpha)$ = 0.108, 24677 reflections measured, 8447 unique (R_{int} = 0.0563) which were used in all calculations. The final wR_2 was 0.1201 (all data) and R_1 was 0.0703 (I > 2(I)).

Compound	**2017sot0006_K_100 K**
Formula	$C_{17}H_{21}F_2NO_4$
$D_{calc.}$/ g cm^{-3}	1.332
μ/mm^{-1}	0.108
Formula Weight	341.35
Colour	clear colourless
Shape	rod
Size/mm^3	0.25×0.04×0.03
T/K	100(2)
Crystal System	orthorhombic
Flack Parameter	0.0(5)
Hooft Parameter	0.0(5)
Space Group	$Pna2_1$
a/Å	9.3962(3)
b/Å	10.8390(3)
c/Å	33.4374(9)
α/°	90
β/°	90
γ/°	90
V/Å^3	3405.45(17)
Z	8
Z'	2
Wavelength/Å	0.71073
Radiation type	MoK_α
Θ_{min}/°	3.760
Θ_{max}/°	28.698
Measured Refl.	24677
Independent Refl.	8447
Reflections Used	6864
R_{int}	0.0563
Parameters	439
Restraints	367
Largest Peak	0.262
Deepest Hole	-0.237
GooF	1.139
wR_2 (all data)	0.1201
wR_2	0.1129
R_1 (all data)	0.0913
R_1	0.0703

A clear colourless rod-shaped crystal with dimensions 0.25×0.04×0.03 was mounted on a MITIGEN holder silicon oil. Data were collected using a Rigaku AFC12 FRE-HF diffractometer equipped with an Oxford Cryosystems low-temperature apparatus operating at T = 100(2) K.

Data were measured using profile data from ω-scans of 1.0° per frame for 20.0 s using MoK_α radiation (Rotating Anode, 45.0 kV, 55.0 mA). The total number of runs and images was based on the strategy calculation from the program **CrysAlisPro** (Rigaku, V1.171.39.9g, 2015). The actually achieved resolution was Θ = 28.698.

Cell parameters were retrieved using the **CrysAlisPro** (Rigaku, V1.171.39.9g, 2015) software and refined using **CrysAlisPro** (Rigaku, V1.171.39.9g, 2015) on 6173 reflections, 25 of the observed reflections.

Data reduction was performed using the **CrysAlisPro** (Rigaku, V1.171.39.9g, 2015) software, which corrects for Lorentz polarisation. The final completeness is 99.70 out to 28.698 in Θ. The absorption coefficient μ of this material is 0.108 at this wavelength (λ = 0.71073) and the minimum and maximum transmissions are 0.59032 and 1.00000.

The structure was solved in the space group $Pna2_1$ (# 33) by Intrinsic Phasing using the **ShelXT** (Sheldrick, 2015) structure solution program and refined by Least Squares using version 2016/6 of **ShelXL** (Sheldrick, 2015). All non-hydrogen atoms were refined anisotropically. Hydrogen atom positions were calculated geometrically and refined using the riding model.

The value of Z' is 2. This means that there are two independent molecules in the asymmetric unit.

The Flack parameter was refined to 0.0(5). Determination of absolute structure using Bayesian statistics on Bijvoet differences using the Olex2 results in 0.0(5). Note: The Flack parameter is used to determine chirality of the crystal studied, the value should be near 0, a value of 1 means that the stereochemistry is wrong and the model should be inverted. A value of 0.5 means that the crystal consists of a racemic mixture of the two enantiomers.

Table 3: Fractional Atomic Coordinates (×10^4) and Equivalent Isotropic Displacement Parameters (Å^2×10^3) for **2017sot0006_K1_100K**. U_{eq} is defined as 1/3 of the trace of the orthogonalised U_{ij}.

Atom	x	y	z	U_{eq}
C101	2564(5)	8478(4)	4498.9(13)	20.9(9)
C102	3611(4)	9412(4)	4333.3(13)	19.4(9)
C103	3736(4)	9080(4)	3893.1(13)	16.7(9)
C104	3726(4)	7675(4)	3902.1(12)	14.4(8)
C105	2940(4)	7137(4)	3544.5(13)	16.1(9)
C106	3138(4)	6762(5)	2850.8(13)	28.2(11)
C107	4362(4)	6374(4)	2588.6(12)	18.8(9)
C108	4496(5)	6833(5)	2208.0(14)	31.7(11)
C109	5607(6)	6446(6)	1963.2(15)	50.1(16)
C110	6570(5)	5588(6)	2102.4(18)	50.3(16)
C111	6429(5)	5124(5)	2483(2)	40.2(13)
C112	5339(5)	5510(4)	2724.3(14)	28.3(10)
C113	2847(4)	6217(4)	4418.9(13)	16.8(9)
C114	3453(4)	4082(4)	4246.5(12)	15.9(9)

Atom	x	y	z	U_{eq}
C115	4217(5)	3747(4)	4631.1(12)	22.5(10)
C116	1907(4)	3667(4)	4248.0(15)	24.9(10)
C117	4211(4)	3586(4)	3882.6(13)	21.5(9)
F101	3140(3)	10618(2)	4381.1(8)	28.4(6)
F102	2515(2)	9511(2)	3697.5(7)	25.9(6)
N101	3013(3)	7381(3)	4278.8(10)	18.2(8)
O101	2156(3)	5968(3)	4715.5(8)	21.8(7)
O102	3552(3)	5426(3)	4184.0(8)	17.2(6)
O103	1783(3)	6676(3)	3557.4(9)	25.2(7)
O104	3732(3)	7267(3)	3216.7(9)	24.2(7)
C201	687(4)	6498(4)	5538.5(11)	14.0(8)
C202	1790(4)	5558(4)	5671.6(12)	15.7(8)
C203	2023(4)	5878(4)	6108.8(13)	15.4(8)
C204	1982(4)	7285(4)	6109.9(12)	14.3(8)
C205	1224(4)	7806(4)	6475.5(12)	14.4(8)
C206	1485(4)	8201(5)	7168.4(13)	25.1(11)
C207	2716(4)	8603(4)	7418.9(12)	17.8(9)
C208	2888(5)	8167(5)	7803.6(12)	27.9(11)
C209	4014(6)	8592(6)	8038.2(14)	47.2(15)
C210	4943(5)	9441(6)	7889.7(17)	47.7(16)
C211	4783(5)	9881(5)	7511(2)	42.3(13)
C212	3680(4)	9461(5)	7274.4(15)	29.6(11)
C213	1093(4)	8740(4)	5590.7(12)	11.9(8)
C214	1781(4)	10864(4)	5762.7(12)	14.5(8)
C215	2513(4)	11218(4)	5375.4(13)	19.9(9)
C216	245(4)	11295(4)	5779.2(13)	19.3(9)
C217	2604(4)	11353(4)	6121.7(13)	18.8(9)
F201	1329(2)	4347(2)	5628.7(8)	24.9(6)
F202	871(2)	5419(2)	6331.9(7)	22.7(6)
N201	1220(3)	7583(3)	5740.9(10)	15.4(7)
O201	418(3)	8999(3)	5297.0(8)	18.4(6)
O202	1864(3)	9521(3)	5823.4(8)	15.5(6)
O203	77(3)	8273(3)	6470.7(8)	21.9(7)
O204	2055(3)	7688(3)	6795.8(8)	22.2(7)

Table 4: Anisotropic Displacement Parameters (×10^4) **2017sot0006_K1_100K**. The anisotropic displacement factor exponent takes the form: $-2\pi^2[h^2a^{*2} \times U_{11} + ... + 2hka^* \times b^* \times U_{12}]$

Atom	U_{11}	U_{22}	U_{33}	U_{23}	U_{13}	U_{12}
C101	29(2)	14(2)	19(2)	-6.0(17)	11.2(18)	1.3(16)
C102	23(2)	14(2)	21(2)	-1.7(18)	4.1(18)	-0.5(16)

Atom	U_{11}	U_{22}	U_{33}	U_{23}	U_{13}	U_{12}
C103	13.9(19)	15(2)	21(2)	1.3(18)	1.3(17)	0.0(15)
C104	14.4(19)	13(2)	15.4(19)	3.3(17)	4.8(16)	1.0(15)
C105	15(2)	13(2)	20(2)	-1.1(17)	6.3(16)	2.3(15)
C106	19(2)	43(3)	23(2)	-10(2)	0.6(18)	-2(2)
C107	18(2)	22(2)	17(2)	-7.4(18)	0.5(17)	-5.2(16)
C108	27(2)	46(3)	23(2)	-2(2)	-6(2)	-8(2)
C109	39(3)	93(5)	18(2)	-19(3)	6(2)	-27(3)
C110	20(3)	81(5)	50(3)	-47(3)	3(2)	-15(3)
C111	16(3)	34(3)	71(3)	-27(3)	-6(3)	2(2)
C112	24(2)	26(3)	35(3)	0(2)	-3(2)	-6.8(18)
C113	19(2)	14(2)	18(2)	-0.9(17)	2.2(17)	0.0(16)
C114	16(2)	13(2)	19(2)	0.9(17)	-3.3(17)	-0.1(15)
C115	31(3)	18(2)	19(2)	3.4(18)	-3.6(19)	-0.1(19)
C116	18(2)	16(2)	41(3)	-4(2)	-2(2)	-2.7(16)
C117	25(2)	17(2)	22(2)	-3.4(18)	-0.4(19)	5.4(17)
F101	40.6(16)	12.3(13)	32.1(15)	-4.6(12)	11.5(12)	1.1(11)
F102	28.7(13)	20.2(14)	28.8(14)	0.5(11)	-3.9(11)	8.8(10)
N101	25.1(19)	13.3(18)	16.2(17)	-4.0(15)	13.1(15)	-0.7(13)
O101	30.7(17)	17.8(17)	17.1(14)	-0.6(13)	12.1(13)	-2.0(13)
O102	21.5(14)	10.8(15)	19.1(15)	-0.2(13)	8.4(12)	0.9(11)
O103	13.7(14)	34(2)	28.1(16)	0.5(15)	3.9(13)	-3.5(13)
O104	19.9(15)	34(2)	18.9(15)	-9.5(14)	6.1(12)	-12.1(13)
C201	13.5(18)	13(2)	15.1(19)	-2.5(16)	-0.5(16)	-1.8(14)
C202	19(2)	10(2)	18(2)	-4.0(17)	0.9(17)	-3.4(14)
C203	14.1(19)	11(2)	21(2)	3.8(18)	0.9(17)	-0.4(15)
C204	17(2)	14(2)	12.4(17)	-1.4(17)	-4.3(16)	0.2(15)
C205	16.3(19)	11(2)	16.1(19)	0.6(16)	-3.3(16)	-2.9(15)
C206	19(2)	41(3)	16(2)	-12(2)	-0.7(18)	4.4(19)
C207	13.3(19)	22(2)	18(2)	-7.5(18)	2.9(16)	6.1(15)
C208	31(2)	38(3)	15(2)	-3(2)	2.1(19)	6(2)
C209	34(3)	92(5)	16(2)	-14(3)	-7(2)	24(3)
C210	19(2)	72(4)	52(3)	-48(3)	-9(2)	8(3)
C211	22(3)	31(3)	73(3)	-17(3)	6(3)	-2(2)
C212	22(2)	31(3)	36(3)	2(2)	2(2)	5.8(19)
C213	11.8(18)	15(2)	9.1(17)	-3.1(16)	3.4(15)	1.3(15)
C214	18.0(19)	9(2)	17(2)	0.4(17)	-0.3(16)	-0.2(14)
C215	20(2)	18(2)	22(2)	2.7(18)	3.4(18)	-2.1(16)
C216	21(2)	15(2)	23(2)	-3.2(19)	1.2(19)	1.1(16)
C217	22(2)	15(2)	20(2)	-0.8(18)	-0.7(18)	-1.5(16)
F201	32.9(14)	11.6(13)	30.0(14)	-4.2(12)	0.3(12)	-0.9(10)
F202	27.6(13)	20.7(14)	19.8(12)	3.3(11)	3.9(11)	-6.6(10)

Atom	U_{11}	U_{22}	U_{33}	U_{23}	U_{13}	U_{12}
N201	19.4(16)	12.4(17)	14.5(17)	1.9(15)	-4.8(14)	0.0(13)
O201	23.2(15)	17.0(16)	14.9(14)	1.0(12)	-4.5(13)	3.6(12)
O202	19.4(14)	11.8(15)	15.4(14)	1.7(12)	-4.9(12)	-1.4(10)
O203	11.0(13)	34.2(19)	20.5(14)	-2.7(13)	-3.7(12)	5.8(13)
O204	19.1(15)	36(2)	11.7(14)	-7.5(14)	-5.1(12)	10.0(13)

Table 5: Bond Lengths in Å for **2017sot0006_K1_100K**.

Atom	Atom	Length/Å	Atom	Atom	Length/Å
C101	C102	1.516(6)	C201	C202	1.520(5)
C101	N101	1.460(5)	C201	N201	1.447(5)
C102	C103	1.520(6)	C202	C203	1.518(6)
C102	F101	1.389(5)	C202	F201	1.390(5)
C103	C104	1.523(6)	C203	C204	1.525(6)
C103	F102	1.401(5)	C203	F202	1.405(4)
C104	C105	1.522(6)	C204	C205	1.523(6)
C104	N101	1.462(5)	C204	N201	1.462(5)
C105	O103	1.197(5)	C205	O203	1.191(5)
C105	O104	1.332(5)	C205	O204	1.332(5)
C106	C107	1.506(6)	C206	C207	1.493(6)
C106	O104	1.452(5)	C206	O204	1.466(5)
C107	C108	1.372(6)	C207	C208	1.380(6)
C107	C112	1.387(6)	C207	C212	1.385(6)
C108	C109	1.391(7)	C208	C209	1.395(7)
C109	C110	1.379(9)	C209	C210	1.362(9)
C110	C111	1.375(9)	C210	C211	1.361(9)
C111	C112	1.369(7)	C211	C212	1.382(7)
C113	N101	1.355(5)	C213	N201	1.356(5)
C113	O101	1.216(5)	C213	O201	1.202(5)
C113	O102	1.338(5)	C213	O202	1.359(5)
C114	C115	1.517(6)	C214	C215	1.516(6)
C114	C116	1.522(6)	C214	C216	1.518(5)
C114	C117	1.509(6)	C214	C217	1.523(6)
C114	O102	1.474(5)	C214	O202	1.471(5)

Table 6: Bond Angles in ° for **2017sot0006_K1_100K**.

Atom	Atom	Atom	Angle/°	Atom	Atom	Atom	Angle/°
N101	C101	C102	99.9(3)	F101	C102	C101	112.3(3)
C101	C102	C103	104.2(4)	F101	C102	C103	111.0(4)

Atom	Atom	Atom	Angle/°
C102	C103	C104	102.6(3)
F102	C103	C102	108.0(3)
F102	C103	C104	109.7(3)
C105	C104	C103	111.8(3)
N101	C104	C103	103.7(3)
N101	C104	C105	111.8(3)
O103	C105	C104	124.9(4)
O103	C105	O104	125.5(4)
O104	C105	C104	109.6(3)
O104	C106	C107	107.6(3)
C108	C107	C106	120.6(4)
C108	C107	C112	119.1(4)
C112	C107	C106	120.2(4)
C107	C108	C109	120.4(5)
C110	C109	C108	119.8(5)
C111	C110	C109	119.7(5)
C112	C111	C110	120.3(5)
C111	C112	C107	120.6(5)
O101	C113	N101	123.4(4)
O101	C113	O102	127.0(4)
O102	C113	N101	109.7(3)
C115	C114	C116	112.2(4)
C117	C114	C115	112.0(3)
C117	C114	C116	110.4(4)
O102	C114	C115	109.1(3)
O102	C114	C116	110.7(3)
O102	C114	C117	102.0(3)
C101	N101	C104	112.9(3)
C113	N101	C101	123.4(3)
C113	N101	C104	123.6(3)
C113	O102	C114	121.2(3)
C105	O104	C106	116.1(3)
N201	C201	C202	99.9(3)
C203	C202	C201	103.1(3)
F201	C202	C201	113.0(3)
F201	C202	C203	111.1(3)
C202	C203	C204	103.1(3)
F202	C203	C202	108.6(3)
F202	C203	C204	109.5(3)
C205	C204	C203	112.6(3)
N201	C204	C203	103.4(3)
N201	C204	C205	111.5(3)
O203	C205	C204	124.7(4)
O203	C205	O204	125.6(4)
O204	C205	C204	109.6(3)
O204	C206	C207	107.7(3)
C208	C207	C206	120.9(4)
C208	C207	C212	118.6(4)
C212	C207	C206	120.4(4)
C207	C208	C209	120.0(5)
C210	C209	C208	120.3(5)
C211	C210	C209	120.3(5)
C210	C211	C212	120.0(5)
C211	C212	C207	120.8(5)
N201	C213	O202	108.5(3)
O201	C213	N201	124.4(4)
O201	C213	O202	127.1(4)
C215	C214	C216	112.6(3)
C215	C214	C217	110.8(3)
C216	C214	C217	110.3(3)
O202	C214	C215	110.2(3)
O202	C214	C216	110.5(3)
O202	C214	C217	102.1(3)
C201	N201	C204	112.6(3)
C213	N201	C201	123.2(3)
C213	N201	C204	124.1(3)
C213	O202	C214	120.6(3)
C205	O204	C206	115.6(3)

Table 7: Hydrogen Fractional Atomic Coordinates (×10^4) and Equivalent Isotropic Displacement Parameters (Å^2×10^3) for **2017sot0006_K1_100K**. U_{eq} is defined as 1/3 of the trace of the orthogonalised U_{ij}.

Atom	x	y	z	U_{eq}
H10A	2675.38	8369.62	4791.28	25
H10B	1567.63	8705.14	4437.46	25
H102	4555.52	9307.84	4466.85	23
H103	4627.88	9413.46	3770.92	20
H104	4725.18	7357.48	3907.85	17
H10C	2554.93	7392.93	2713	34
H10D	2525.2	6044.2	2912.18	34
H108	3826.95	7417.97	2111.16	38
H109	5701.67	6773.03	1700.93	60
H110	7327.97	5317.68	1935.96	60
H111	7091.53	4531.8	2579.42	48
H112	5251.27	5184.51	2986.86	34
H11A	5198.67	4049.78	4620.34	34
H11B	4221.26	2847.91	4663.23	34
H11C	3723.67	4125.17	4858.38	34
H11D	1444.66	3949.81	4494.28	37
H11E	1864.87	2764.65	4234.43	37
H11F	1413.85	4019.33	4016.29	37
H11G	3673.83	3804.33	3641.68	32
H11H	4285.34	2686.02	3902.68	32
H11I	5167.27	3944.37	3867.25	32
H20A	683.81	6604.24	5244.4	17
H20B	-280.32	6274.5	5630.53	17
H202	2693.99	5682.31	5518.83	19
H203	2953.03	5556.11	6209.57	18
H204	2972.75	7618.32	6096.33	17
H20C	921.01	7569.17	7311.76	30
H20D	858.04	8912.85	7109.7	30
H208	2241	7576.69	7908.68	33
H209	4132.43	8289	8302.61	57
H210	5706.41	9726.73	8051.19	57
H211	5429.89	10477.6	7409.95	51
H212	3581.41	9763.48	7009.27	35
H21A	3505.89	10943.87	5382.72	30
H21B	2480.87	12116.53	5342.75	30

Atom	x	y	z	U_{eq}
H21C	2023.69	10824.27	5150.18	30
H21D	-266.16	10991.33	5543.32	29
H21E	217	12198.32	5783.21	29
H21F	-208.26	10972.29	6021.61	29
H21G	2156.54	11059.6	6368.74	28
H21H	2595.87	12257.32	6117.58	28
H21I	3588.8	11057.97	6109.76	28

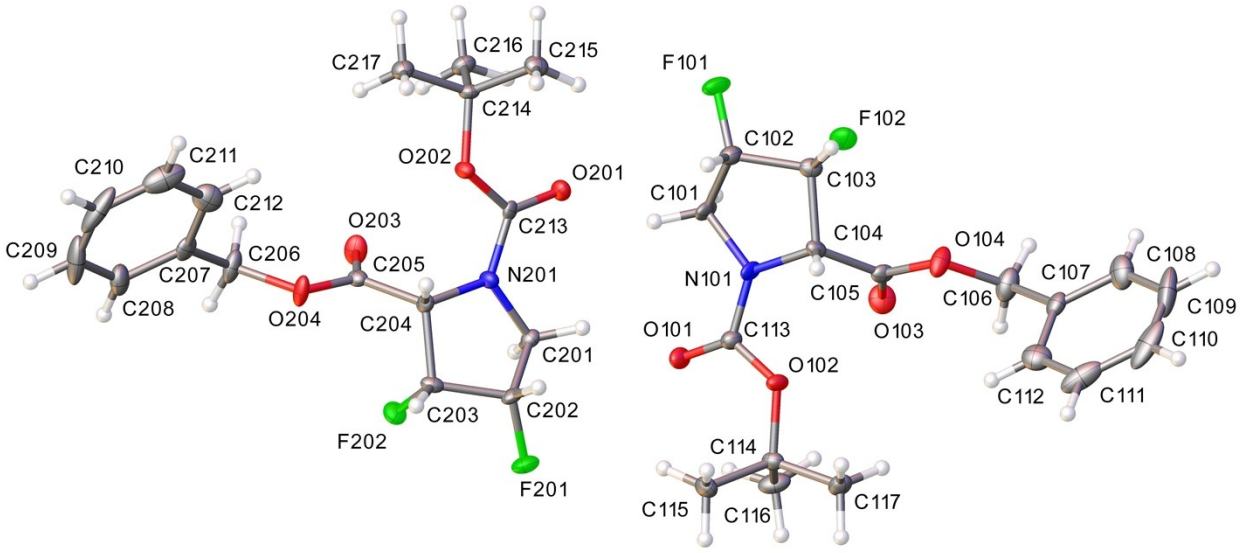

Figure 2. Thermal ellipsoids drawn at the 50% probability level.

Citations

CrysAlisPro Software System, Rigaku Oxford Diffraction, (2015).

O.V. Dolomanov and L.J. Bourhis and R.J. Gildea and J.A.K. Howard and H. Puschmann, Olex2: A complete structure solution, refinement and analysis program, *J. Appl. Cryst.*, (2009), **42**, 339-341.

Sheldrick, G.M., Crystal structure refinement with ShelXL, *Acta Cryst.*, (2015), **C27**, 3-8.

Sheldrick, G.M., ShelXT-Integrated space-group and crystal-structure determination, *Acta Cryst.*, (2015), **A71**, 3-8.

5 H, C, F spectra of all compounds:

5.1 (2S)-N-t-Butyloxycarbonyl-3,4-dehydroproline benzyl ester 9

5.1.1 ^{1}H NMR (400 MHz, $CDCl_3$)

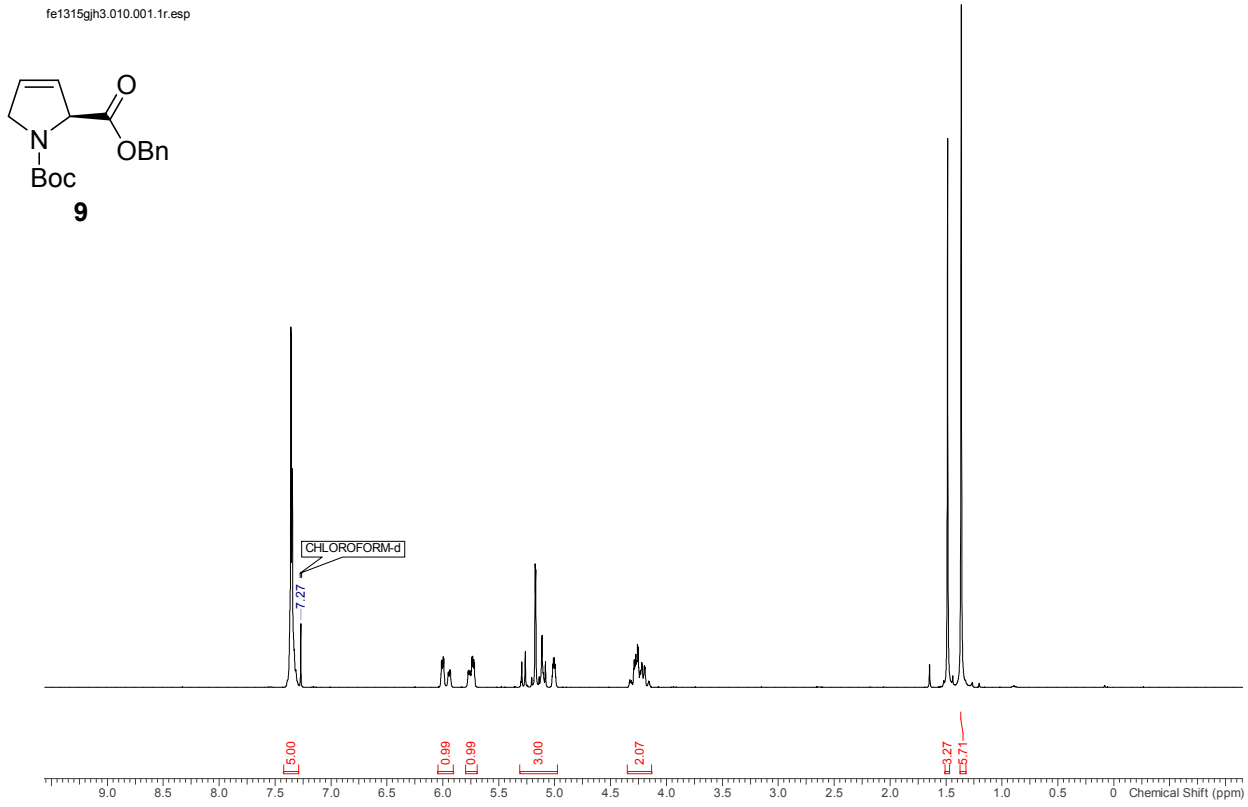

5.1.2 ^{13}C NMR (100 MHz, $CDCl_3$)

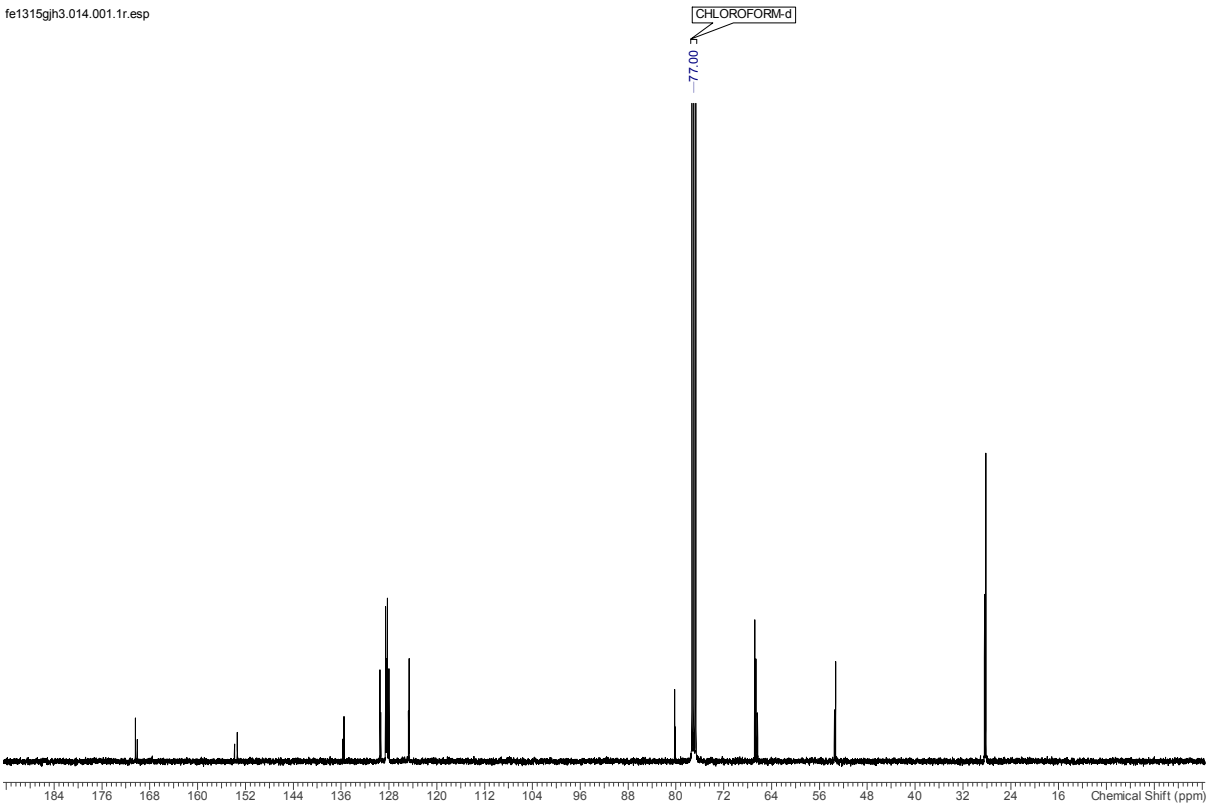

5.2 (2S,3R,4S)-N-t-Butyloxycarbonyl-3,4-dihydroxyproline benzyl ester 10

5.2.1 ^{1}H NMR (400 MHz, $CDCl_3$)

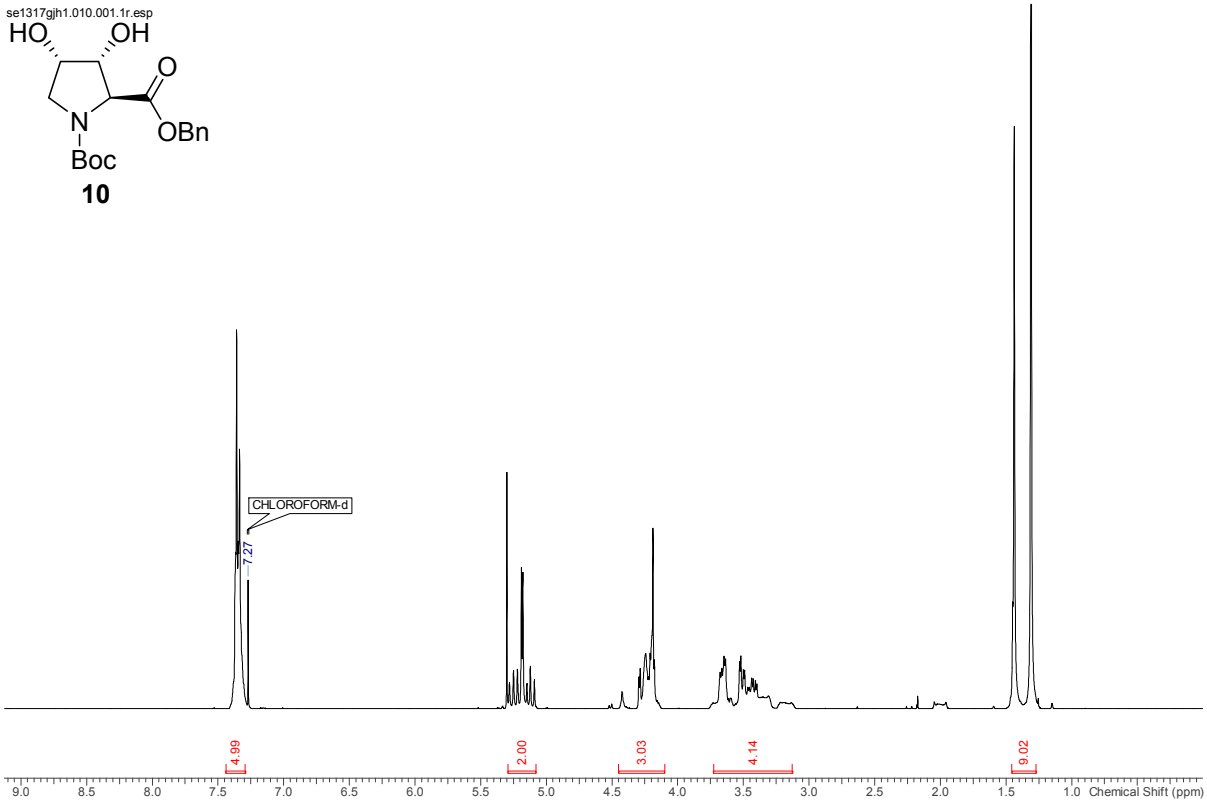

5.2.2 ^{13}C NMR (100 MHz, $CDCl_3$)

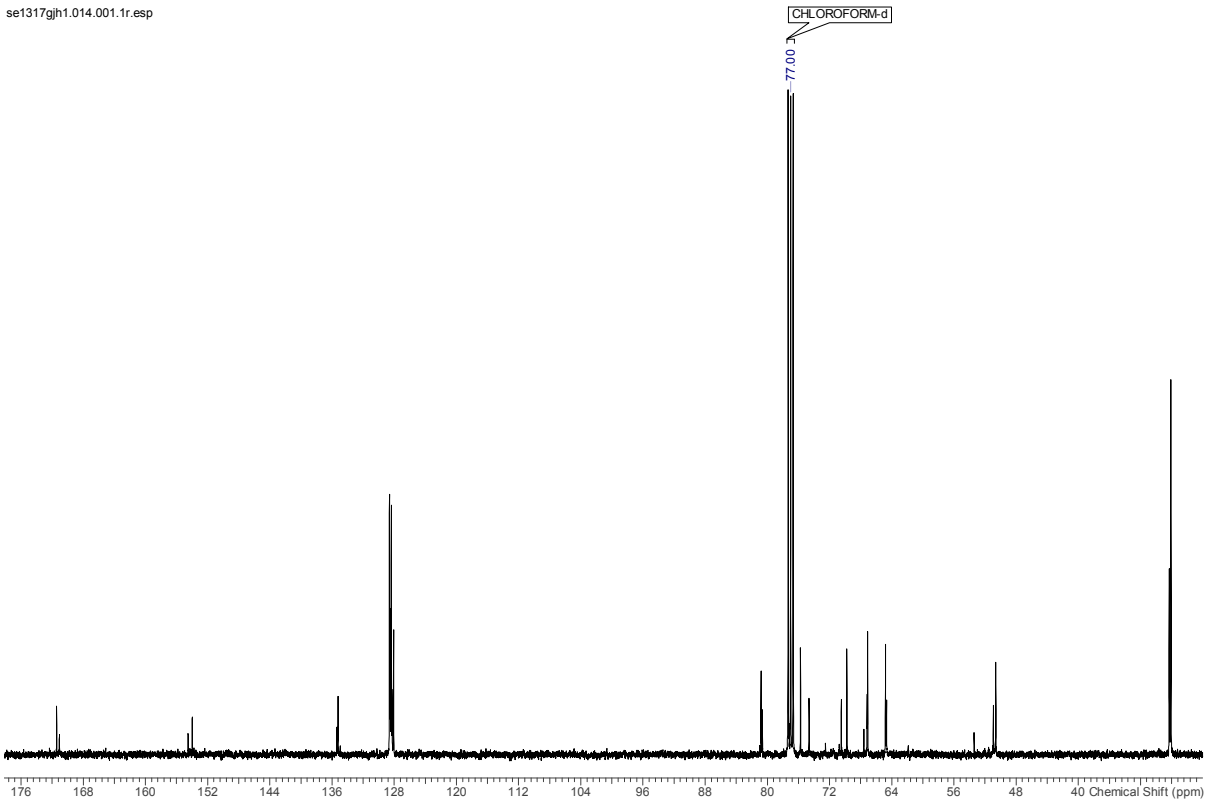

5.3 (2*R*,3*S*,4*R*)-*N*-*t*-Butyloxycarbonyl-3,4-difluoroproline benzyl ester 11

5.3.1 ^{1}H NMR (400 MHz, $CDCl_3$)

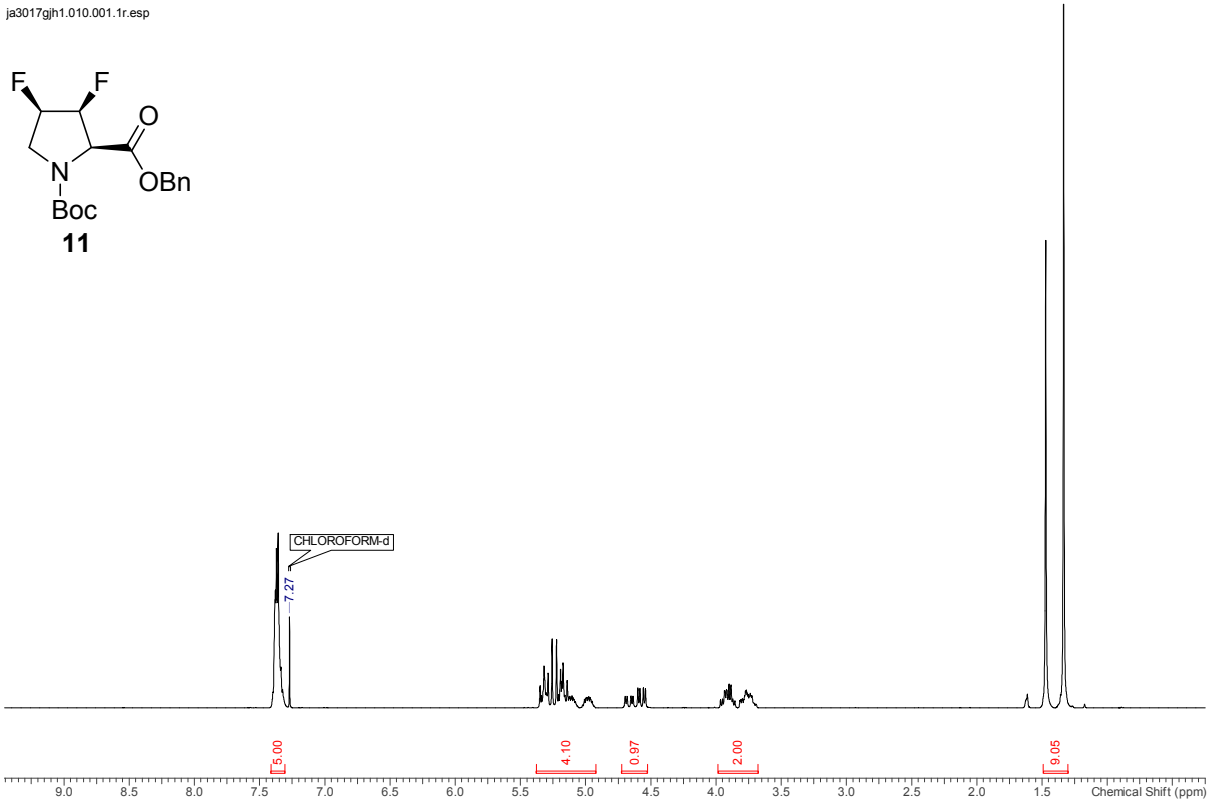

5.3.2 ^{13}C NMR (100 MHz, $CDCl_3$)

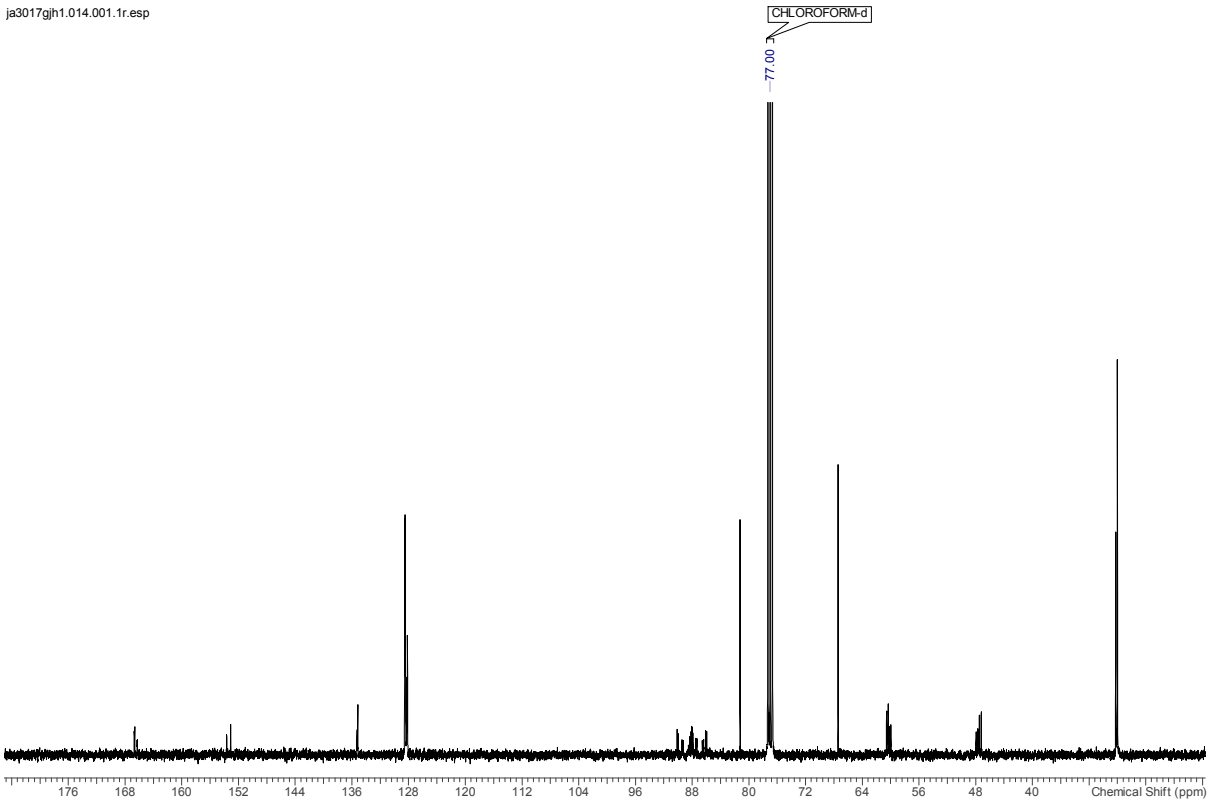

5.3.3 ^{19}F NMR (376 MHz, $CDCl_3$)

ja3017gjh1.017.001.1r.esp

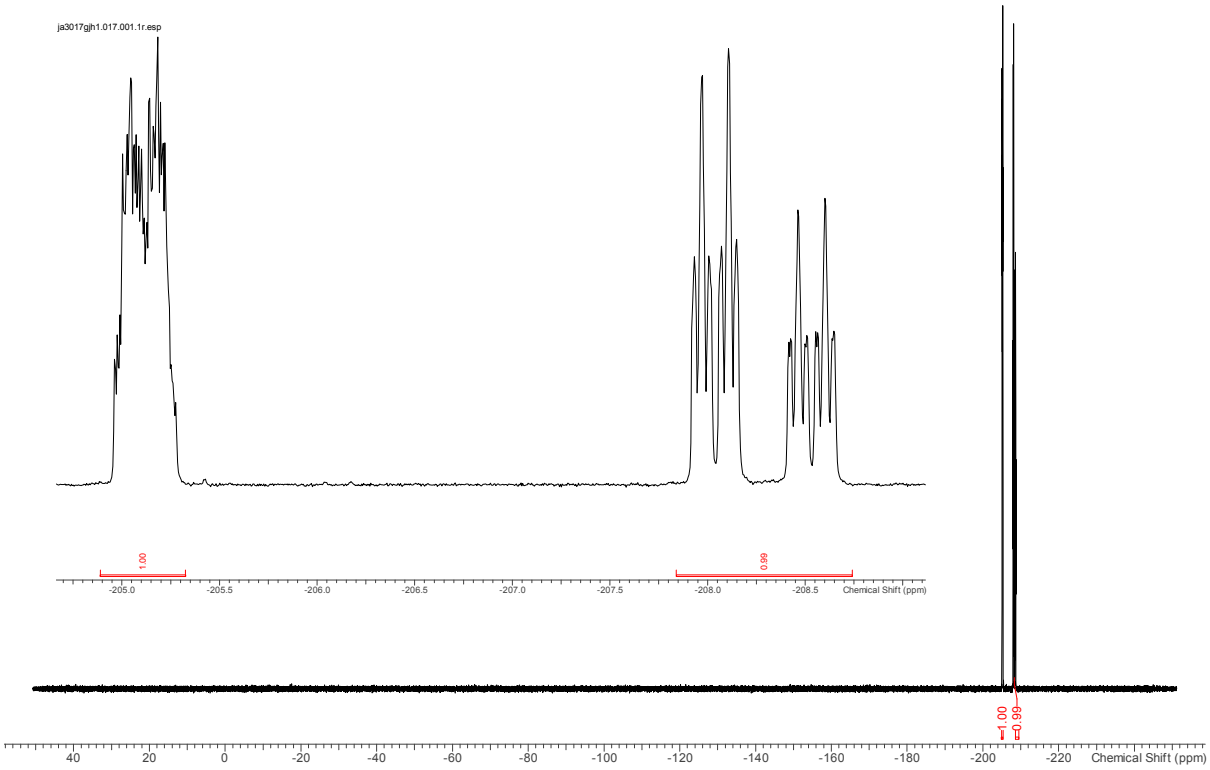

5.3.4 ^{19}F {^{1}H} NMR (376 MHz, $CDCl_3$)

ja3017gjh1.018.001.1r.esp

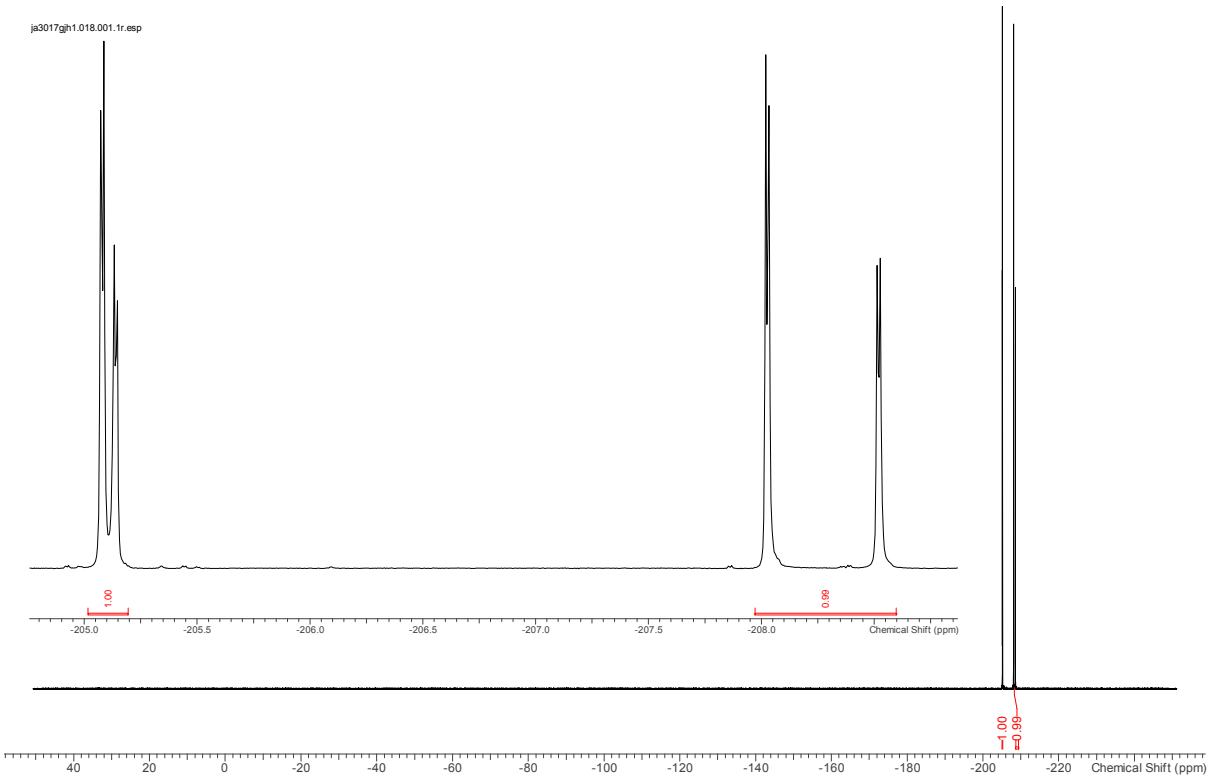

5.4 (2S)-N-t-Butyloxycarbonyl-3,4-dehydro-3-nonafluorobutylsulfonyloxyproline benzyl ester 12

5.4.1 ^{1}H NMR (500 MHz, $CDCl_3$)

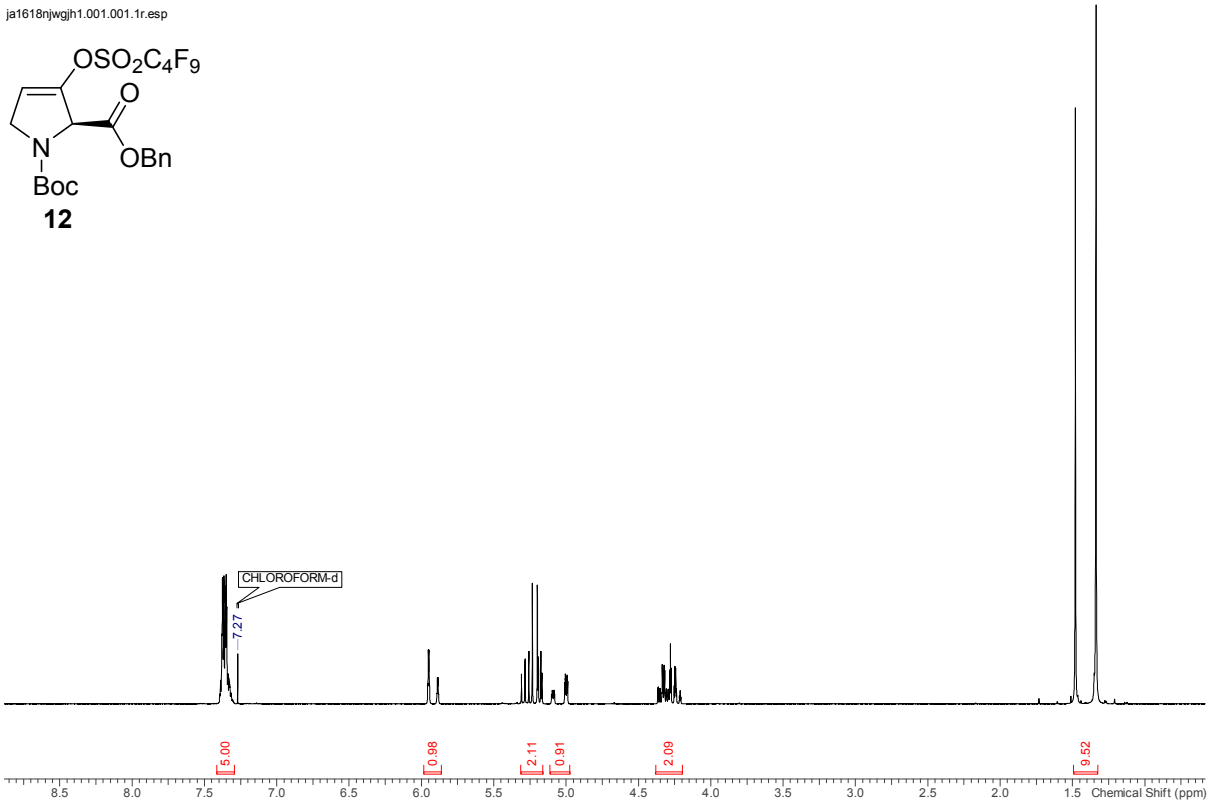

5.4.2 ^{13}C NMR (100 MHz, $CDCl_3$)

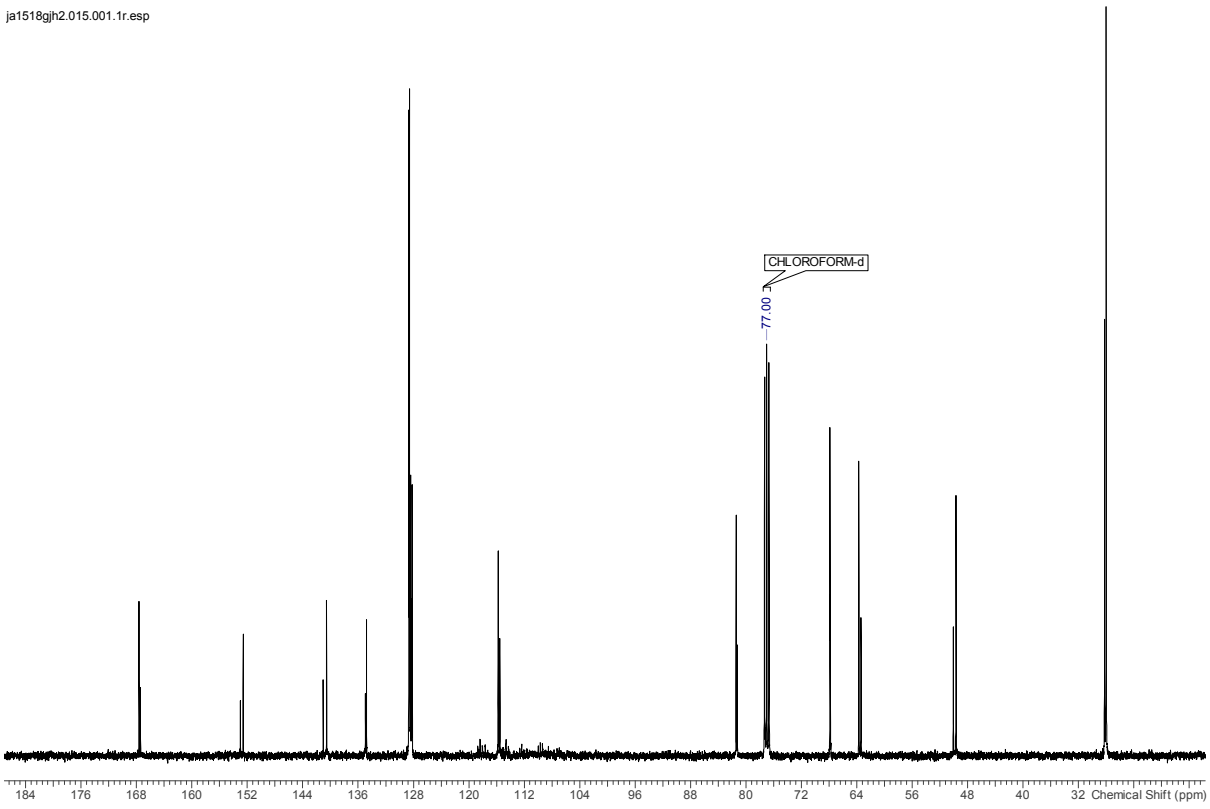

5.4.3 ^{19}F NMR (376 MHz, $CDCl_3$)

ja1518gjh2.017.001.1r.esp

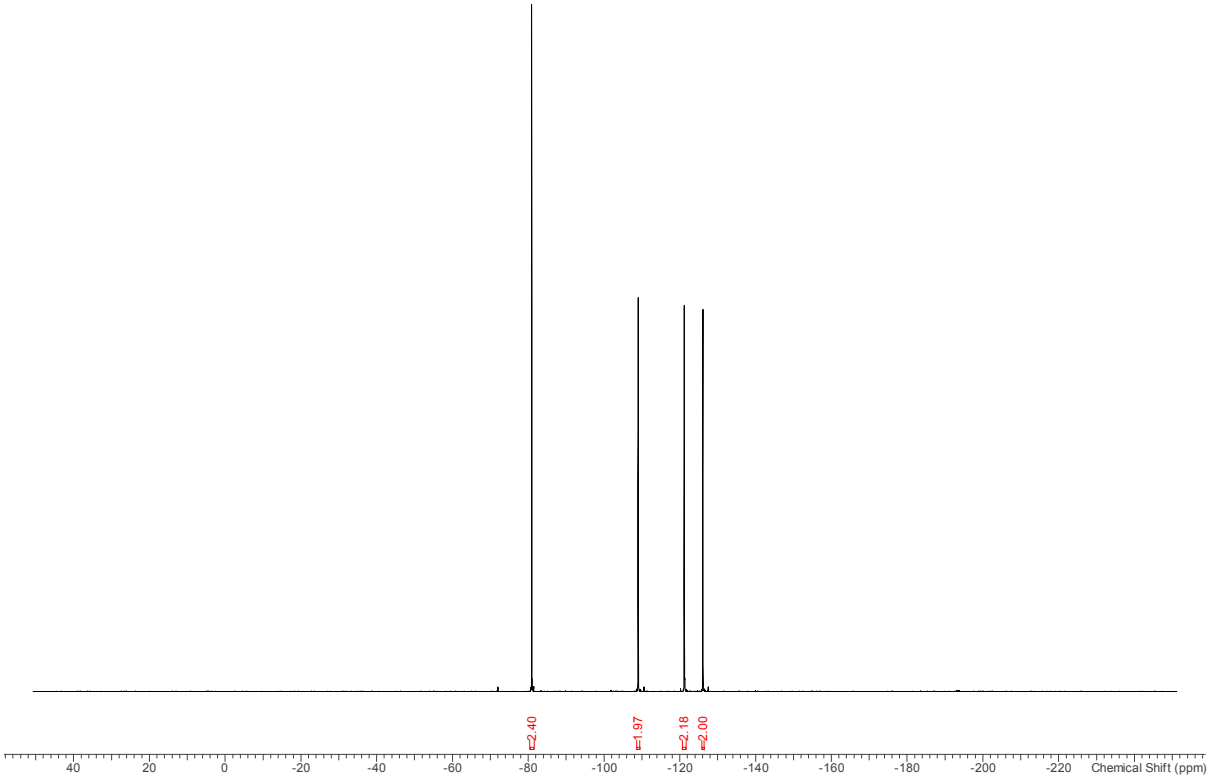

5.4.4 ^{19}F {^{1}H} NMR (376 MHz, $CDCl_3$)

ja1518gjh2.018.001.1r.esp

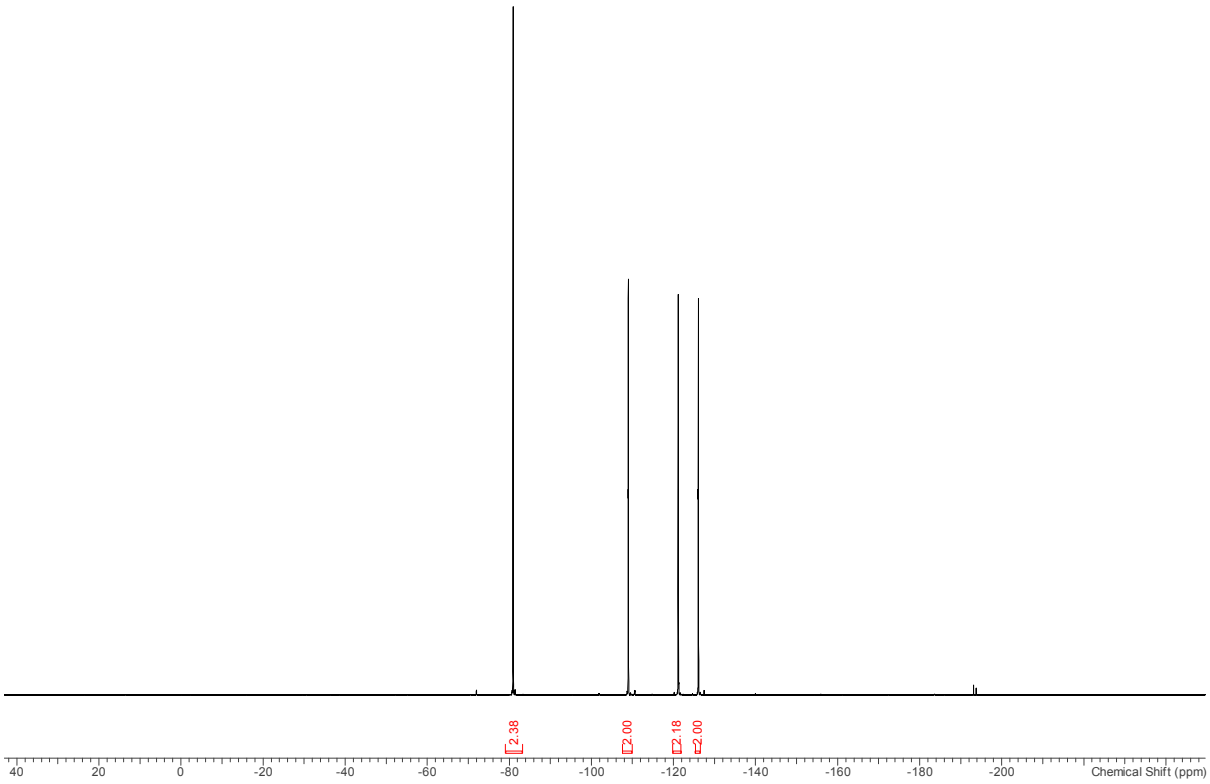

5.5 (2R,3S,4R)-N-Acetyl-3,4-difluoroproline methyl ester 7

5.5.1 ^{1}H NMR (400 MHz, $CDCl_3$)

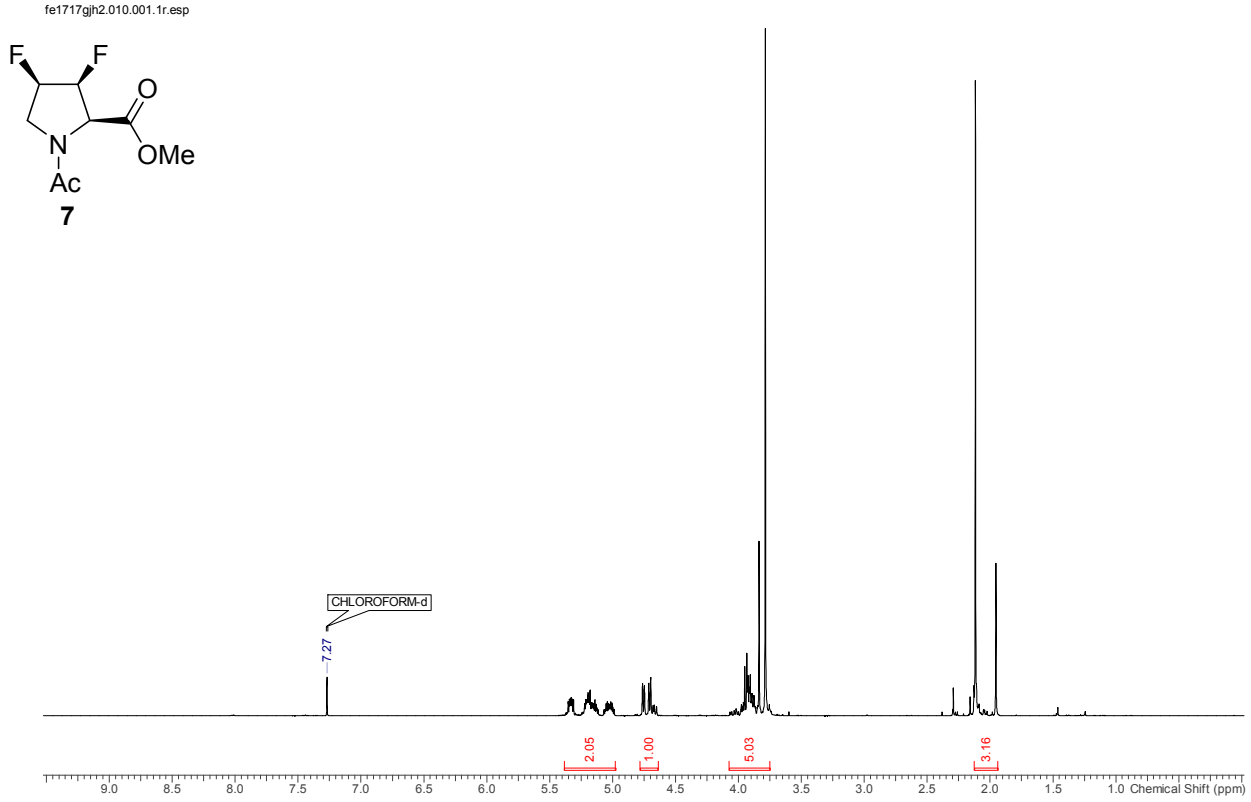

5.5.2 ^{13}C NMR (100 MHz, $CDCl_3$)

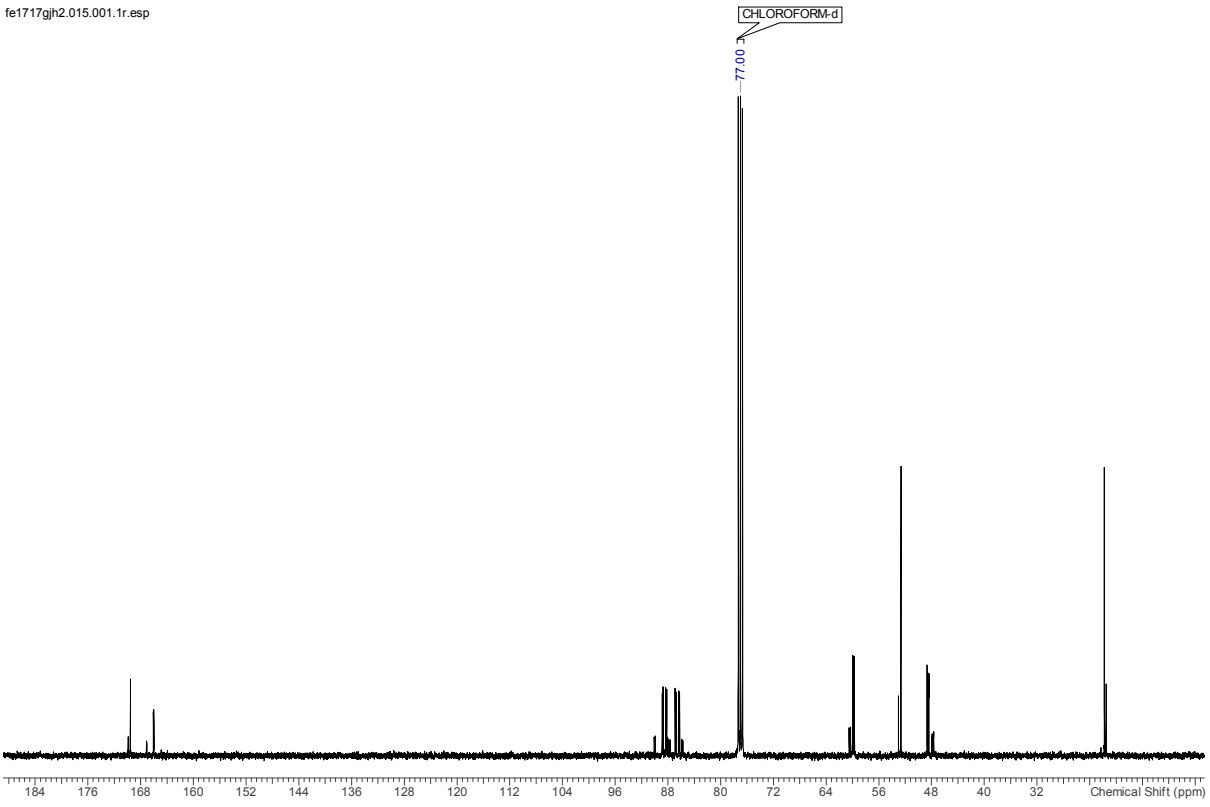

5.5.3 **^{19}F NMR** (376 MHz, $CDCl_3$)

fe1717gjh2.017.001.1r.esp

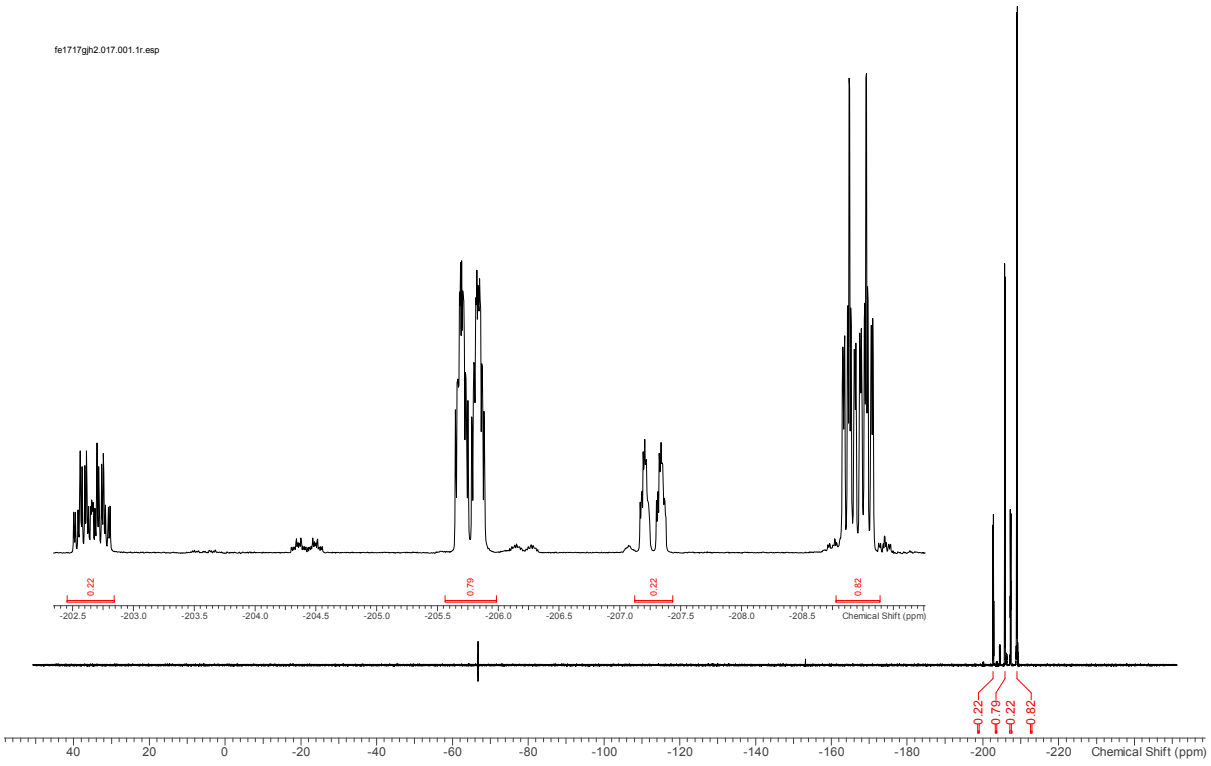

5.5.4 **^{19}F {^{1}H} NMR** (376 MHz, $CDCl_3$)

fe1717gjh2.018.001.1r.esp

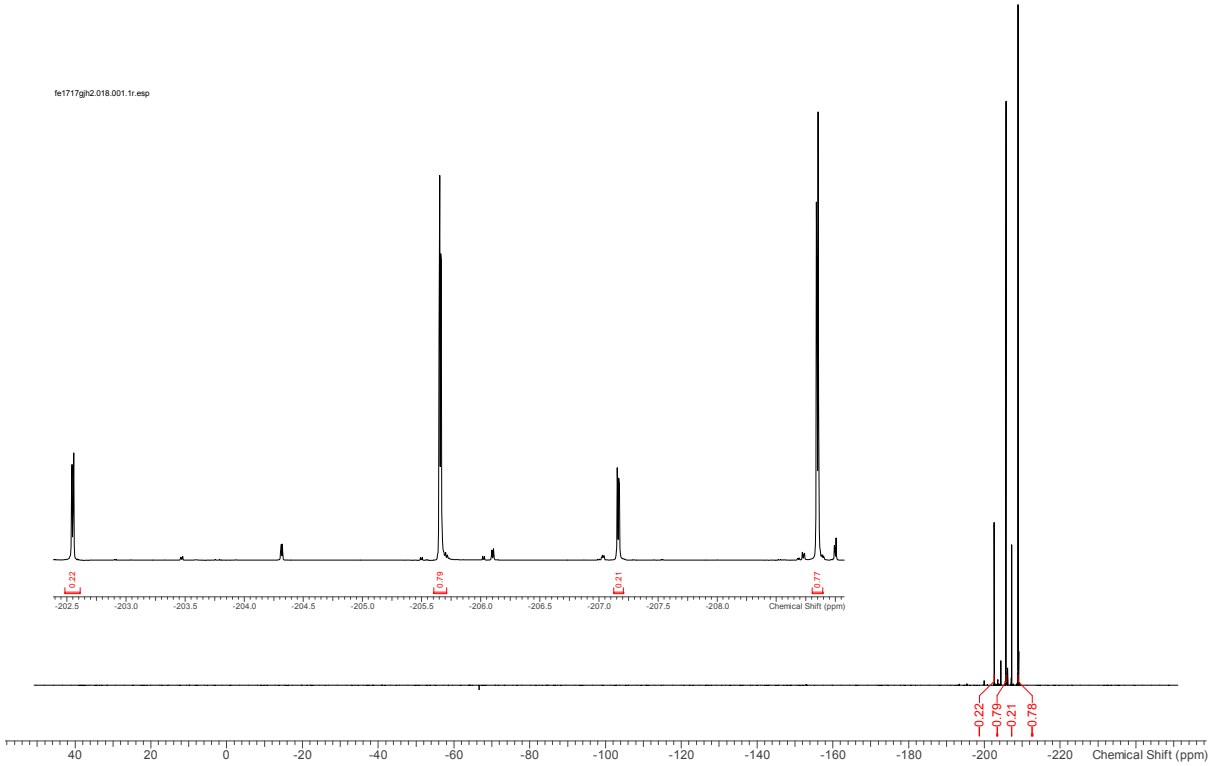

1. *US Pat.,* WO2005/87731, 2005.

2. *US Pat.,* WO2017/35360, 2017.

3. C. Priem, A. Wuttke, M. Berditsch, A. S. Ulrich and A. Geyer, *J. Org. Chem.*, 2017, **82**, 12366-12376.

4. C. Renner, S. Alefelder, J. H. Bae, N. Budisa, R. Huber and L. Moroder, *Angewandte Chemie-International Edition*, 2001, **40**, 923-925.

5. M. J. Frisch, G. W. Trucks, H. B. Schlegel, G. E. Scuseria, M. A. Robb, J. R. Cheeseman, G. Scalmani, V. Barone, B. Mennucci, G. A. Petersson, H. Nakatsuji, M. Caricato, X. Li, H. P. Hratchian, A. F. Izmaylov, J. Bloino, G. Zheng, J. L. Sonnenberg, M. Hada, M. Ehara, K. Toyota, R. Fukuda, J. Hasegawa, M. Ishida, T. Nakajima, Y. Honda, O. Kitao, H. Nakai, T. Vreven, J. A. Montgomery Jr., J. E. Peralta, F. Ogliaro, M. J. Bearpark, J. Heyd, E. N. Brothers, K. N. Kudin, V. N. Staroverov, R. Kobayashi, J. Normand, K. Raghavachari, A. P. Rendell, J. C. Burant, S. S. Iyengar, J. Tomasi, M. Cossi, N. Rega, N. J. Millam, M. Klene, J. E. Knox, J. B. Cross, V. Bakken, C. Adamo, J. Jaramillo, R. Gomperts, R. E. Stratmann, O. Yazyev, A. J. Austin, R. Cammi, C. Pomelli, J. W. Ochterski, R. L. Martin, K. Morokuma, V. G. Zakrzewski, G. A. Voth, P. Salvador, J. J. Dannenberg, S. Dapprich, A. D. Daniels, Ö. Farkas, J. B. Foresman, J. V. Ortiz, J. Cioslowski and D. J. Fox, *Journal*, 2009.

6. Y. Zhao and D. G. Truhlar, *Theor. Chem. Acc.*, 2008, **120**, 215-241.

7. A. V. Marenich, C. J. Cramer and D. G. Truhlar, *J. Phys. Chem. B*, 2009, **113**, 6378-6396.